12-13-2014

Impacts of Feedstock Bark Addition and Centrifugal Filtration on Pyrolysis Oil Properties and Storage Stability

Anandavalli Varadarajan

Impacts of feedstock bark addition and centrifugal filtration on pyrolysis oil properties and storage stability

By

Anandavalli Varadarajan

A Thesis
Submitted to the Faculty of
Mississippi State University
in Partial Fulfillment of the Requirements
for the Degree of Master of Science
in Chemical Engineering
in the School of Chemical Engineering

Mississippi State, Mississippi

December 2014

Impacts of feedstock bark addition and centrifugal filtration on pyrolysis oil properties and storage stability

By

Anandavalli Varadarajan

Approved:

_____

Keisha B. Walters
(Major Professor)

_____

Jason M. Keith
(Committee Member)

_____

Billy B. Elmore
(Committee Member)

_____

W. Todd French
(Graduate Coordinator)

_____

Jason M. Keith
Interim Dean
Bagley College of Engineering

Name: Anandavalli Varadarajan

Date of Degree: December 13, 2014

Institution: Mississippi State University

Major Field: Chemical Engineering

Major Professor: Keisha B. Walters

Title of Study: Impacts of feedstock bark addition and centrifugal filtration on pyrolysis oil properties and storage stability

Pages in Study: 127

Candidate for Degree of Master of Science

The physicochemical properties of pyrolysis oil have been shown to be dependent on feedstock composition. Accelerated aging tests were performed to understand the effects of feedstock, condensate fraction collected, and filtration on the stability of pyrolysis oil. In this study, pyrolysis oil properties critical for downstream upgrading were measured and compared for different feedstock weight ratios of pine clearwood and pine bark. Post-condensation filtration of pyrolysis oil was evaluated using both lab-scale and pilot plant-scale centrifugal filtration with several operational parameters evaluated. The pilot-plant centrifuge can be used as a three-phase separator [light liquid-heavy liquid-solids] or a two-phase clarifier [liquid-solid]. Since pyrolysis oil is an oil-water micro-emulsion, separation of the heavy and light liquid phases is difficult; therefore, emulsion destabilization studies were performed in concert with centrifugation. Physicochemical properties were monitored to determine the impact of the production and processing parameters on the oil properties critical to biofuel applications.

DEDICATION

I would like to dedicate this work to my family especially to my husband and daughter for their love and support throughout my Graduate program.

ACKNOWLEDGEMENTS

I would like to thank my advisor, Dr.Keisha Walters who has always been there to teach, motivate and help. I would also like to thank the members of my committee, Dr.Jason Keith and Dr.B.Elmore for their time and suggestions. I am also thankful to all members of my research group for their timely help.

TABLE OF CONTENTS

APPENDIX

LIST OF TABLES

LIST OF FIGURES

CHAPTER I

INTRODUCTION

1.1 Current and Future Trends in Energy Supply and Demand

During the last two centuries, global population has increased from 1 billion to 7 billion (Exxon Mobil, 2014) and quality of life has advanced owing to economic development and modern technologies. Population growth is expected to continue to increase, 25% over the next 20 years, with developing countries such India and China showing the most growth (Chevron, 2014). Global primary energy consumption for 2013 showed a 2.3% increase over 2012 (BP Statistical Review, 2014). Overall, world energy consumption is projected to increase by 56% between 2010 and 2040 (Table 1.1). India and China combined were responsible for 24% of world's total energy consumption in 2010; their consumption is expected to increase to 34% by 2040 with China consuming twice the quantity required by United States (Figure 1.1).

Table 1.1 Historical and projected global energy consumption in quadrillions of Btus.

Year							Average annual percent change, 2010-2040
2010	**2015**	**2020**	**2025**	**2030**	**2035**	**2040**	
524	572	630	680	729	777	820	1.5

(EIA, 2013)

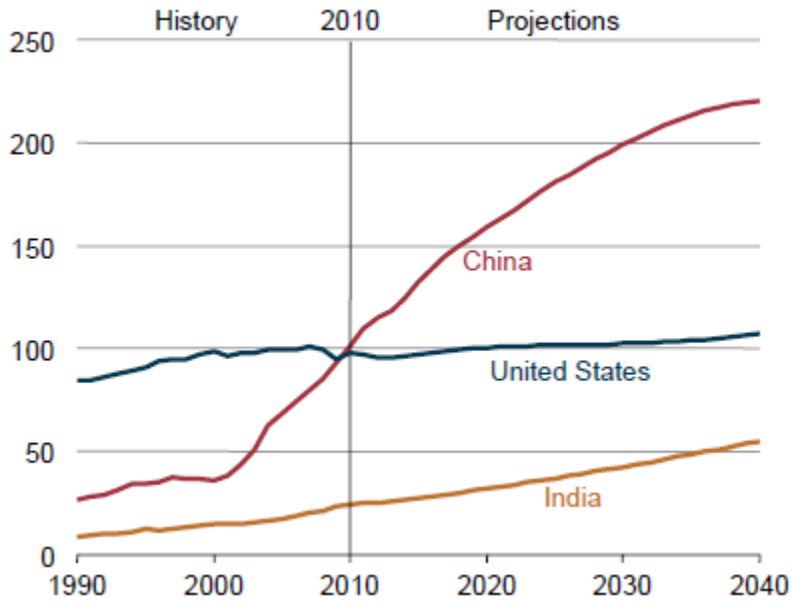

Figure 1.1 Energy consumption from 1990 to 2040 in quadrillion Btu (EIA, 2013).

The world's fastest growing form of energy is electricity whose generation increased by 93%, at an average annual rate of 2.2%, over the 2010-2040 period (EIA 2013). Though coal remains the major source for electricity generation so far, the contribution of renewable energy towards electricity generation is expected to increase at an average annual rate of 2.8%. U.S. energy consumption in 2013 showed electric power as the primary form of energy consumption with petroleum and natural gas the major energy sources (Figure 1.2). The outlook on world energy consumption in the short- and long-term shows considerable continued increase in energy demand mainly due to increases in population. Continued growth in energy demand, coupled with environmental considerations, has generated interest in renewable energy and significant increase in the development of renewable energy methods and renewable energy

production making renewable energy as one of the fastest growing energy sources, increasing at an average annual rate of 2.5% over the 2010-2040 period (EIA, 2013).

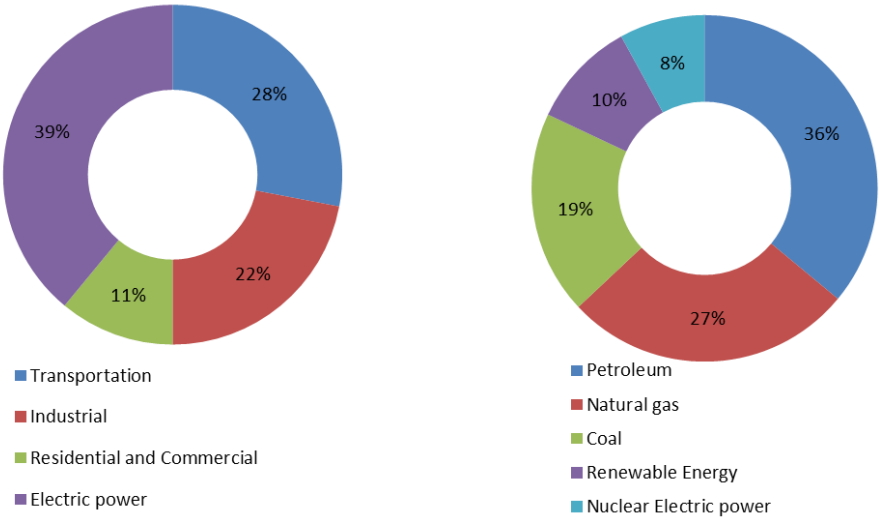

Figure 1.2 Primary U.S. energy consumption in 2013 by usage sector and feedstock source

(EIA 2013).

1.2 Need for Renewable Energy

Fossil fuel contributes 80% towards the current global energy demand and is expected to decline by 5% between now and 2035 (IEA, 2013). Though fossil fuel resources are plentiful, most of them require advanced recovery technologies which increase fuel prices (IEA, 2013). With continued global increase in energy demand, there will be a push towards converting resources to reserves which will eventually increase fuel prices. Another major concern in utilizing fossil fuels is the emission of greenhouse gases. Energy-related CO_2 emission for the world is expected to increase by 46 % between 2010 and 2040 (Table 1.2). The predicted global CO_2 emission for 2040 is 45.5

billion metric tons. Interest in environmentally friendly fuels supports the development of alternate energy sources with reduced carbon emissions.

Table 1.2 Historical and projected global energy-related CO_2 emission in billions of metric tons.

Year					Average annual percent change, 2010-2040
1990	2010	2020	2030	2040	
21.5	31.2	36.4	41.5	45.5	1.3

(EIA, 2013)

1.3 Biomass and Biomass Conversion

Biomass is the most abundant and widely used source of renewable energy. It is defined as the biological matter derived from plant material and animal manure (Demirbaş, 2001). Biomass is the only available renewable carbon based energy source which can be converted into solid, liquid and gaseous fuels (Demirbaş, 2001). Compared with other alternative energy resources, only biomass has the potential to produce a liquid fuel which could be utilized as a transportation fuel (EERE, 2013). Biomass is comprised mainly of carbon, hydrogen, and nitrogen, with sulfur and some other elements in small concentrations, including alkali, alkaline earth, and heavy metals (Yaman, 2004). Biomass falls into four broad categories (Demirbaş, 2001):

1) Wastes, such as agricultural production and processing wastes, wastes from lumber mills, waste from food processing, municipal solid wastes, and animal wastes;
2) forest products, including virgin wood, bark/saw dust from forest clearings and lumber mills, and logging residues;

3) energy crops (e.g., herbaceous, starch, sugar, oilseed); and

4) aquatic plants, such as algae, water weed, and water hyacinth.

Energy available from biomass is solar energy stored through the process of photosynthesis, and is called biomass energy or bioenergy. Globally, photosynthesis helps plants to fix 200 billion tons of carbon resulting in a stored energy content of 3000 billion GJ/year (Demirbaş, 2001). Biomass can be utilized in different forms such as biofuels, biopower and bioproducts (NREL). Fossil fuels are the remains of the plants and animals fossilized for up to millions of years. Both biomass and fossil fuels release greenhouse gases, such as carbon dioxide, when burned. The major difference between fossil fuels and bioenergy is that bioenergy has a closed carbon cycle. Biomass releases the same amount of carbon dioxide it absorbed while growing thereby not adding additional CO_2 into the atmosphere, unlike the combustion of fossil fuels (Demirbaş, 2001). Utilization of biomass results in the development of managed forests as crops, increased CO_2 absorption from the atmosphere (and generating carbon credits, as applicable) (AEBIOM, 2012). Another way biomass-based fuels have reduced environmental impact is the 90% reduction in the release of harmful gases, such as sulfur dioxide and nitrogen oxides, in comparison to burning coal (Demirbaş, 2001).

There are three methods to convert biomass: thermochemical, biochemical, and agrochemical (Demirbaş, 2001; McKendry, 2002a). For thermochemical conversion processes, the most sui biomass feedstocks are wood, woody residues, and low moisture herbaceous plants (Demirbaş, 2001). Thermochemical conversion includes direct combustion, gasification, pyrolysis and direct liquefaction (Küçük and Demirbaş, 1997). Fermentation and digestion in the presence of microorganisms are biochemical

conversion techniques (Küçük and Demirbaş, 1997; McKendry, 2002b) which are used on energy crop and manure feedstocks (Demirbaş, 2001). Agrochemical processes involve extraction of oils from plants such as rapeseed, sunflower, soybean; and these oils can be used directly as a biofuel (e.g., biodiesel) (Demirbaş, 2001). The viability of biomass as an energy source and appropriate conversion technologies are determined by properties such as moisture content, calorie content, cellulose-lignin ratio, concentration of alkali metal and fixed carbon, and volatiles produced (McKendry, 2002c). Cellulose-lignin ratio plays an important role in biochemical conversion as the biodegradability of cellulose is greater than that of lignin and high cellulose content is required for high yields. Other properties are important factors for thermochemical conversion (McKendry, 2002b).

Transportation fuels are responsible for ~30 % of CO2 emissions in developed countries and 98 % of transportation fuels are derived from petroleum (Gomez et al., 2008). The goals to replace (and/or supplement) petroleum-derived transportation fuels and reduce transportation-related CO2 emissions has driven a strong interest in the last 10 years to produce carbon neutral, liquid fuels. Liquid fuels obtained from biomass are called biofuels, and can be divided into first, second and third generation fuels. Biodiesel produced from oil crops and bioethanol from sugar-rich plants are first generation biofuels (Damartzis and Zabaniotou, 2011). The main concern with first generation fuels are high costs due to limited feedstock species and the utilization of food crops creating a food versus fuel competition (Damartzis and Zabaniotou, 2011). Second generation fuels are produced from lignocellulosic biomass and so avoids competition with food sources. With second generation fuels, either biochemical pathways are used to produce cellulosic

ethanol or thermochemical conversions are used to produce solid, liquid, and gas fuels. Third generation biofuels utilize microbes and microalgae as the biomass source, also avoiding food competition (Nigam and Singh, 2011). Finding economically viable ways of growing microalgae and extracting lipids from microbial biomass are under research. This study is focused on second generation biofuels utilizing lignocellulosic biomass.

1.4 Second Generation Biofuels

Second generation biofuels are mainly produced from lignocellulosic feedstock (Naik et al., 2010). Lignocellulosic biomass is the non-food material available in abundance in plants (Gomez et al., 2008). Production of second generation fuels is not yet commercialized due to some difficulties involved in increasing the yield and technical production issues such as selecting proper reactor configuration, heat transfer rate, feed preparation, liquid collection and char separation methods to improve the product quality (Bridgwater et al., 1999; Damartzis and Zabaniotou, 2011). Some pilot plant studies for cellulosic ethanol have been successful but commercialization still faces financial difficulties. There are only two commercial-scale facilities available in United States for the production of second generation biofuels, INEOS Bio in Florida which produces ethanol from waste and KiOR in Mississippi which utilizes wood to produce diesel and fuel oil blendstocks (icct 2013). Though both thermochemical and biochemical conversion can be utilized for lignocellulosic biomass (Damartzis and Zabaniotou, 2011; Nigam and Singh, 2011), in biochemical conversion acid/enzymatic hydrolysis is required before fermentation due to the presence of longer-chain polysaccharide molecules (McKendry, 2002b). The major advantage of thermal processes is all organic material present in the biomass is converted, unlike the biochemical pathway which

concentrates only on polysaccharides (Gomez et al., 2008). Of the thermochemical processes, the majority of research has focused on pyrolysis as the liquid product obtained from pyrolysis has high energy density (Bridgwater and Grassi, 1991; Küçük and Demirbaş, 1997).

1.5 Pyrolysis and Woody Biomass

Pyrolysis is one of the thermochemical conversion methods available to convert solid biomass to liquid fuel. Pyrolysis is the thermal decomposition of biomass in the absence of oxygen which can produce gases rich in hydrocarbon, solids rich in carbon (can be utilized as energy source for domestic purpose), and liquids which resembles oil (Demirbaş, 2001). The liquid product obtained from this process is called pyrolysis oil or bio-oil and has the potential to be used as transportation fuel. Pyrolysis can be divided in to three categories (Jahirul et al., 2012) based on the operating conditions.

- Slow pyrolysis. This method utilizes a very slow heating rate (0.1-1 °C/s), and it has been used conventionally to produce charcoal. Due to the high residence time, the gaseous products react with one another resulting in a carbon-rich solid, charcoal, and therefore oil yields are typically only about 30 %.
- Fast pyrolysis. This method utilizes a much faster heating rate (10-200 °C/s) compared to slow pyrolysis. This higher heating rate results in the formation of three product phases: solid (15-20 wt%), liquid (60-75 wt%), and non-condensable gases (10-20 wt %).

- Flash pyrolysis. Very high heating rates (>1000 °C/s) are utilized in this process. Very small biomass particle size of biomass is required due to the extremely small residence times. Flash pyrolysis results in higher oil yields, in comparison to the other two processes.

Fast pyrolysis gives higher oil yields versus slow pyrolysis (Jahirul et al., 2012). Flash pyrolysis gives even higher oil yields; however, the oil produced displays poor thermal stability, high corrosiveness, and higher solids contents (Cornelissen et al., 2008). In addition to producing a viable liquid biofuels at reasonable yields, fast pyrolysis also has a low investment cost and high energy efficiency—in comparison to slow and flash pyrolysis (Jahirul et al., 2012).

1.5.1 Details on Fast Pyrolysis

Fast pyrolysis produces high liquid yields when operating conditions can be well-controlled. Typical operating parameters such as heating rate of 10-200 °C/s, temperature range of 450 °C-550 °C and vapor residence time of <1 s (Bridgwater et al., 1999). The major advantage of fast pyrolysis is that there is no secondary conversion of products due to high heating rates and quick quenching of liquid products (Klass, 1998). Both residence time of vapor and temperature plays a major role in minimizing the secondary reactions (Bridgwater et al., 1999). Decomposition of volatiles takes place at temperature above 500 °C and condensation reactions occur when the temperature is maintained below 400 °C. When very low residence times are utilized, incomplete depolymerisation of lignin occurs resulting in a non-homogenous product while very high residence times leads to secondary cracking of products reducing yields and adversely impacting in oil

properties (Bridgwater, 1999; Bridgwater et al., 1999). With fast pyrolysis, maximum liquid yields up to 80 wt % (dry feed basis) can be obtained from wood under controlled operating conditions (Bridgwater, 1999). Although the resultant liquid product from fast pyrolysis has a heating value half that of conventional fuels (Bridgwater, 1999), it has the potential to be used to as an environmentally-friendly substitute for fuel oil and an alternative source to produce specialty chemicals (Bridgwater, 2007; Oasmaa and Czernik, 1999).

1.5.2 Biomass Used for Pyrolysis

Wood is a commonly used feedstock for pyrolysis due to its compositional consistency (Bridgwater, 2007); wood is generally comprised mainly of cellulose (40-50 wt%), hemicellulose (25-35 wt%), and lignin (18-35 wt%) (Pettersen, 1984). Other materials, such as organic extractives and inorganic ash, are also present in small quantities (4-10 wt%) (Pettersen, 1984). The chemical composition of any particular wood sample not only varies with the species and age of the tree, but also with the parts of the same tree. Other factors that contribute to compositional variations include geographic location, climate, and soil type (Pettersen, 1984). Lignocellulose is a natural composite material with cellulose proving skeletal structure, strength, and rigidity (Gomez et al., 2008; Yaman, 2004). Cellulose constitutes 50 % of the cell wall material and is insoluble in water (Yaman, 2004). Hemicelluloses are polysaccharides covering the cellulose which acts as plasticizer to provide flexibility (Gomez et al., 2008). Hemicellulose has a branched structure of 50-200 monomeric units and some sugar residues with xylan in plenty and they are soluble in alkali solution (Yaman, 2004). Lignins are three dimensional, highly branched phenolic polymer network and they are

bound to cellulosic fibers. Lignin content in any hardwood and softwood normally falls in the range of 20-40 wt% on dry basis (Yaman, 2004). All these three components decompose at different rates and mechanism due to the difference in their molecular structures (Jahirul et al., 2012). Hemicellulose has an amorphous structure and is rich in saccharides whereas cellulose has a strong structure with a long polymer of glucose and lignin is rich in aromatic rings with various branches and the chemical bonds in lignin are active for the wide range of temperature (Yang et al., 2007). Hence hemicellulose remains as the easiest one to be pyrolyzed followed by cellulose and lignin (Wang et al., 2008). As lignin has a great thermal stability they need wider temperature range to decompose compared with cellulose and hemicellulose (Bridgwater et al., 1999). Lignin and cellulose affects the pyrolysis of cellulose but they do not affect each other (Wang et al., 2008). The decomposition of cellulose components results in oil yield whereas decomposition of lignin leads to char (Yang et al., 2006). The product yields are also affected by the reactor configuration as it has influence over the secondary reactions (Bridgwater et al., 1999). The decomposition also depends on process parameters such as temperature, rate of heating and pressure (Bridgwater et al., 1999; Jahirul et al., 2012).

1.6 Pyrolysis Oil Characteristics

Pyrolysis oil is a dark brown liquid (Oasmaa and Czernik, 1999) with a distinctive acrid or smoky odor (Bridgwater, 2003; Czernik and Bridgwater, 2004). Pyrolysis oil is a complex mixture of oxygenated hydrocarbons with molecules of different sizes. The elemental composition of pyrolysis oil resembles that of the feedstock biomass as the product is formed from depolymerization and fragmentation reactions (Czernik and Bridgwater, 2004; Oasmaa and Czernik, 1999). Pyrolysis oil is comprised of water,

solids and more than 400 organic compounds that include functional groups such as hydroxyaldehydes, hydroxyketones, sugars, carboxylic acids, and phenolics (Diebold, 2000; Lu et al., 2009; Milne et al., 1997; Oasmaa and Czernik, 1999). It can be described as a micro-emulsion with a continuous aqueous phase including decomposition products of holocellulose which stabilizes the discontinuous phase of lignin macromolecules through hydrogen bonding (Bridgwater, 2003). The properties of pyrolysis oil are very much dependent on feedstock type, feedstock pretreatment, pyrolysis conditions, liquid collection method, and char removal techniques (Lu et al., 2009).

1.6.1 Homogeneity and multiphase structure

Most pyrolysis oils are homogenous unless they are derived from a feedstock rich in extractives, such as forestry residues (Lu et al., 2009; Oasmaa and Czernik, 1999). Oil produced from extractives differs in solubility, polarity, and density (Oasmaa et al., 2002). Pyrolysis oil derived from extractive-rich biomass can separate into two phases with the top phase rich in extractives and the bottom phase having properties similar to pyrolysis oil produced from feedstocks without extractives (Garcìa-Pérez et al., 2007; Oasmaa et al., 2002). Phase separation can also occur in pyrolysis oil with high water content (>30-35 wt%) (Oasmaa and Czernik, 1999). Pyrolysis oil derived from biomass with small concentrations of extractives does not phase separate since at low concentrations, the extractives remain well dispersed (Lu et al., 2009). Garcìa-Pérez et al. showed that pyrolysis oil having an apparent single phase still showed multiphase structure at the microscopic scale, with distinct char particles, aqueous droplets, and heavy compound micelles present (Garcìa-Pérez et al., 2005).

1.6.2 Heating value

Heating value can be defined as the amount of heat released during the combustion of a specified mass of a given material. Lower heating value (LHV) and higher heating value (HHV) are two different types of heating values reported in the technical and commercial literature. Higher heating value is obtained by adding the heat of vaporization of the liquid water content to the lower heating value. Lower heating value determination assumes that all the water content in the fuel is in vapor state at the end of combustion and the energy required to vaporize will not be released as heat (Carpenter, 2014)

Compared to traditional hydrocarbon fuels, pyrolysis oil has a lower heating value (LHV) ranging from 14-18 MJ/Kg, which is 40-50 % of the value for traditional hydrocarbon fuels. This is due to high water and oxygen contents of the oil (Oasmaa and Czernik, 1999). The heating value of pyrolysis oil derived from oil plant biomass is higher than for the oil derived from wood or agricultural residue biomass. Woody biomass produces higher yield than plant biomass (Zhang et al., 2007).

1.6.3 Water content

Water in the pyrolysis oil results from both the original moisture present in the feedstock and water produced from dehydration reactions. The amount of water produced varies considerably with the feedstock type and process conditions (Oasmaa and Czernik, 1999). Water in the pyrolysis oil is miscible with the lignin derived compounds until the concentration of 30 wt% (Oasmaa and Czernik, 1999). More water leads to phase separation with an aqueous phase and thick, tar-like phase (Diebold and Czernik, 1997). Although higher water content leads to lower heating values, it improves

flow characteristics leading to better atomization and lower NOx emissions (Oasmaa and Czernik, 1999).

1.6.4 Oxygen content

Pyrolysis oil has fairly oxygen contents ranging between 35-40 % (Oasmaa and Czernik, 1999; Scholze and Meier, 2001), as the oil contains all oxygen present in the original biomass (Lu et al., 2009). The presence of oxygen is the major cause for the noted differences between pyrolysis oil and hydrocarbon fuels (Zhang et al., 2007). Oxygen makes the pyrolysis oil polar making it immiscible with non-polar petroleum fuels (Lu et al., 2009). High oxygen content also makes pyrolysis oil corrosive, less s, and a lower heating value (Lu et al., 2009; Zhang et al., 2007).

1.6.5 Corrosiveness

The pH of pyrolysis oil is usually in the range of 2-3 due to the presence of carboxylic acids, mainly formic and acetic acid (Oasmaa and Czernik, 1999). Acetic acid is produced by the deacetylation of hemicellulose (Alén et al., 1996). Due to low pH, pyrolysis oil corrodes carbon steel and aluminum (Jay et al., 1995) and this corrosiveness is increased at high temperatures and high water contents (Aubin and Roy, 1990).

1.6.6 Solids content

Char particles are a major source of the solids in pyrolysis oil, although there can be some entrained fluidized bed materials or other heat transfer media (Lu et al., 2009; Oasmaa and Czernik, 1999). Char particles remains as unburned particles in the flue gas as it forms carbonaceous cenospheres (Lu et al., 2009). Solid content can be as high as 3 wt%, even after separating solids from the pyrolysis vapors (for example, with a cyclone

separator), and the particle sizes range between 1-200 µm (Lu et al., 2009; Oasmaa and Czernik, 1999). Most of the particles are below 10 µm, which makes them more difficult to remove (Lu et al., 2009). The presence of char leads to problems such as erosion and clogging in fuel injection systems (Lu et al., 2009). Char particles also act as catalysts for aging reactions that have been shown to increase the viscosity of the oil (Agblevor and Besler, 1996). However Naske at al. observed that char removal did not prevent aging related physicochemical property changes in pyrolysis oil (Naske et al., 2011).

1.6.7 Ash

Inorganic materials present in the feedstock are generally sequestered into the char during pyrolysis and these char particles (Agblevor and Besler, 1996; Lu et al., 2009). During storage, alkali metals do not leach from the char into pyrolysis oil (Agblevor and Besler, 1996). Most commercial filtration methods do not help in removing the ash content since ash particles are submicron in size (Agblevor and Besler, 1996). Ash in pyrolysis oil leads to difficulties such as erosion and corrosion in engines and valves; significant deterioration can occur with ash content higher than 0.1 wt% (Zhang et al., 2007). Sodium and potassium are primarily responsible for corrosion at the high temperatures experienced during combustion (Zhang et al., 2007).

1.6.8 Viscosity

Viscosity plays a major role in determining the atomization and combustion properties of the fuel oil. So viscosity values need to be considered while designing the fuel injection system (Lu et al., 2009). The viscosity of pyrolysis oils vary widely (10-100 cP @ 40 °C), and has been shown to be highly dependent on the feedstock type and

pyrolysis conditions (Lu et al., 2009; Zhang et al., 2007). Pyrolysis oil with high water content and less water insoluble components are less viscous compared to the one with low water content (Zhang et al., 2007).

1.6.9 Toxicity

Pyrolysis oil is found to be an irritant to eyes, skin and respiratory system and it may even cause some irreversible damage (LaClaire et al., 2004). Swallowing, inhaling and direct exposure to eyes have harmful effects. Also pyrolysis oil produced at temperatures greater than 600 °C can have mutagenic effects due to the presence of polycyclic aromatic hydrocarbons (Lu et al., 2009; Oasmaa and Peacocke, 2010). Pyrolysis oil has the tendency to penetrate into the skin and could even cause damage to internal organs. Inhalation of pyrolysis oil can lead to lung damage (LaClaire et al., 2004). The toxicity of pyrolysis oil is due to the presence of aldehydes, unsaturated oxygenates, and furans (Diebold, 1999). As these compounds are unstable, the toxicity might reduce over time (Lu et al., 2009). Ingestion of pyrolysis oil at levels of 700 mg per 1 kg of body weight has been shown to cause acute effects (Lu et al., 2009). There would be safety concerns involved with the development of a large-scale pyrolysis plant, due to the oil's toxicity and health hazards (Gratson, 1994). However, pyrolysis oil is less toxic and has less environmental impact, as compared to petroleum fuels (Oasmaa and Czernik, 1999).

1.7 Stability

The main drawback in commercial application of pyrolysis oil is that it is unstable during storage. Pyrolysis oil is not at thermodynamic equilibrium; hence it undergoes

property changes due to thermal and oxidative degradation in an attempt to move towards equilibrium during storage (Diebold, 2000; Hilten and Das, 2010). This instability is caused by the presence of volatiles and non-volatile oxygenated compounds at higher concentrations (Oasmaa and Kuoppala, 2003). The instability of pyrolysis oil presents as an increase in viscosity, increase in solids, and oxidation of volatile components (Hilten and Das, 2010; Oasmaa and Kuoppala, 2003; Oasmaa and Peacocke, 2001). Both thermal and oxidative degradation results in viscosity increase, with the former caused by loss of volatiles and the later by polymerization (Diebold, 2000; Diebold and Czernik, 1997; Hilten and Das, 2010; Oasmaa and Kuoppala, 2003). Some post-condensation chemical reactions such as polymerization of double bonded compounds, etherification, and esterification result in water as a byproduct leading to increases in water content during storage (Czernik et al., 1994; Oasmaa and Czernik, 1999). These processes result in property changes over time (and/or at elevated temperatures) and so it is referred to as 'aging' (Oasmaa and Czernik, 1999). Changes in properties associated with aging in pyrolysis oil are highly dependent on feedstock and storage temperature. A study conducted by Oasmma and Kuoppala showed that most of the aging reactions and physicochemical changes in pyrolysis oil at ambient temperature take place during the first six months of storage (Oasmaa and Kuoppala, 2003)

Aldehydes play a major part in the aging process as they are the most unstable functional groups found in pyrolysis oil (Lu et al., 2009). Some of the reactions of aldehydes (Diebold, 2000; Lu et al., 2009) include (1) reaction with water to form hydrates, (2) reaction with phenolics to form resins and water, (3) reaction with alcohols to form acetals, hemiacetals and water, (4) reaction with proteins to form dimers, and (5)

reaction with each other to form oligomers and resins. Other reactions responsible for aging in pyrolysis oil include reactions between acids and alcohols to form esters and water and the polymerization of olefins resulting in the formation of oligomers and polymers (Lu et al., 2009). Polymerization reactions can be catalyzed by acids and peroxides produced by the oxidation of pyrolysis oil (Lu et al., 2009). Aging reactions also changes the polarity of pyrolysis oil as highly polar acids and alcohols are converted to less polar esters and extremely polar water during esterification (Lu et al., 2009).

Aging mechanisms are accelerated at high temperatures (Lu et al., 2009). Change in properties of oil as a function of time and temperature during storage is an important factor to be considered for fuel applications (Czernik et al., 1994). During heating pyrolysis oil undergoes changes such as thickening, phase separation, gummy formation and coke formation (Oasmaa and Peacocke, 2010). Aging of pyrolysis oil can also be measured through increases in molecular weight due to the increase in water-insoluble fractions composed of lignin-derived materials and polymerization reactions (Oasmaa and Czernik, 1999). Increase in molecular weight also causes an increase in viscosity (Oasmaa and Czernik, 1999). Phase separation is another phenomenon that happens during storage. Phase separation occurs due to increase in water content resulting as a byproduct in some of the chemical reactions during aging. Polymerization also leads to phase separation caused by the formation of larger molecules resembling tar which settles at the bottom leaving top phase as high water content and acidic (LaClaire et al., 2004). Normally, viscosity of pyrolysis oil decreases with the increase in water content. But during aging both viscosity and water content increases attributed to the fact that increase in water content is small compared to the increase in average molecular weight (Oasmaa

and Czernik, 1999). The rate of aging is depends on many factors such as feedstock, pyrolysis conditions, liquid collection and char removal methods.

1.8 Upgrading

Pyrolysis oil has many deleterious properties such as high viscosity, high solids, high oxygen content, lower heating value and instability which provides an obstacle to replace fossil fuels with pyrolysis oil (Zhang et al., 2007). Pyrolysis oil can be upgraded by physical, chemical and catalytic means (Bridgwater, 2012a). The heating value of pyrolysis oil can be increased by catalytic hydrotreatment or catalytic cracking but these processes have drawbacks such as lower liquid yields and more capital investment (Oasmaa and Czernik, 1999; Solantausta et al., 1992).

Physical means of upgrading can be utilized for controlling the solids in pyrolysis oil. Cyclone separator is commonly used to separate char from pyrolysis vapors. But cyclones are not efficient in removing particle of below 10 μm (Bridgwater, 2012a; Oasmaa and Czernik, 1999). Pressure filtration to remove particles is not efficient as the char and pyrolytic lignin agglomerates to form a gel that clogs the filter resulting in pressure loss and loss of oil (Bridgwater, 2012a; Elliott, 1994; Oasmaa and Czernik, 1999). Another method of filtration which is hot gas filtration has proven to be effective in reducing ash content to less than 0.01 % and the alkali content to <10 ppm but it has drawbacks such as high pressure loss leading to lower yields (Bridgwater, 2012b). Char cake clogging the filters can be removed by frequent backflushing is more expensive (Bridgwater, 2012a; Hoekstra et al., 2009; Oasmaa and Czernik, 1999).

Solvent addition helps in overcome the viscosity increase during storage or heating. Polar solvents help in homogenizing and reducing the viscosity of pyrolysis oil

(Boucher et al., 2000; Diebold and Czernik, 1997; Oasmaa et al., 2004). Solvents work through three different mechanisms (Oasmaa and Czernik, 1999; Xiu and Shahbazi, 2012) in reducing the viscosity, (1) physical dilution (2) molecular level dilution changing the microstructure of the oil or reducing the chemical reaction rates (3) solvents react with the components of oil and prevents polymerization. When alcohols are used as solvent they react with acids and aldehydes in pyrolysis oil leading to esterification and acetalization which results in decrease in acidity and increase in heating value of pyrolysis oil (Oasmaa and Czernik, 1999; Xiu and Shahbazi, 2012). A study conducted by Diebold and Czernik proved that the rate at which viscosity increase is almost 10 times less for pyrolysis oil with 10 wt % methanol than the pyrolysis oil without additives (Diebold and Czernik, 1997).

Catalytic means of upgrading helps in reducing the oxygen content of pyrolysis oil. Methods include hydrotreating, hydrocracking, and steam reforming (Zhang et al., 2007). Hydrotreating is a simple hydrogenation process commonly used in petroleum refineries (Xiu and Shahbazi, 2012). Hydrocracking is performed at high temperatures (> 350 °C) and pressures (100-2000 psi) with removal of oxygen as H_2O, CO_2 or CO, resulting in the formation of hydrocarbons (Bridgwater, 2012a; Xiu and Shahbazi, 2012; Zhang et al., 2005). Hydrotreating results in coke formation and is not economical / energy efficient due to the requirement of high temperature and pressure (Xiu and Shahbazi, 2012). Hydrotreating pyrolysis oil results in producing naptha-like compounds requiring a refining process (Bridgwater, 2012a) and the coke formation (8-25 %) leads to a poor quality pyrolysis oil (Xiu and Shahbazi, 2012). Hydrocracking, catalytic reaction with hydrogen, helps in removing oxygen in the form of water, but is not

economical and energy efficient due to the high temperature and pressure employed. Steam reforming produces hydrogen which is a clean energy source but the process is complicated and requires high energy due to the high temperature employed (Xiu and Shahbazi, 2012).

1.9 Emulsification

Pyrolysis oil can be blended with diesel oil to utilize it as transportation fuel (Zhang et al., 2007). Since pyrolysis oil is not miscible with hydrocarbon fuels, it can be emulsified with the aid of surfactants (Oasmaa and Czernik, 1999). CANMET Energy Technology Center developed a process to produce a s microemulsion containing 5-30 % pyrolysis oil in diesel fuel (Oasmaa and Czernik, 1999). While emulsification does not involve chemical transformation, the process requires significant energy and therefore has a high cost. Pyrolysis oil might also be corrosive to engine and related assemblies (Zhang et al., 2007).

1.10 Economics

A way to estimate the capital cost for a pyrolysis plant and the production cost of for the pyrolysis oil has been proposed by Bridgwater et al. (Bridgwater, 2012b).

$$Capital\ cost, euros\ million\ 2011 = 6.98 \times (biomass\ feed\ rate, t/h)^{0.67} \quad \text{Eq. 1.1}$$

$$Production\ cost, t^{-1} pyrolysis\ oil_{2011} = 1.1 \times [(B) + (H \times 16{,}935 \times F^{-0.33})]Y^{-1} \quad \text{Eq. 1.2}$$

B = Biomass cost £ dry t^{-1}

H = Capital and capital related charges, default value = 0.18

F = Capital and capital related charges, default value = 0.18

Y = Fractional bio-oil yield, wt., default value = 0.75 for wood, 0.60 for grasses

Developing fast pyrolysis technologies at a commercial scale is still expensive when compared with fossil fuels. The properties of the oil require post-condensation processing or upgrading to make the oil usable as a stand-alone product, source of specialty chemicals, or as an extender for petroleum fuels. Therefore, economic and technical barriers still remain in order to allow for the commercially-viable production and use of pyrolysis oil (Anex et al., 2010; Bridgwater, 2012b).

1.11 References

Agblevor, F.A., and Besler, S. (1996). Inorganic Compounds in Biomass Feedstocks. 1. Effect on the Quality of Fast Pyrolysis Oils. Energy Fuels 10, 293–298.

Agblevor, F., Besler, S., Montane, D., and Evans, R. (1995). Influence of inorganic-compounds on char formation and quality of fast pyrolysis oils. (Amer chemical soc PO box 57136, Washington, DC 20037-0136), p. 8 – cell.

Akhtar, J., and Saidina Amin, N. (2012). A review on operating parameters for optimum liquid oil yield in biomass pyrolysis. Renew. Sustain. Energy Rev. 16, 5101–5109.

Alén, R., Kuoppala, E., and Oesch, P. (1996). Formation of the main degradation compound groups from wood and its components during pyrolysis. J. Anal. Appl. Pyrolysis 36, 137–148.

Anex, R.P., Aden, A., Kazi, F.K., Fortman, J., Swanson, R.M., Wright, M.M., Satrio, J.A., Brown, R.C., Daugaard, D.E., Platon, A., et al. (2010). Techno-economic comparison of biomass-to-transportation fuels via pyrolysis, gasification, and biochemical pathways. Techno-Econ. Comp. Biomass--Biofuels Pathw. 89, Supplement 1, S29–S35.

Aubin, H., and Roy, C. (1990). Study on the corrosiveness op wood pyrolysis oils. Pet. Sci. Technol. 8, 77–86.

Ba, T., Chaala, A., Garcia-Perez, M., and Roy, C. (2003). Colloidal Properties of Bio-Oils Obtained by Vacuum Pyrolysis of Softwood Bark. Storage Stability. Energy Fuels 18, 188–201.

Ba, T., Chaala, A., Garcia-Perez, M., Rodrigue, D., and Roy, C. (2004). Colloidal Properties of Bio-oils Obtained by Vacuum Pyrolysis of Softwood Bark. Characterization of Water-Soluble and Water-Insoluble Fractions. Energy Fuels 18, 704–712.

Biofuels Digest. (2013). Ineos Bio produces cellulosic ethanol from waste, at commercial scale. http://www.biofuelsdigest.com/bdigest/2013/08/01/ineos-bioproduces-Cellulosic-ethanol-from-waste-at-commercial-scale.

Boucher, M.., Chaala, A., and Roy, C. (2000). Bio-oils obtained by vacuum pyrolysis of softwood bark as a liquid fuel for gas turbines. Part I: Properties of bio-oil and its blends with methanol and a pyrolytic aqueous phase. Biomass Bioenergy 19, 337–350.

BP. BP Statistical Reviewof World Energy June 2014. http://www.bp.com/en/global/corporate/about-bp/energy-economics/statistical-review-of-world-energy.html. accessed September 12, 2014.

Bridgwater, A.. (2003). Renewable fuels and chemicals by thermal processing of biomass. Chemreactor - 15 SI 91, 87–102.

Bridgwater, A. (2007). The production of biofuels and renewable chemicals by fast pyrolysis of biomass. Int. J. Glob. Energy Issues 27, 160–203.

Bridgwater, A.V. (1999). Principles and practice of biomass fast pyrolysis processes for liquids. J. Anal. Appl. Pyrolysis 51, 3–22.

Bridgwater, A.V. (2012a). Upgrading biomass fast pyrolysis liquids. Environ. Prog. Sustain. Energy 31, 261–268.

Bridgwater, A.V. (2012b). Review of fast pyrolysis of biomass and product upgrading. Overcoming Barriers Bioenergy Outcomes Bioenergy Netw. Excell. 2003 – 2009 38, 68–94.

Bridgwater, A.V., and Grassi, G. (1991). Biomass pyrolysis liquids: upgrading and utilisation (Springer).

Bridgwater, A.V., Meier, D., and Radlein, D. (1999). An overview of fast pyrolysis of biomass. Org. Geochem. 30, 1479–1493.

Carpenter, N.E. (2014). Chemistry of Sustainable Energy (CRC Press).
Chevron. "Energy Supply and Demand." May 2014. http://www.chevron.com/globalissues/energysupplydemand, accessed September 12, 2014.

Cornelissen, T., Yperman, J., Reggers, G., Schreurs, S., and Carleer, R. (2008). Flash co-pyrolysis of biomass with polylactic acid. Part 1: Influence on bio-oil yield and heating value. Fuel 87, 1031–1041.

Czernik, S., and Bridgwater, A.V. (2004). Overview of Applications of Biomass Fast Pyrolysis Oil. Energy Fuels 18, 590–598.

Czernik, S., Johnson, D.K., and Black, S. (1994). Stability of wood fast pyrolysis oil. Biomass Bioenergy 7, 187–192.

Damartzis, T., and Zabaniotou, A. (2011). Thermochemical conversion of biomass to second generation biofuels through integrated process design—A review. Renew. Sustain. Energy Rev. 15, 366–378.

Demirbaş, A. (2001). Biomass resource facilities and biomass conversion processing for fuels and chemicals. Energy Convers. Manag. 42, 1357–1378.

Diebold, J.P. (1999). A review of the toxicity of biomass pyrolysis liquids formed at low temperatures. Fast Pyrolysis Biomass Handb. 1, 135–163.

Diebold, J.P. (2000). A review of the chemical and physical mechanisms of the storage stability of fast pyrolysis bio-oils (National Renewable Energy Laboratory Golden, CO).

Diebold, J.P., and Czernik, S. (1997). Additives To Lower and Stabilize the Viscosity of Pyrolysis Oils during Storage. Energy Fuels 11, 1081–1091.

Elliott, D.C. (1994). Water, alkali and char in flash pyrolysis oils. Biomass Bioenergy 7, 179–185.

Elliott, D.C., Oasmaa, A., Preto, F., Meier, D., and Bridgwater, A.V. (2012). Results of the IEA Round Robin on Viscosity and Stability of Fast Pyrolysis Bio-oils. Energy Fuels 26, 3769–3776.

Energy Information Administration (EIA). (2013). International Energy Outlook 2013. Washington, DC: US Department of Energy.

European Biomass Association (AEBIOM). AEBIOM statement. Biomass delivers climate change benefits. November 5, 2012. http://www.biomassenergycentre.org.uk/, accessed September 10, 2014.

ExxonnMobil. The Outlook for Energy: A View to 2040. 2014. http://www.exxonmobil.com/energyoutlook, accessed September 12, 2014.

Garcìa-Pérez, M., Chaala, A., Pakdel, H., Kretschmer, D., Rodrigue, D., and Roy, C. (2005). Multiphase Structure of Bio-oils. Energy Fuels 20, 364–375.

Garcìa-Pérez, M., Chaala, A., Pakdel, H., Kretschmer, D., Rodrigue, D., and Roy, C. (2005). Multiphase Structure of Bio-oils. Energy Fuels 20, 364–375.

Garcìa-Pérez, M., Chaala, A., Pakdel, H., Kretschmer, D., and Roy, C. (2007). Vacuum pyrolysis of softwood and hardwood biomass: Comparison between product yields and bio-oil properties. J. Anal. Appl. Pyrolysis 78, 104–116.

Gomez, L.D., Steele-King, C.G., and McQueen-Mason, S.J. (2008). Sustainable liquid biofuels from biomass: the writing's on the walls. New Phytol. 178, 473–485.

Gratson, D. (1994). Results of toxicological testing of whole wood oils derived from the fast pyrolysis of biomass. pp. 203–211.

Hilten, R.N., and Das, K.C. (2010). Comparison of three accelerated aging procedures to assess bio-oil stability. Fuel 89, 2741–2749.

Hoekstra, E., Hogendoorn, K.J.A., Wang, X., Westerhof, R.J.M., Kersten, S.R.A., van Swaaij, W.P.M., and Groeneveld, M.J. (2009). Fast Pyrolysis of Biomass in a Fluidized Bed Reactor: In Situ Filtering of the Vapors. Ind. Eng. Chem. Res. 48, 4744–4756.

Ingram, L., Mohan, D., Bricka, M., Steele, P., Strobel, D., Crocker, D., Mitchell, B., Mohammad, J., Cantrell, K., and Pittman, C.U. (2007). Pyrolysis of Wood and Bark in an Auger Reactor: Physical Properties and Chemical Analysis of the Produced Bio-oils. Energy Fuels 22, 614–625.

International energy Agency (IEA). Executive summary, Resources to Reserves 2013. http://www.iea.org/Textbase/npsum/resources2013SUM.pdf, accessed September 8, 2014.

Jahirul, M.I., Rasul, M.G., Chowdhury, A.A., and Ashwath, N. (2012). Biofuels production through biomass pyrolysis—a technological review. Energies 5, 4952–5001.

Jay, D.C., Rantanen, O., Sipilä, K., and Nylund, N. (1995). Wood pyrolysis oil for diesel engines. pp. 24–27.

Klass, D.L. (1998). Biomass for renewable energy, fuels, and chemicals (Academic press).

Küçük, M.M., and Demirbaş, A. (1997). Biomass conversion processes. Energy Convers. Manag. 38, 151–165.

LaClaire, C., Barrett, C., and Hall, K. (2004). Technical, environmental and economic feasibility of bio-oil in new hampshire's north country. Durh. NH Univ. N. H.

Lu, Q., Li, W.-Z., and Zhu, X.-F. (2009). Overview of fuel properties of biomass fast pyrolysis oils. Energy Convers. Manag. 50, 1376–1383.

McKendry, P. (2002a). Energy production from biomass (part 1): overview of biomass. Rev. Issue 83, 37–46.

McKendry, P. (2002b). Energy production from biomass (part 2): conversion technologies. Rev. Issue 83, 47–54.

McKendry, P. (2002c). Energy production from biomass (part 1): overview of biomass. Rev. Issue 83, 37–46.

McKendry, P. (2002d). Energy production from biomass (part 2): conversion technologies. Rev. Issue 83, 47–54.

Milne, T., Agblevor, F., Davis, M., Deutch, S., and Johnson, D. (1997). A review of the chemical composition of fast-pyrolysis oils from biomass. In Developments in Thermochemical Biomass Conversion, (Springer), pp. 409–424.

Naik, S.N., Goud, V.V., Rout, P.K., and Dalai, A.K. (2010). Production of first and second generation biofuels: A comprehensive review. Renew. Sustain. Energy Rev. 14, 578–597.

Naske, C.D., Polk, P., Wynne, P.Z., Speed, J., Holmes, W.E., and Walters, K.B. (2011). Postcondensation Filtration of Pine and Cottonwood Pyrolysis Oil and Impacts on Accelerated Aging Reactions. Energy Fuels 26, 1284–1297.

Nigam, P.S., and Singh, A. (2011). Production of liquid biofuels from renewable resources. Prog. Energy Combust. Sci. 37, 52–68.

Oasmaa, A., and Czernik, S. (1999). Fuel Oil Quality of Biomass Pyrolysis OilsState of the Art for the End Users. Energy Fuels 13, 914–921.

Oasmaa, A., and Kuoppala, E. (2003). Fast Pyrolysis of Forestry Residue. 3. Storage Stability of Liquid Fuel. Energy Fuels 17, 1075–1084.

Oasmaa, A., and Peacocke, C. (2001). A guide to physical property characterisation of biomass-derived fast pyrolysis liquids (Technical Research Centre of Finland Espoo).

Oasmaa, A., and Peacocke, C. (2010). Properties and fuel use of biomass-derived fast pyrolysis liquids. VTT Finl.

Oasmaa, A., Kuoppala, E., Gust, S., and Solantausta, Y. (2002). Fast Pyrolysis of Forestry Residue. 1. Effect of Extractives on Phase Separation of Pyrolysis Liquids. Energy Fuels 17, 1–12.

Oasmaa, A., Kuoppala, E., and Solantausta, Y. (2003). Fast Pyrolysis of Forestry Residue. 2. Physicochemical Composition of Product Liquid. Energy Fuels 17, 433–443.

Oasmaa, A., Kuoppala, E., Selin, J.-F., Gust, S., and Solantausta, Y. (2004). Fast Pyrolysis of Forestry Residue and Pine. 4. Improvement of the Product Quality by Solvent Addition. Energy Fuels 18, 1578–1583.

Office of the Biomass Program, Energy Efficiency and Renewable Energy (EERE). Multi-year program plan (2013). US Department of Energy, May 2013. www1.eere.energy.gov/biomass/pdfs/mypp.pdf, accessed October 12, 2014).

Pettersen, R.C. (1984). The chemical composition of wood. Chem. Solid Wood 207, 57–126.

Scholze, B., and Meier, D. (2001). Characterization of the water-insoluble fraction from pyrolysis oil (pyrolytic lignin). Part I. PY–GC/MS, FTIR, and functional groups. J. Anal. Appl. Pyrolysis 60, 41–54.

Solantausta, Y., Beckman, D., Bridgwater, A., Diebold, J., and Elliott, D. (1992). Assessment of liquefaction and pyrolysis systems. Biomass Bioenergy 2, 279–297.

The International council on clean transporation (icct). Measuring and addressing Investment risk in the secondgeneration, December 2013. http://www.theicct.org, accessed September 12, 2014.

Wang, G., Li, W., Li, B., and Chen, H. (2008). TG study on pyrolysis of biomass and its three components under syngas. 9th China–Japan Symp. Coal C1 Chem. 87, 552–558.

Xiu, S., and Shahbazi, A. (2012). Bio-oil production and upgrading research: A review. Renew. Sustain. Energy Rev. 16, 4406–4414.

Yaman, S. (2004). Pyrolysis of biomass to produce fuels and chemical feedstocks. Energy Convers. Manag. 45, 651–671.

Yang, H., Yan, R., Chen, H., Lee, D.H., and Zheng, C. (2007). Characteristics of hemicellulose, cellulose and lignin pyrolysis. Fuel 86, 1781–1788.

Zhang, Q., Chang, J., Wang, T., and Xu, Y. (2007). Review of biomass pyrolysis oil properties and upgrading research. Energy Convers. Manag. 48, 87–92.

Zhang, S., Yan, Y., Li, T., and Ren, Z. (2005). Upgrading of liquid fuel from the pyrolysis of biomass. Bioresour. Technol. 96, 545–550.

CHAPTER II

IMPACTS OF FEEDSTOCK BARK ADDITION ON PYROLYSIS OIL PROPERTIES AND STORAGE STABILITY

2.1 Introduction

In U.S, the energy production and consumption for 2013 was 82 and 98 quadrillion Btu, respectively (EIA, 2013), with the trend of energy consumption surpassing production not likely to change in the near future. The gap between production and consumption is rising due to increases in population and demand. Increased demand drives the necessity to find and utilize new and multiple energy options. The fast depletion of fossil fuel and resultant increases in fuel costs are driving interest in renewable energy resources. There is also a strong societal desire for environmentally-friendly fuels, due to concern for protecting the environment from the effects of toxic emissions and greenhouse gases. Out of the available alternative energy resources, in the southeastern U.S biomass is a major contributor due to the opportunity for localized energy production. Biomass energy production in US was 5 quadrillion Btu in 2013 (EIA, 2013), which makes it a leader in renewable energy production. One major advantage of utilizing biomass for energy production is that it does not build up CO2 in the atmosphere as it has a closed carbon cycle (McKendry, 2002c).

Biomass is a generic term for organic matter derived from living organisms; generally in energy production, plant and plant derived materials are the dominant

sources (Biomass Energy Center, 2012). Biomass falls into five basic categories, virgin wood, energy crops, agricultural residue, food waste, industrial waste & co-products (Biomass Energy Center, 2012), with virgin wood is the primary source (EIA, 2013). The components of any wood resource include cellulose, hemicellulose, lignin and extractives in varying amounts. Woody plant species have high proportions of lignin indicated by the tightly bound fibers that provide a hard external surface. The relative proportions of cellulose and lignin plays a major role in the suitability of the biomass as an energy source (McKendry, 2002c).

To utilize biomass as energy, different methods, such as thermochemical, biochemical and mechanical extraction with esterification (McKendry, 2002b) can be used. Some factors that influence the choice of method include biomass type, end use, and economic conditions (McKendry, 2002b). Thermochemical is a suitable technique for converting woody biomass to fuel, as the conversion of lignocellulosic biomass using the other methods is more complex due to the presence of longer chain polysaccharide molecules. Pyrolysis is one of the thermochemical conversion methods available; it is more efficient in terms of conversion when compared with combustion and in terms of economy when compared with liquefaction (McKendry, 2002d). Fast pyrolysis at high temperatures, high heating rates, and short residence times is much preferred as it produces higher yields and minimizes secondary reactions (Bridgwater, 1999). The condensable liquid from pyrolysis to be used as fuel is known as pyrolysis oil, bio-oil or bio-crude.

Pyrolysis oil is a complex mixture of organics, inorganics, water and solid char; more than 400 organic compounds are present (Diebold, 2000). As the pyrolysis

involves many mechanisms, such as dehydration, charring, decomposition and volatilization, the properties of the products obtained are very much influenced by the biomass type, type of reactor, and processing parameters (Akhtar and Saidina Amin, 2012). Even the varying only the parts of the same tree used as feedstock will affect the pyrolysis oil properties, as each tree part contains cellulose, hemicellulose, lignin and extractives in different proportions. The bark portion of the tree is rich in lignin derivatives and extractives. Lignin is a three dimensional polymer network and extractives includes fatty acids, fatty alcohols, terpenes, resin acids, and terpenoids (Oasmaa et al., 2003). Lower liquid yields have been observed with feedstocks containing bark, as compared to bark free (or clear) wood (Oasmaa et al., 2003). This is partially due to the higher levels of volatiles present in bark (Oasmaa et al., 2003). In bark, there are 4-5 times more extractives present versus bark-free wood which is mainly composed of high-molecular weight polyphenols and suberine. In pyrolysis oil derived from bark, the low oxygen content extractives can separate from the polar matrix resulting in a two phase product. In addition, the lignin present in the bark leads to char residue due to the higher temperatures required for its decomposition, as compared to cellulose and hemicellulose, which contributes to its structural stability (Akhtar and Saidina Amin, 2012).

Pyrolysis oil has drawbacks related to its usage as a fuel. Corrosion, fouling, low heating value, and storage instability have been observed for pyrolysis oil irrespective of the biomass type and process parameters utilized in its production. As pyrolysis involves the partial decomposition of biomass, the resultant products tend to move towards thermal, mechanical, radiative and chemical equilibrium through one or more chemical

mechanisms, with most of these mechanisms unknown (Diebold, 2000). Many probable mechanisms have been well explained by Diebold (Diebold, 2000). During storage, the pyrolysis oil undergoes oxidative and thermal degradation leading to polymerization and volatilization. Both of these processes eventually result in increased viscosity (Hilten and Das, 2010). Additionally, increases in water content, phase separation, and particle growth have also been observed; these changes during storage or elevated temperature conditions are commonly referred to as 'aging'. These physical and chemical changes interfere with upgrading processes needed to improve the products quality to be usable as a fuel. In addition, aging is accelerated at higher temperatures which create problems when the pyrolysis oil is preheated for atomization for use as a fuel oil. Aging rates and properties changes vary considerably based on the initial properties of the oil. The char and inorganic content present in the pyrolysis oil act as catalysts for the polymerization reactions (Diebold, 2000). Minerals present in the pyrolysis oil also catalyze some of the aging mechanisms, and these minerals are concentrated in the char (Diebold, 2000). An accelerated aging study is the quickest way of testing for time- and temperature-related physical and chemical changes in the properties of particular pyrolysis oil. It has been found that the viscosity increase observed for 24 h of 'aging' at 80 °C matches the viscosity increase when the pyrolysis oil is stored for 1 year at room temperature (Czernik et al., 1994). Results of a 'round robin' test in 2012 showed that the viscosity increase for the filtered bio-oil (<0.1% filterable solids) when aged at 80 °C for 24 h was similar to that of oil stored at room temperature for 6 months (Elliott et al., 2012). This indicates that the solids content plays a major role in the aging reactions.

Lumber manufacturing and papermaking process leaves bark as residue and it can be used as feedstock to produce pyrolysis oil; thereby competition with the timber industry can be avoided. Since the properties of pyrolysis oil vary with the type of feedstock used, the suitability of bark to produce better quality of pyrolysis oil can be studied. The objective of this study is to understand the change in physical and chemical properties of pyrolysis oil produced from the feedstock containing pine clear wood and pine bark, in varying proportions. Accelerated aging tests were also performed to understand the aging changes observed in relation to biomass type and solids content.

2.2 Methods and Materials

2.2.1 Feedstock composition

The biomass used as feedstock in this study was southern yellow pine (*Pinus palustris*, *Pinus elliottii*, *Pinus echinata*, and/or *Pinus taeda*) collected by Southern Timber Products (Ackerman, MS). The pine was collected from a planer and had ~ 16% moisture content as determined by OHAUS moisture analyzer. The material was screened to a particle range of 0.5 mm to 4 mm using a vibrating screen (Universal Vibrator Screen) and then dried in an oven (JPW Design & Mfg., Inc.) at 212 °F to final moisture contents ranging from 1.4 to 4.0 wt%. Different ratios of pine clear wood (CW) and pine bark (B) prepared in the manner described above were mixed and utilized as feedstock for producing pyrolysis oil. The CW/B ratios utilized in terms of weight percentage were: 100/0; 80/20; 60/40, and 50/50.

2.2.2 Pyrolysis and sample collection

Pyrolysis oil used for this study was produced using a lab scale auger reactor at MSU's Forest Products Laboratory. The auger reactor processes the biomass at around 7 kg/h. The reactor is constructed from a pipe that is 3" in diameter and 40" in length with 18" heated. Heat is provided by 5 ceramic band heaters on the outside of the pipe and an internal heater inside the auger pipe. The feedstock drops into the reactor pipe through a rotary airlock valve which along with a nitrogen purge keeps oxygen from entering the reactor and process gases from exiting. The biomass is then fed through the heated zone by an auger (~ 4.5 rpm). The residence time of the biomass in the heated zone (450 °C) is ~1 min. Char drops out of the reactor into a sealed collection vessel and process gases (420 °C) are sent to the condensers for pyrolysis oil production. Multiple condensers in series are utilized at ~20 °C to condense the hot gases to oil. Samples can be collected from one or more of the condensers, if desired. For this study, samples were collected as Total (from all the condensers), Fractionate I (excludes product from one condenser with high water content), and Fractionate II (product from condenser with high water content). All the collected samples were placed in a refrigerator (5 °C) to minimize the aging effects prior to analysis.

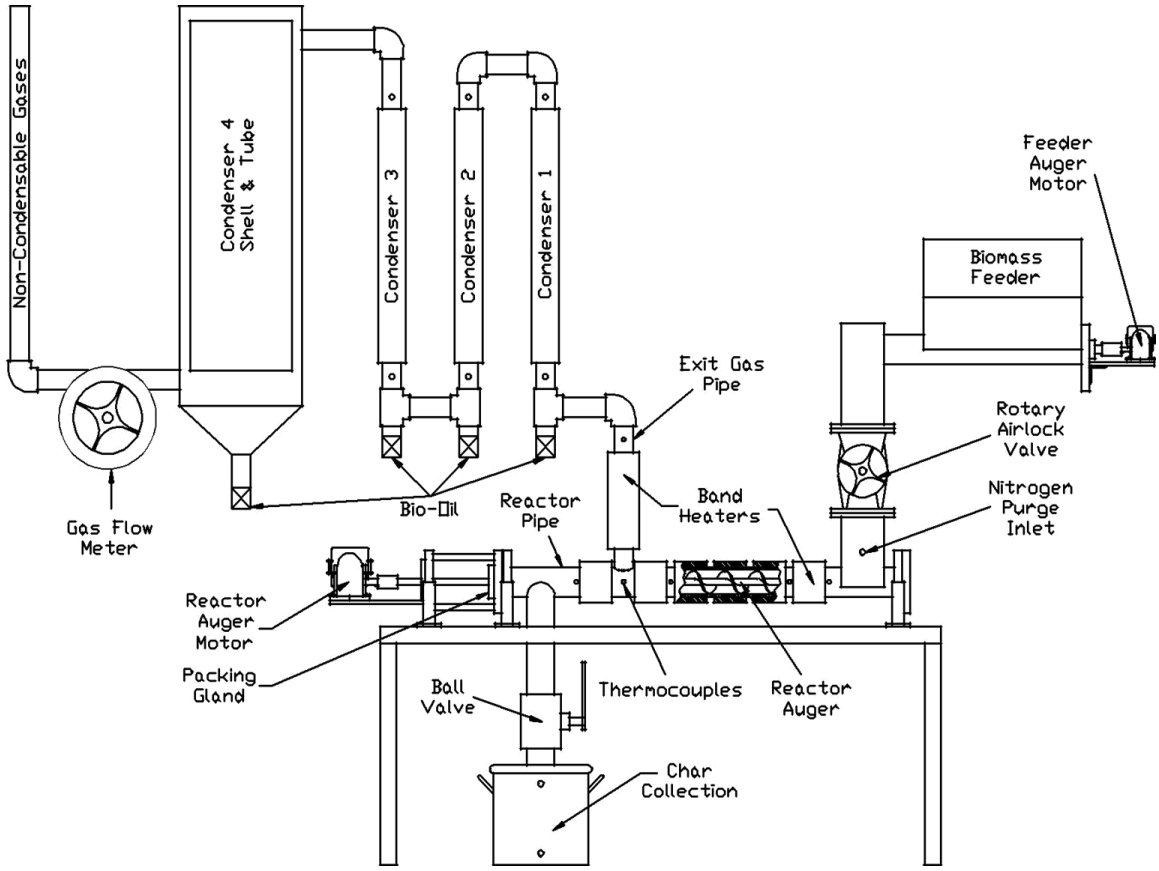

Figure 2.1 Schematic of the lab-scale pyrolysis reactor and condensers (Li et al., 2013)

2.2.3 Filtration

Serial filtration was performed using stainless steel (SS) wire mesh filters and Whatman filter papers. The pore sizes of the filters are as follows: SS wire mesh, 1184 μm; SS wire mesh, 84 μm; Whatman grade 41 filter paper, 20-25 μm; Whatman grade 40 filter paper, 8 μm; Whatman grade 5 filter paper, 2.5 μm. Filtration under vacuum was performed when filter papers were used.

2.2.4 Accelerated aging conditions

For the aging test, 30 mL amber jars were charged with 27 mL sample. This sample volume was chosen based on previous studies to allow enough head space for gas evolution without excessive pressure developing in the jars. The aging temperature was 80 °C, which is the most common temperature used in pyrolysis oil aging studies in the literature (Oasmaa et al. 1997). Aging times were 6, 24, and 48 h which would give viscosity changes in the filtered pyrolysis oil equivalent to aging at room temperature for 3 months, 6 months and 1 year, respectively (Oasmaa et al. 1997). Note that for unfiltered pyrolysis oil, these aging times must be doubled (Elliott et al., 2012). A convection oven was used to heat/age the samples and frequent retightening of the vial caps is necessary to minimize sample loss, as the test should be repeated if the net weight loss is above 0.1 wt% of the initial weight (Oasmaa et al. 1997). To determine sample loss during aging, initial and final weights of the sample vials were measured. Sample loss was found to be less than 0.1 wt%. Triplicates were prepared for each sample per aging time.

2.2.5 Characterization methods

2.2.5.1 Ultimate analysis

An Exeter Analytical Inc. CE-440 Elemental Analyzer was used to determine carbon, hydrogen and nitrogen content in the pyrolysis oil following ASTM D5291 method. Helium was used as carrier and purging gas.

2.2.5.2 pH

To measure pyrolysis oil pH, a Mettler Toledo SevenEasy S20 pH meter was used. Buffer solutions of pH 2, 4, 7, 10, and 12 were used to calibrate the meter. Three measurements were taken for each sample to obtain average pH values and 95% confidence interval (CI).

2.2.5.3 Density

A known volume of the oil was weighed and density was calculated.

2.2.5.4 Water content

Water content was determined using Mettler Toledo's EasyPlus^{TM} KFV titrator following ASTM 203-01 method. Hydranal 5E titrant and Hydranal Chloroform-Methanol (CM) solvent were used. Three measurements were taken to obtain the average and 95% confidence interval (CI).

2.2.5.5 Solids content

Solids content in the pyrolysis oil were measured as weight percentage of Methanol Insoluble Materials (MIM wt%). Sample size of 1-3 mg was used for the solvent amount of 100 mL. The solution was filtered through the 1μm Whatman filter paper. The filter was then weighed after drying and the solid content was calculated based on the weight on the sample used initially.

2.2.5.6 Viscosity

Dynamic viscosity was measured using Brookfield DVI viscometer for all the unfiltered, unaged samples. Spindles were chosen (S61/S62) based on the sample. To measure the dynamic viscosity of the filtered unaged and aged samples, TA instruments

AR 1000N rheometer was used. Step flow shear test was conducted using 60 mm aluminum parallel plate accessory. All measurements were taken over the shear rate range of 0.1 - 1000 s^{-1} with 10 points per decade at 40 °C. The gap distance was chosen based on the viscosity of the sample. Rheology advantage data analysis software (version 5.7.0) was used for data collection.

2.2.5.7 FTIR spectroscopy

Attenuated Total reflectance (ATR) FTIR spectroscopy was used for the identification of the functional groups present in the pyrolysis oil. The spectra were collected using Nicolet 6700 spectrometer with MIRacle accessory containing diamond-ZnSe crystal. DTGS detector was used with 4 cm-1 resolution and 256 scans. Thermo Electron Omnic software (version 8.2) was used for spectra collection and analysis. A minimum of three spectra were collected for each sample and all spectra were ATR corrected prior to analysis.

2.2.5.8 Particle size distribution

An Olympus BX 51 optical microscope was used to collect the images of the pyrolysis oil by smearing the sample on the slide. Images were collected at 10X and 20X magnifications. ImageJ software (version 1.45s) was used for the analysis of particle size.

2.3 Results and Discussion

2.3.1 Physical appearance and phase separation

The pyrolysis oil produced from 100/0 CW/B was mostly homogenous with solid particles dispersed throughout. All the samples produced from bark added feedstock had

high solids content with larger size particles. Unique phase separation was observed in the 50/50 CW/B samples. The non-fractionated sample (Total) had a layer of solids content settled at the bottom. Particles precipitated quickly in the high water content sample, and the particles may be lignin-derived materials (Ba et al., 2004). All of the Fractionate II samples produced from bark added feedstock had a less dense layer of sticky slimy layer at the top. The sticky layer seems to be the agglomeration of particles which are rich in waxy materials like fatty acids (Ba et al., 2003, 2004).

2.3.2 Property differences in Pyrolysis oil based on feedstock

Physico-chemical properties such as water content, solids content, pH, density, viscosity and chemical composition were measured and compared for the pyrolysis oil produced from different ratios of pine clear wood and pine bark were measured and compared. This study helped to understand the effects of utilizing bark in feedstock on the properties of pyrolysis oil. Yield and chemical composition were also measured.

2.3.2.1 Yield

Biomass composition plays a major role in the degree of decomposition and the composition of products during pyrolysis. The bark portion of the tree is rich in lignin derivatives and extractives. Pyrolysis of cellulose or hemicellulose produces more oil yield than lignin. Also lignin requires wider temperature range for decomposition. Lignin in the bark attributes to the decrease in liquid yield. Also decrease in oil yield was dependent on the amount of bark added. Decrease in yield was around 17 % when the clear wood was replaced by 50 % bark (wt%). The char content has increased with the

addition of bark as lignin in the biomass leads to the formation of char residue. Table 2.1 shows the data for the yield of oil and char from different feedstock.

Table 2.1 Yields (in wt%) of pyrolysis oil and char from different feedstock ratios of clear wood (CW) and bark (B): 100/0; 80/20; 60/40; 50/50 CW/B (wt%).

	Feedstock (CW/B wt%)			
	100/0	**80/20**	**60/40**	**50/50**
Oil (wt%)	58.3	51.7	43	41.2
Char (wt%)	23.7	25.7	29.1	30.9

2.3.2.2 Ultimate analysis of biomass, pyrolysis oil, and char

Elemental compositions of the biomass, char and pyrolysis oil are provided in Table 2.2. The elemental composition in the biomass differed only by ±2 % with the addition of bark. Fractionate-I samples had the highest carbon content and Fractionate-II samples had the lowest values when compared with non-fractionated (Total) samples. No trend was observed with the amount of bark added. However, elemental composition of the pyrolysis oil varied considerably with the amount of bark added in the feedstock. Carbon content in the non-fractionated pyrolysis oil decreased when the bark was added to the feedstock. The percentage increase/decrease was dependent on the amount of bark added. Around 13.5% decrease was observed for the non-fractionated oil when 50 wt% of clear wood feedstock was replaced by bark. Only small increase in the hydrogen content was observed in the non-fractionated pyrolysis oil with the addition of bark. No trend was seen for the nitrogen with the addition of bark. For the non-fractionated samples, the nitrogen content increased when 50 wt% bark was utilized in the feedstock, but it decreased with the addition of 20 and 40 wt% bark. The oxygen content

(calculated by difference) was observed to be increased with the bark addition. The high oxygen content is indicative of the presence of many highly polar groups leading to high viscosities and boiling points as well as relatively poor chemical stability (Bridgwater et al., 1999). The pyrolysis oil rich in polar groups will be immiscible with the non-polar petroleum fuels which will create problem while blending. Also the increase in oxygen will lead to the decrease in the energy density of the fuel.

Table 2.2 Elemental analysis of carbon, hydrogen, nitrogen and oxygen (by difference) of pyrolysis oil derived from different feedstock ratios of clear wood (CW) and bark (B): 100/0; 80/20; 60/40; 50/50 CW/B (wt%).

Biomass	**% C**	**% H**	**% N**	**% O**
100/0	49.00	6.49	0.37	44.13
80/20	50.59	6.25	0.41	42.75
60/40	50.15	6.13	0.50	43.22
50/50	51.05	6.05	0.44	42.45
Char	% C	% H	% N	% O
100/0	77.79	4.08	0.84	17.28
80/20	74.78	3.80	0.64	20.77
60/40	76.45	3.65	0.89	19.01
50/50	76.64	3.55	0.60	19.21
Non-fractionated (Total) Pyrolysis oil	**% C**	**% H**	**% N**	**% O**
100/0	41.41	8.06	0.48	50.05
80/20	34.83	8.23	0.25	56.69
60/40	30.14	8.32	0.32	61.22
50/50	27.98	8.44	0.85	62.73
Fractionate I	**% C**	**% H**	**% N**	**% O**
100/0	44.64	7.75	0.56	47.06
80/20	46.83	7.55	0.36	45.26
60/40	42.39	7.78	0.42	49.42
50/50	39.07	7.91	0.35	52.67
Fractionate II	**% C**	**% H**	**% N**	**% O**
100/0	31.90	8.86	0.40	58.84
80/20	21.58	9.50	0.25	68.87
60/40	24.72	9.26	0.33	65.68
50/50	34.83	8.36	0.15	56.67

2.3.2.3 Water content

Water content in pyrolysis oil plays a major role in the storage and utilization of pyrolysis oil. It was important to measure the water content of the pyrolysis oil produced from the different clear wood/ bark feedstock ratios. Pyrolysis oil water content increased with bark addition, and the water content increase was proportional to the bark wt% in the feedstock. This additional water in the condensed pyrolysis product is due to the high yield of reaction water resulting from the cracking of volatile vapors caused by higher concentration of alkali metals in bark (Oasmaa et al., 2002). Water contents varied from ~30-50 wt% for the non-fractionated samples. The increase was around 20 % when 50 wt% bark was added in the feedstock. All the Fractionate I samples had less water content compared to the non-fractionated sample as it excludes collection from the high water content condenser. The Fractionate II samples showed high water content as expected. Though the water content had increased, no phase separation of oil and water was observed. The water content data measured for all the samples are shown in Figure 2.2.

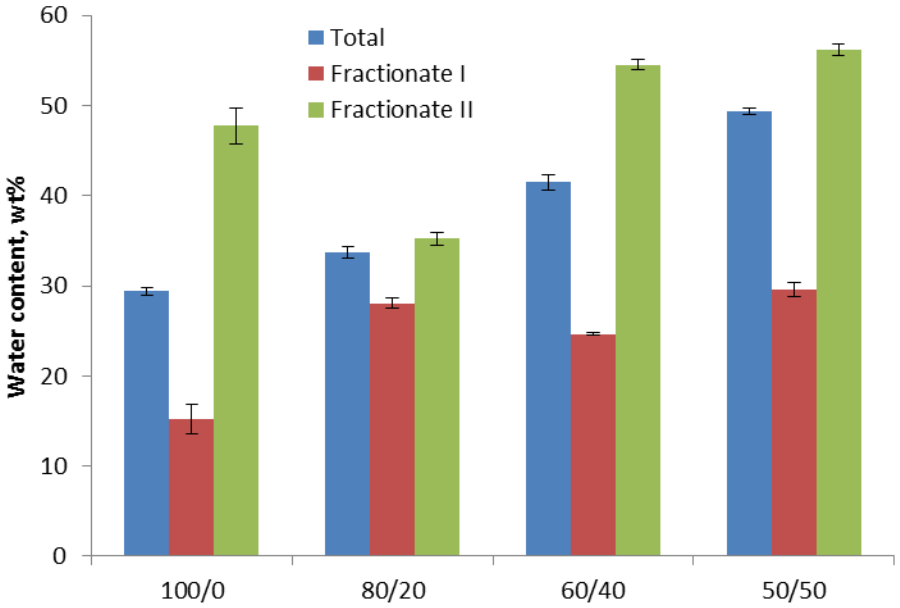

Figure 2.2 Average water content (wt%) of the pyrolysis oil derived from different ratios of clear wood (CW) and bark (B) feedstock: 100/0; 80/20; 60/40; 50/50 CW/B (wt%).

Error bars represent 95% confidence intervals.

2.3.2.4 Solids content

Solids contents measured as methanol insoluble materials (MIM, wt%) increased considerably when bark was used in the feedstock (Figure 2.3). The increase in solids content of the non-fractionated samples derived from 80/20 CW/B and 60/40 CW/B was 6X and 8X respectively compared with the sample derived from 100/0 CW/B. The additional precipitated solids may be derived from the high lignin content of the bark. But the solid content in the sample derived from 50/50 CW/B was only 5X higher than the 100/0 CW/B sample. This may be due to particulate matter in that sample apparently being more dense than in the other bark-containing samples, and so they settled out quickly even after vigorous shaking. This might have led to some error when representative MIM aliquots were collected for analysis.

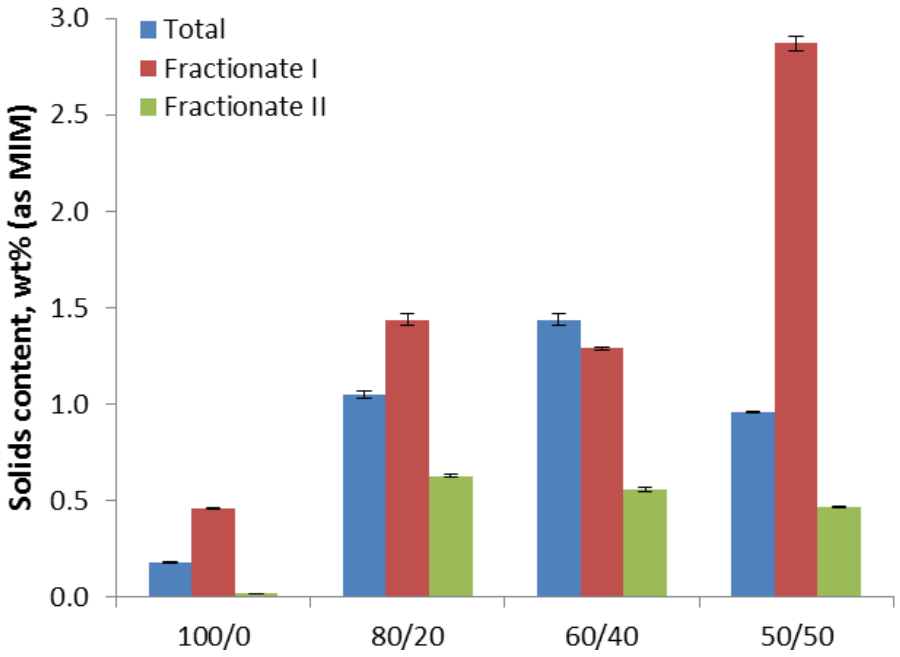

Figure 2.3 Average solids content (as MIM, wt%) of the pyrolysis oil derived from different ratios of clear wood (CW) and bark: 100/0; 80/20; 60/40; 50/50 CW/B (wt%).

Error bars represent 95% confidence intervals.

2.3.2.5 pH

All the pyrolysis oil samples were acidic (pH ~2.5) irrespective of the feedstock and collection method (Figure 2.4). Increases in pH were observed for all the samples produced from bark feedstock, in comparison to the oil produced from 100/0 CW/B. It is justified by the increase in water content and decrease in the carbonyl groups related to carboxylic acid (1708-1716 cm^{-1}) observed from FTIR. All the Fractionate II samples had higher pH compared to the non-fractionated samples as expected due to the high water content. Although a trend of increasing pH was observed in all fractions as the wt% of bark used in the feedstock increased, there was no statistical difference in the pH of the total pyrolysis oil samples irrespective of bark weight % used in the feedstock. For the fractionated samples, the pH was significantly higher for the bark-derived pyrolysis oils.

Since acidic catalysis of pyrolysis oil can lead to esterification (Diebold, 2000), the increased pH of the bark-derived pyrolysis oil may retard chemical changes during aging

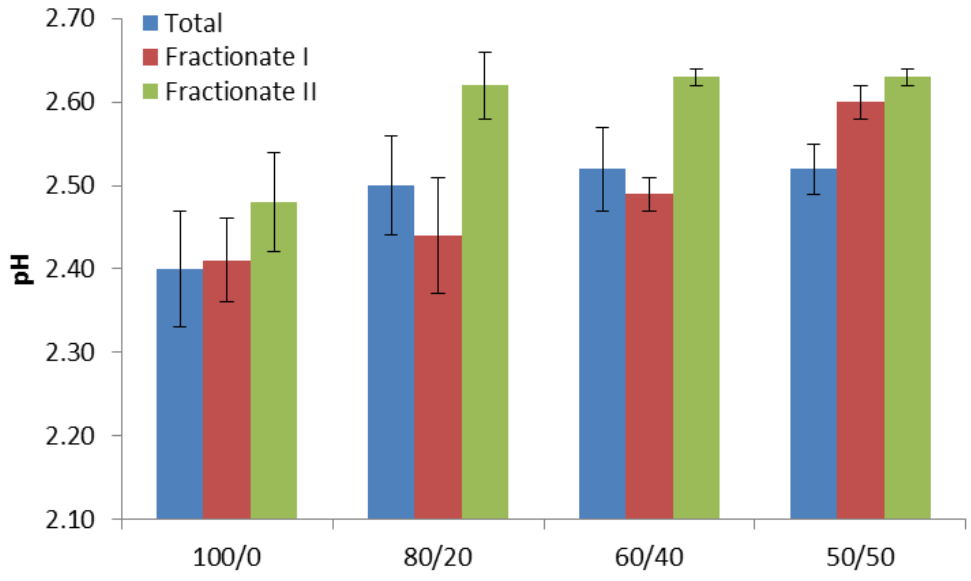

Figure 2.4 Average pH values of the pyrolysis oil derived from different ratios of clear wood (CW) and bark: 100/0; 80/20; 60/40; 50/50 CW/B (wt%).

Error bars represent 95% confidence intervals.

2.3.2.6 Density

The densities for all the samples were ranging from 1 to 1.3 g/mL (Figure 2.5). The variability in the data was high for the non-fractionated oil which is due to the larger particle size or the separation of solid and liquid phase leading to the error in taking representative samples for the measurement. The density was slightly higher for all the samples produced from the bark added feedstock compared to the oil produced from 100/0 CW/B. No trend was observed with the amount of bark added. The density for the Fractionate II samples were slightly lower than the non-fractionated samples due to the high water content and change in the chemical composition. Density for the Fractionate I

samples were slightly higher than Fractionate II and non-fractionated samples as expected.

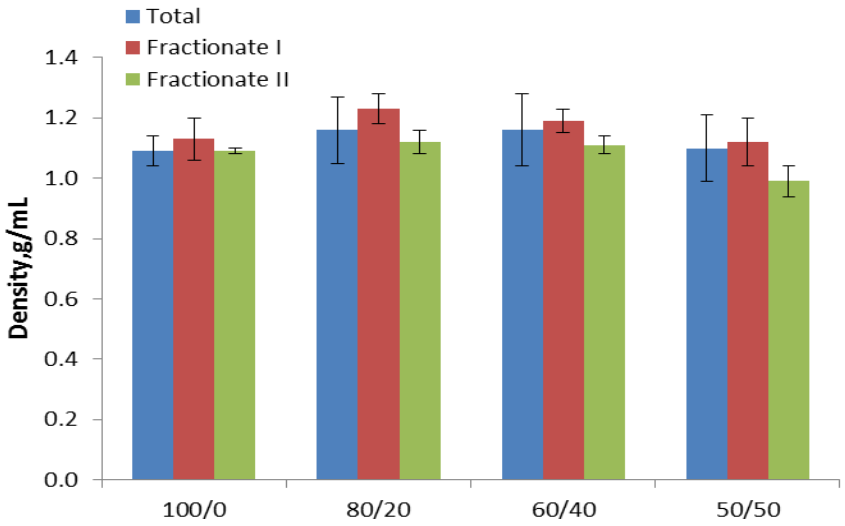

Figure 2.5 Average density values of the pyrolysis oil derived from different ratios of clear wood (CW) and bark: 100/0; 80/20; 60/40; 50/50 CW/B (wt%). Error bars represent 95% confidence intervals.

2.3.2.7 Viscosity

Dynamic viscosity measured using viscometer was observed to be increased for the pyrolysis oil produced from 80/20 CW/B and 60/40 CW/B compared to the sample derived 100/0 CW/B. Increase in solids content seems to the reason for the viscosity increase. But the sample produced from 50/50 CW/B exhibited less viscosity which is possibly due to the quick settling of solids. All the Fractionate I samples were more viscous compared with non-fractionated samples which correlates well with the decrease in water content in Fractionate I samples. Fractionate II samples exhibited low viscosity in all the cases. All the samples with high solids content exhibited high viscosity due to the presence of heavy weight aromatics in the solids.

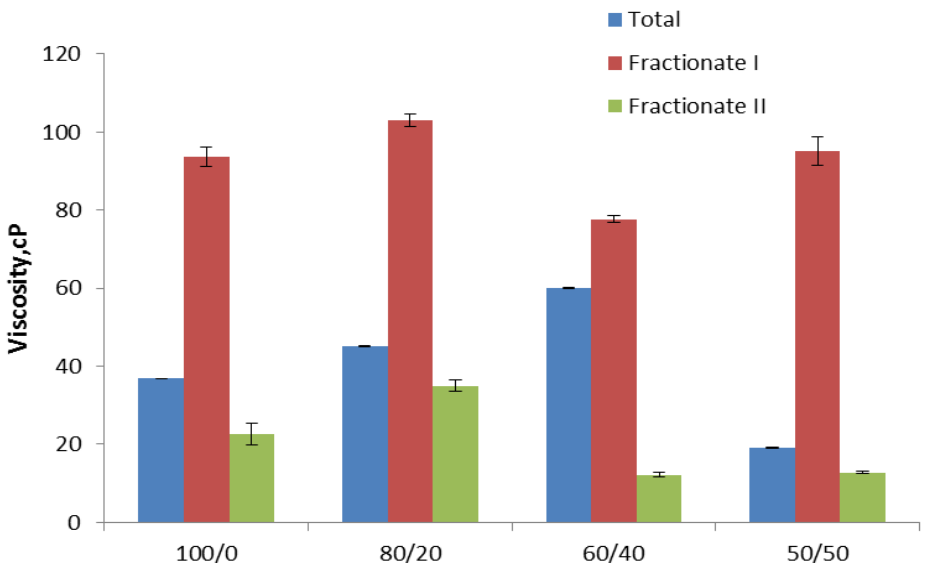

Figure 2.6 Average viscosity values of the pyrolysis oil derived from different ratios of clear wood (CW) and bark: 100/0; 80/20; 60/40; 50/50 CW/B (wt%).

Error bars represent 95% confidence intervals.

2.3.2.8 FTIR spectroscopy

ATR-FTIR spectroscopy was performed to identify any change in chemical composition. Most of the peaks were identified at the same frequency range for all the fractionated and non-fractionated samples.

2.3.2.8.1 Peak identification

The functional groups in the pyrolysis oil samples were identified from the peaks observed and they are summarized in Figure 2.3. The peak identified in the absorbance range of 3370-3415 cm-1 is due to the stretching of O-H bond indicates the presence of alcohols, phenols and water. The presence of alkanes is shown by the peak around 2930 cm-1 which is due to the asymmetric stretching of C-H bond and vibration of aliphatic C-H2 and C-H3 bonds. A consistent peak in the absorbance range of 1708-1715 cm-1 was observed in all the samples which is due to the stretching of C=O bonds of carbonyl

groups and it indicates the presence of aliphatic ketones, conjugated aldehydes and alpha-beta unsaturated and benzoate esters. A peak was identified at around 1650 cm-1 which might have caused by C=C symmetrical stretching of unconjugated linear alkenes and C=O stretching of amides or intramolecular hydrogen bonded carboxylic acid. The absorbance peak at 1515 cm-1 caused by C=C-C (ring stretching) or N=O (stretching) indicates the presence of aromatics and aromatic nitrogen-containing compounds. A peak was observed at 1463 cm-1 for all pyrolysis oil produced from the bark containing feedstocks, which corresponds to the asymmetric C-H bending of alkanes. The absorbance peak at 1366 cm-1 is due to the symmetric deformation of C-H in methyl groups. A peak was observed at 1271-1274 cm-1 which is due to the asymmetric stretch of C-O bond in alkyl aryl ethers. Peaks were observed at 1153 cm-1 and 1123 cm-1 are due to deformation vibrations of C-H bonds in benzene rings and aromatic in plane C-H bending respectively. The absorbance peak at 1123 cm-1 may also be due to the stretching of C-O bond and it indicates the presence of unsaturated and cyclic tertiary alcohols. The absorbance peak found at 1052 cm-1 could correspond to the rocking vibration of C-H3 bond or C-N stretching vibrations or stretching of C-O bond indicating the presence of aromatics or aliphatic amines or primary alcohols respectively. A peak was absorbed at 1035 cm-1 due to deformation vibrations of C-H bond in aromatic rings. Peaks were observed in the broad absorbance range of 775-570 cm-1 due to the stretching of C-Cl and a C-Br bond indicates the presence of alkyl halides. Two peaks observed around 1500 cm-1 and 1370 cm-1 together indicates the presence of aryl nitro compounds.

Table 2.3 Identification of peaks from FTIR spectra and corresponding functional groups.

Peak Wavenumber (cm^{-1})	Functional Groups	Compound Class(es)	References
3390-3412	O-H (stretching)	Phenols, Alcohols, Water	Pretsch, Nakanishi
	N-H/N-H_2(stretching)	Amines, Amides, Imines	www.science-and-fun.de
2927-2938	C-H,C-H_2,C-H_3 (stretching)	Alkanes, Ketones	Silverstein, Prtesch, Nakanishi
1708-1716	C=O (stretching)	Ketones, Aldehydes, Carboxylic acids	Silverstein, Prtesch, Nakanishi
1642-1657	C=C (stretching)	Alkenes	Silverstein, Kupotsav
	C=O (stretching)	Amides, Intramolecular hydrogen bonded carboxylic acids	www.science-and-fun.de
1515	C-H,C=C-C (ring stretching)/N=O (stretching)	Aromatics	Pretsch, Nakanishi
	NO_2 (asymmetric stretching)	Aromatic nitro compounds	www.science-and-fun.de
1463	C-H (deformation vibration/scissoring)	Alkanes	Pretsch, Nakanishi
	C-H (asymmetric deformation)	Ethers	www.science-and-fun.de
	C-H_2 (symmetric deformation)	Esters/Amides	www.science-and-fun.de
1360-1368	CO-CH_3 (bending)	Aromatics	Pretsch, Nakanishi
1265-1277	C-C,C-O,C=O (stretching)	Aromatics	Silverstein, Prtesch, Kupotsav
	C-N (stretching)	Aromatic amines	www.science-and-fun.de

Table 2.3 (Continued)

1123	C-O (stretching)	Saturated secondary alcohols, Unsaturated & cyclic tertiary alcohols, Ethers, Esters	Silverstein, Nakanishi, Kupotsav
	C-O-C stretching vibration	Aromatics	Nakanishi, www.science-and-fun.de
1052	$C-H_3$ (rocking)/C-C (skeleton)	Aromatics	Pretsch, Kupotsav, www.science-and-fun.de
	C-N stretching vibrations	Aliphatic amines	Silverstein, Prtesch, www.science-and-fun.de
	C-O (stretching)	Primary alcohols, Esters	Nakanishi, Kupotsav, www.science-and-fun.de
1032	C-H (deformation)	Ethers	Prtesch, Nakanishi, www.science-and-fun.de
	C-O (stretching)	Primary alcohols	Silverstein, Prtesch, Nakanishi
	C-N stretching vibrations	Aliphatic amines	www.science-and-fun.de
775-570	C-Cl/C-Br (stretching)	Alkyl halides	www.science-and-fun.de

2.3.2.8.1.1 Non-fractionated samples

The FTIR spectra for the non-fractionated samples produced from all ratios of clear wood and bark feedstock were compared to identify any changes in chemical composition. Though most peaks were consistent in all samples, a few differences were observed. The alkane absorbance peak found at 1463 cm^{-1} in the bark samples was not present in the 100/0 CW/B sample. A peak identified at ~1650 cm^{-1}, corresponding to alkenes, amides and/or intramolecular hydrogen bonded carboxylic acids, was present in 60/40 CW/B and 50/50 CW/B samples but not present in 100/0 CW/B and 80/20 CW/B samples. Similarly, peaks observed at 1153 cm^{-1} and 1123 cm^{-1}, corresponding to aromatic ring structures, were present for non-fractionated samples produced from 60/40

CW/B and 50/50 CW/B but were not present in the 100/0 CW/B and 80/20 CW/B samples. At bark concentrations at or above 40 wt%, there are no chemical composition changes detectable by FTIR spectroscopy.

The separated solid and liquid phases of 50/50 CW/B sample were analyzed separately. The solid phase showed the presence of alkanes, alkenes, aldehydes, ketones, carboxylic acids, ethers and aromatic nitrogen-containing compounds. The liquid phase contained phenols, alcohols and methyl groups.

2.3.2.8.1.2 Fractionated samples

Peaks identified in the fractionated samples were compared with the non-fractionated samples to look for differences in functional groups between the samples. A peak observed at 1463 cm^{-1} in the non-fractionated samples produced from the bark added feedstock was not present in all Fractionate I samples. This indicates the absence of alkanes. Absence of aromatic rings in the Fractionate I samples was observed by the absence of peaks at 1153 and 1123 cm^{-1}. The absorbance peak at 1035 cm^{-1} due to deformation vibrations of C-H bond in aromatic rings was present only in the sample produced from 100/0 CW/B among all Fractionate I samples. No spectral differences were observed between the Fractionate I samples.

2.3.2.8.2 Quantitative analysis

Figure 2.7 represents the comparison of PHR for all the peaks identified from the all of the non-fractionated samples. The spectra obtained for the total samples from all the feedstock using ATR-FTIR were compared and no significant change was found. So to determine the quantitative change peak height ratio was measured. Normalization for

the Peak Height Ratios (PHRs) are based on the peak height for the peak apex falling in the 1265-1277 cm^{-1} wavelength (C-C, C-O, C=O) a common and very consistent peak from sample-to-sample. When bark was added in the feedstock PHR for the O-H stretch (3390-3412 cm^{-1}) increased which indicates the increase in phenols, water and alcohols. It correlates with the presence of lignin-derived compounds; Alkenes or amides present in the samples produced from 60/40 CW/B and 50/50 CW/B increased with the increase in the amount of bark added. PHR for C=C-C (ring stretching) or N=O (stretching) increased with the addition of bark which indicates the increase in aromatics and aromatic nitro compounds. Aromatics increase is also shown by the increase in PHR for the $C\text{-}H_3$ (rocking) or C-C (skeleton) (1052 cm^{-1}) and deformation vibrations of C-H bond in aromatic rings (1035 cm^{-1}). Increased ether and ester was also observed which corresponds to C-H (deformation vibration/scissoring), C-H (asymmetric deformation), $C\text{-}H_2$ (symmetric deformation) at 1463 cm^{-1}. Increase in alkyl halides (775-570 cm^{-1}) also observed with the addition of bark. Decrease in carbonyl groups was observed with the bark addition which could correspond to decrease in aldehydes, ketones or carboxylic acid. Increase in the PHR of O-H stretch (alcohols, water) and decrease in the PHR of C=O (carboxylic acid) correlates well with the increase in pH.

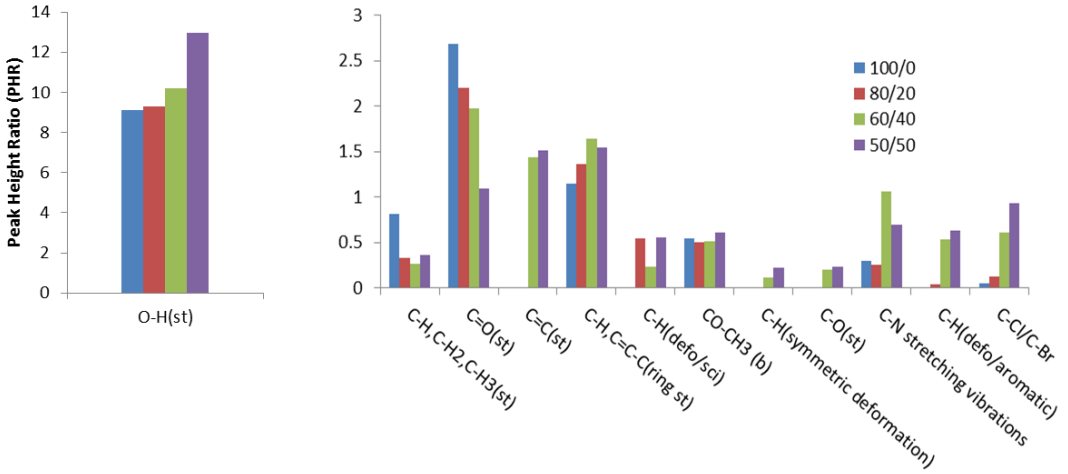

Figure 2.7 Average PHR values for the peaks found in the non-fractionated samples derived from different ratios of clear wood (CW) and bark: 100/0; 80/20; 60/40; 50/50 CW/B (wt%).

2.3.2.9 Optical microscopy

Measured solids content in this study showed high particulate loading in pyrolysis oil produced from bark added feedstock. Similar result was observed in a study by Ingram et al., when pyrolysis oil produced from pine wood and pine bark were compared (Ingram et al., 2007). Ba et al. revealed that solids content (measured as MIM) of softwood-bark derived pyrolysis oil includes not only charcoal particles but also waxy materials. Visual observation of the oil samples in this study clearly revealed the presence of larger particles in bark-derived oil. Determining the size of particles present in pyrolysis oil is crucial in identifying sui upgrading method and application. Particulate structure and particle size distributions were determined using optical microscopy and ImageJ software.

2.3.2.9.1 Particulate structures

The pyrolysis oil produced from softwood bark residues was found to be a complex colloidal multi-dispersed system consisting of solid particles, droplets and structured materials (Ba et al., 2004). Agglomeration of particles was observed in all samples, although the particle content, degree of agglomeration, and agglomerate shapes varied. More agglomeration was observed in samples with higher solids content. Some rod-like structures were observed in the liquid portion of Fractionate II samples derived from 50/50 CW/B. Emulsion droplets were observed in the 50/50 CW/B samples confirming phase separation (Ingram et al., 2007). Imaging the solid/sludge portion of the phase separated samples was difficult due to the opacity of the sample smear.

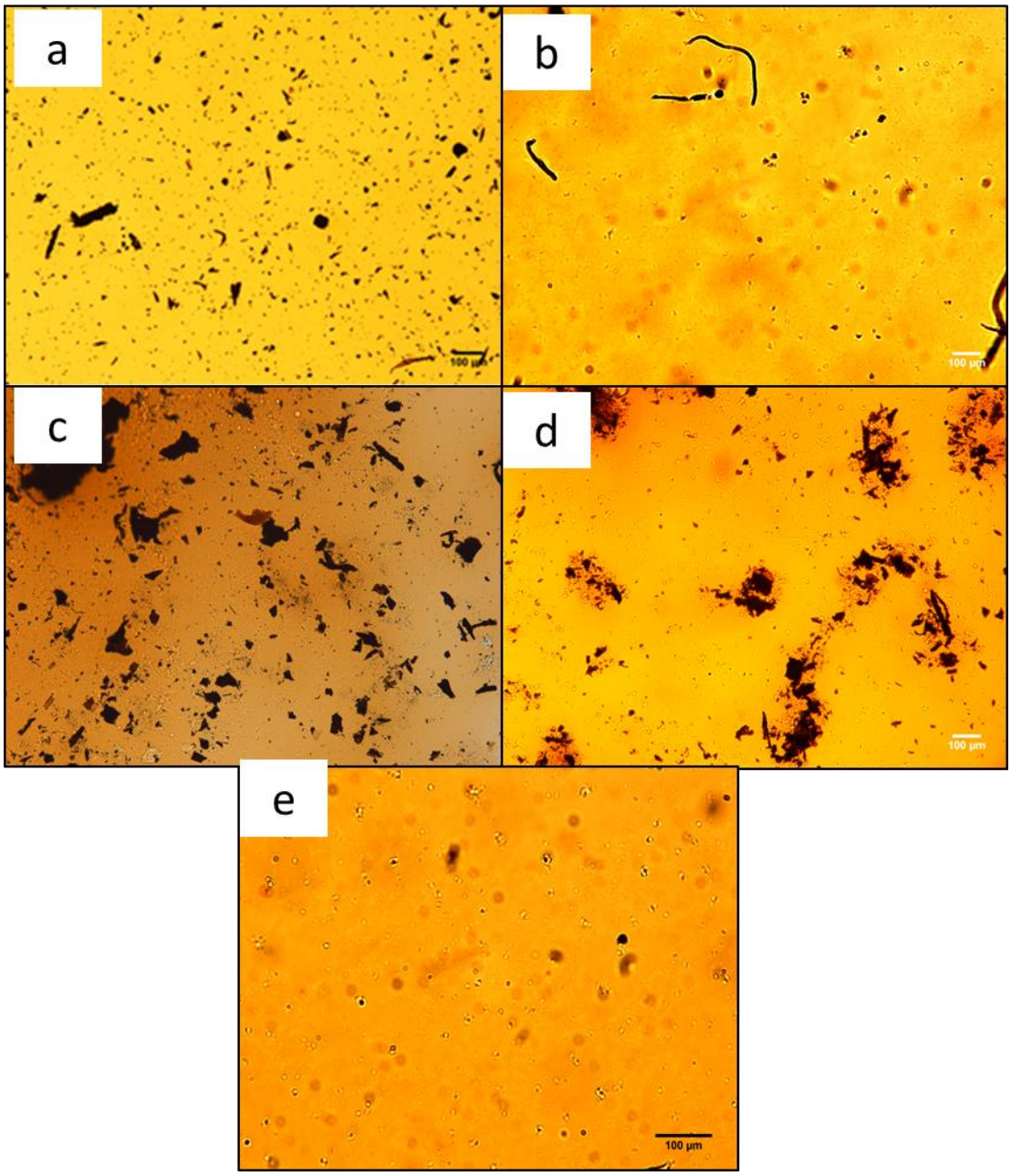

Figure 2.8 Representative optical micrographs for pyrolysis oil samples derived from different ratios of clear wood (CW) and bark:

At 10X magnification (a) Total (non-fractionated) 100/0 CW/B sample showing the presence of relatively small particles; (b) Fractionate II derived from 50/50 CW/B (50/50 CW/B-F II) showing the presence of rod like structures; (c) Non-fractionated sample from 80/20 CW/B showing larger size/agglomerated particles; and(d) Fractionate I derived from 50/50 CW/B (50/50 CW/B-F I) showing small droplets. Shown at 20X magnification is (e) Fractionate II derived from 50/50 CW/B (50/50 CW/B-F II) showing droplets containing particles

ImageJ (version 1.45s) software was used to analyze particle size and determine the particle size distributions (PSD) for each sample pre/post treatment. Samples derived from 100/0 CW/B and 50/50 CW/B were analyzed. Particle counts for all the samples correlates with the solids content measured as MIM (wt%). 50CW/50B samples had larger size particles than did samples derived from 100/0 CW/B. The solid and liquid phases of the phase separated samples were analyzed separately. The particle count was very less in the liquid portion of the Fractionate II samples derived from50/50 CW/B.

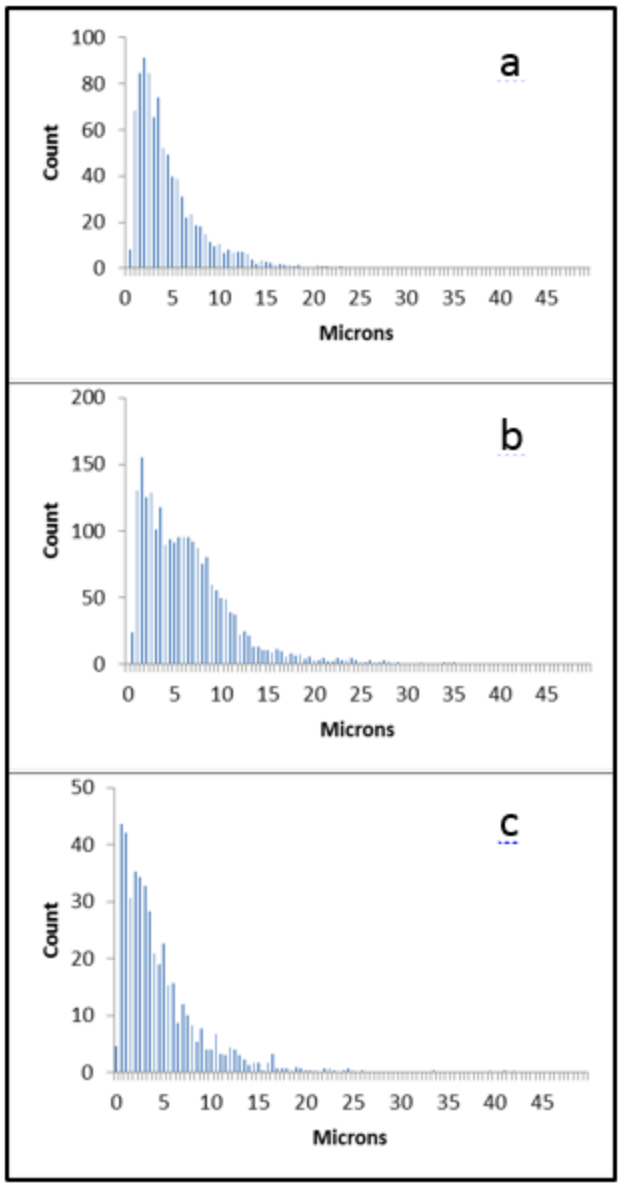

Figure 2.9 Representative particle size distribution (PSD) histograms of the samples derived from 100/0 CW/B

(a) 100/0 CW/B –Total; (b) 100/0 CW/B --Fractionate I; (c) 100/0 CW/B --Fractionate II.

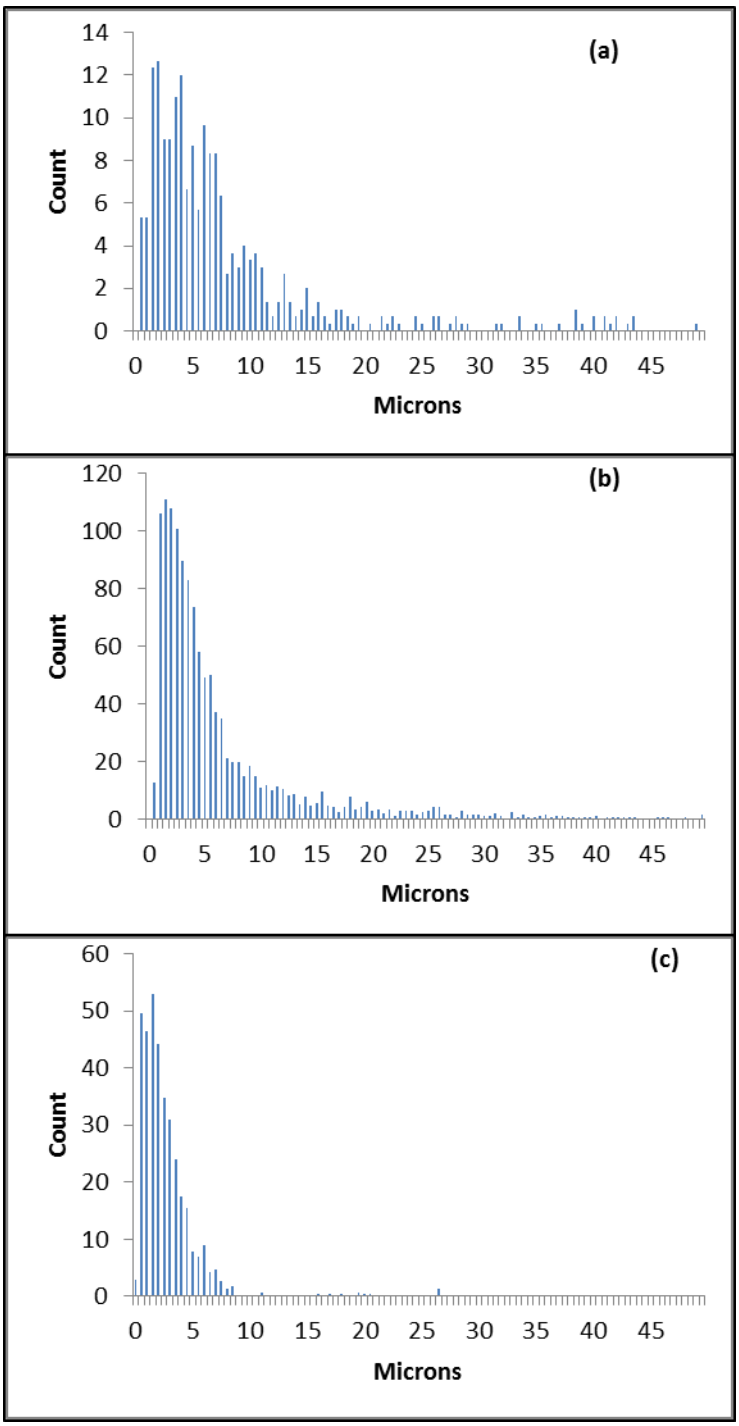

Figure 2.10 Representative particle size distribution (PSD) histograms for the solids within the liquid phase of phase separated samples

(a) 50/50 CW/B –Total; (b) 50/50 CW/B --Fractionate I; (c) 50/50 CW/B --Fractionate II.

2.3.3 Post-filtration changes in pyrolysis oil properties

Char removal is inevitable for the commercial application and upgrading of pyrolysis oil. Present study is to understand the role of char in the properties of pyrolysis oil and how it changes after the char removal. Crucial properties such as solids, water content and viscosity were measured.

2.3.3.1 Solids content

Figure 2.11 shows the average solids content data for unfiltered and filtered non-fractionated samples. The non-fractionated samples produced from four different feed stocks were filtered using serial filtration method. To understand the amount of solids removed, the solids content were measured as Methanol Insoluble Materials in the filtered sample and compared with the un-filtered sample. Considerable removal of solids was observed in all the samples. The solids content in the filtered samples was less than 0.2 wt%. Solids content for the 100/0 CW/B samples reduced from 0.18% to 0.12%. Percentage reduction was 0.06%.Similarly reduction in solid content for 80/20 CW/B; 60/40 CW/B and 50/50 CW/B were 0.96, 1.3, and 0.8 respectively. Percentage reduction varied between the samples based on the particle size. It shows that the particles in the pyrolysis oil produced from bark added feed stock were bigger than in the 100/0 CW/B sample. It was justified by the particle size distribution analysis which showed more number of larger particles in the bark samples.

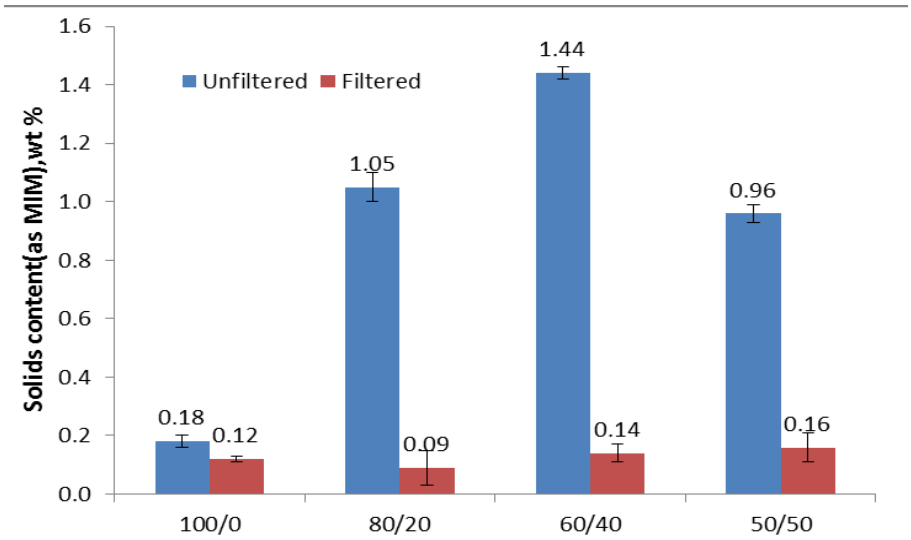

Figure 2.11 Average solids content for un-filtered and filtered non-fractionated pyrolysis oil derived from different ratios of clear wood (CW) and bark: 100/0; 80/20; 60/40; 50/50 CW/B (wt%).

Error bars represent 95% confidence intervals.

2.3.3.2 Water content

Water content increased after filtration in all the samples. This may be due to the removal of material causing increase in water weight percentage as water content is measured based on the weight of the sample.

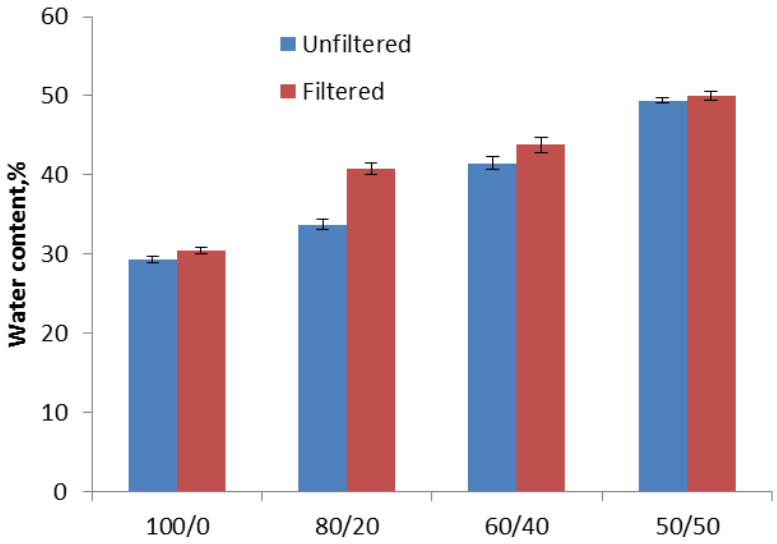

Figure 2.12 Average water content data for un-filtered and filtered non-fractionated pyrolysis oil derived from different ratios of clear wood (CW) and bark: 100/0; 80/20; 60/40; 50/50 CW/B (wt%).

Error bars represent 95% confidence intervals.

2.3.3.3 Viscosity

After filtration, the viscosity decreased drastically for all the samples. The viscosity for 100/0 CW/B sample was higher than other samples. This might be due to the fact that 100/0 CW/B samples had small particles dispersed throughout the sample might not have removed through filtration. Percentage reduction in viscosity was high for 80/20 CW/B (94.76%) and 60/40 CW/B (93.63%) samples as most of the larger size particles could be removed through filtration. The average viscosity data are shown in Figure 2.13.

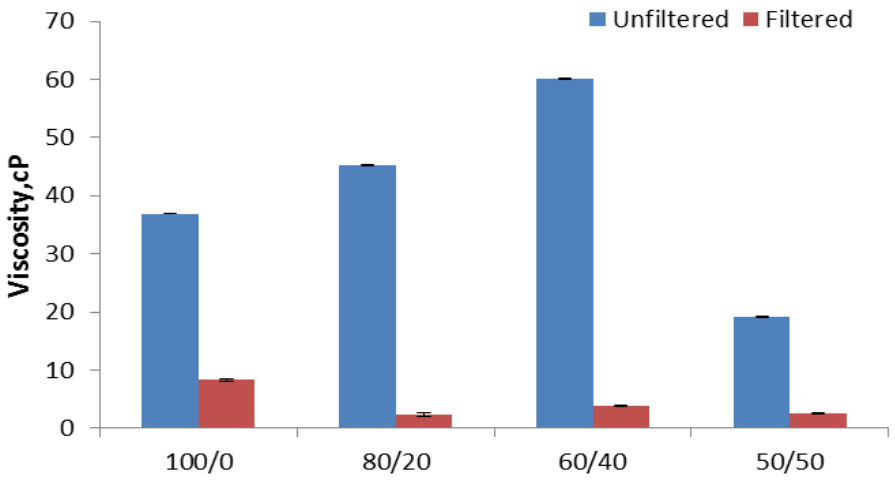

Figure 2.13 Average viscosity for un-filtered and filtered non-fractionated pyrolysis oil derived from different ratios of clear wood (CW) and bark: 100/0; 80/20; 60/40; 50/50 CW/B (wt%).

Error bars represent 95% confidence intervals.

2.3.4 Post-accelerated aging changes in pyrolysis oil properties

Pyrolysis oil undergoes various chemical reactions leading to undesirable changes in properties such as viscosity increase, increase in water etc; content during storage (Oasmaa and Czernik, 1999). This unstable nature of pyrolysis oil is a concern during storage and transportation. The chemical reactions during storage are strongly dependent on the compounds present in the oil and the composition of pyrolysis oil varies with the feedstock used for the production. Accelerated aging study was conducted and physic-chemical properties of pyrolysis oil were measured to understand the effects of feedstock on the stability of pyrolysis oil. Char particles were found to catalyze some of the reactions leading to aging in pyrolysis oil (Agblevor et al., 1995). Thus aging study was performed for the filtered samples to understand the effects of char on the stability of pyrolysis oil.

2.3.4.1 Water content

Water content was measured for both the unfiltered and filtered aged samples. Figure 2.14 and 2.15 shows the data for different aging hours.

2.3.4.1.1 Pre-filtration.

Water content for the 100 CW/0 B sample remained almost constant when it was aged for 6 h. The water content increased from 29.4% to 34.5% and 36.4% when it was aged for 24 h and 48 h respectively. Surprisingly the water content decreased after 6 h of aging in 80/20 CW/B and 60/40 CW/B samples. Like 100 CW/0 B samples, the water content for 50 CW/50 B also remained constant for 6 h of aging. In all the samples the water content increased when aged for 24 h and 48 h, though the percentage increase differed. Maximum increase was observed for 60 CW/40 B sample and it was notices as ~10%. Very less increase was observed in the 50/50 CW/B sample for any hours of aging. Percentage increase compared to unaged samples for different aging hours are shown in Figure 2.4.

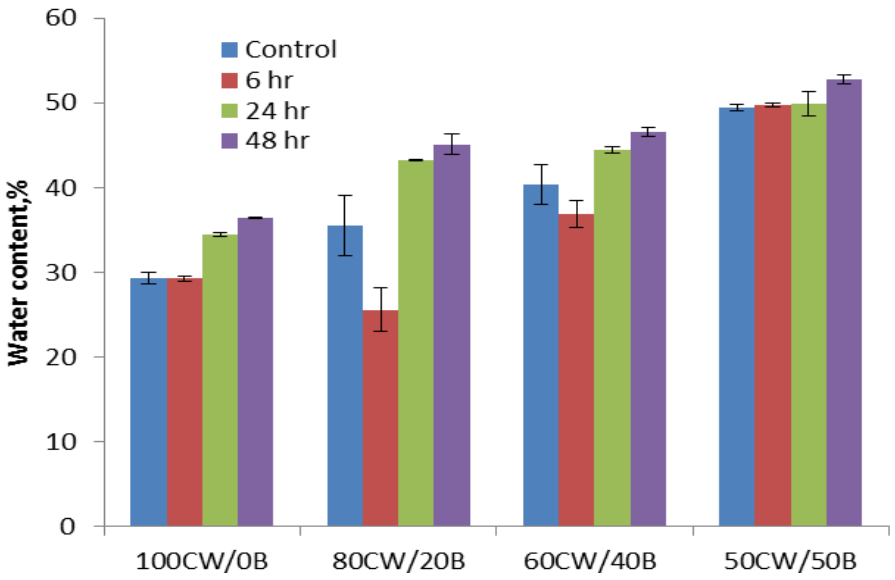

Figure 2.14 Average water content for un-filtered aged samples derived from different ratios of clear wood (CW) and bark: 100/0; 80/20; 60/40; 50/50 CW/B (wt%).

Error bars represent 95% confidence intervals.

Table 2.4 Change in water content (in %) for unfiltered aged samples derived from different ratios of clear wood (CW) and bark: 100/0; 80/20; 60/40; 50/50 CW/B (wt%).

Change in water content (%)				
Aging Time	**100/0**	**80/20**	**60/40**	**50/50**
6 h	(-0.12)	(-9.94)	(-3.49)	0.35
24 h	5.10	7.69	4.15	0.51
48 h	7.02	9.57	6.23	3.40

2.3.4.1.2 Post-filtration.

The change in water content after aging for the filtered samples varied completely from the data obtained for the unfiltered samples. A very little or no difference was observed when all the samples were aged for 6 h and 24 h. No difference was observed with the addition of in the aging based on water content. The water content increased

between ~1.0 to 2.3% in all the samples when aged for 48 h. The filtration seems to help in retarding the aging and minimizing the effects caused by aging. This validates the fact that the particle present in the pyrolysis oil catalyzes the aging and by removing the particles by filtration helps in minimizing the aging effects. The increase in water content is well explained in many literatures as due to the polycondensation reaction and etherification/acetalization producing water as a byproduct. The average water content data for the filtered aged samples are shown in Figure 2.14. Percentage increase compared to unaged samples for different aging hours are shown in Table 2.5.

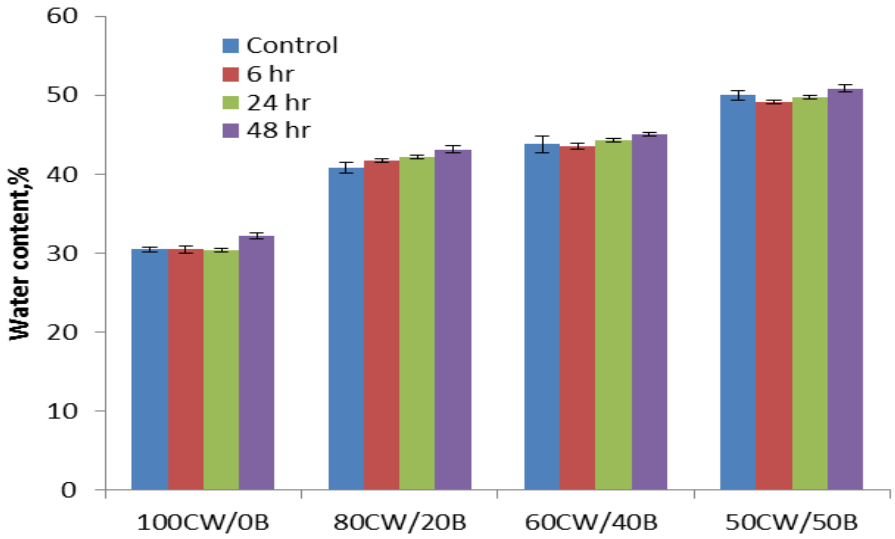

Figure 2.15 Average water content for filtered aged samples derived from different ratios of clear wood (CW) and bark: 100/0; 80/20; 60/40; 50/50 CW/B (wt%).

Error bars represent 95% confidence intervals.

Table 2.5 Change in water content (in %) for filtered aged samples derived from different ratios of clear wood (CW) and bark: 100/0; 80/20; 60/40; 50/50 CW/B (wt%).

	Change in water content (%)			
	100/0	**80/20**	**60/40**	**50/50**
6 h	0.01	0.94	(-0.22)	(-0.87)
24 h	(-0.07)	1.37	0.50	(-0.24)
48 h	1.71	2.34	1.23	0.86

2.3.4.2 Solids content.

2.3.4.2.1 Pre-filtration

The solids content increased when the samples were aged for long hours (Table 2.6). It was difficult to take representative samples for all the bark added sample was non-homogenous and the particle sizes were big due to which they were separating from the liquid even after vigorous shaking which caused the difference in solid content for the samples taken for aging with the control.

Table 2.6 Solids content of the unfiltered aged samples derived from different ratios of clear wood (CW) and bark: 100/0; 80/20; 60/40; 50/50 CW/B (wt%).

Feedstock	**MIM (wt%)**		
	6 h	**24 h**	**48 h**
100/0	0.39	0.50	0.92
80/20	0.35	0.44	0.54
60/40	0.54	0.58	0.77
50/50	0.56	0.44	0.91

2.3.4.2.2 Post-filtration

Increase in solids content was observed when the samples were aged, though the percentage increase was very less. Percentage increase in solids content varied between

0.04 to 0.06% highest being for 100/0 CW/B samples. This confirms that the chemical composition of the bark added samples differ from the CW samples which might have led to different aging reactions resulting in the formation of solids. Also the sample produced from 100/0 CW/B was always more acidic than other samples which might have led to reactions catalyzed by the low pH.

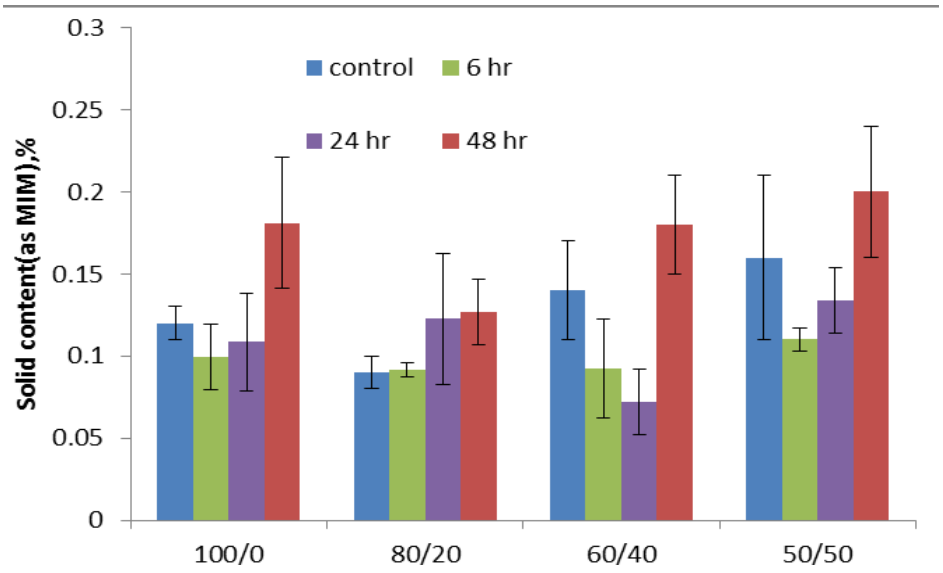

Figure 2.16 Average solids content for filtered aged samples derived from different ratios of clear wood (CW) and bark: 100/0; 80/20; 60/40; 50/50 CW/B (wt%).

Error bars represent 95% confidence intervals.

2.3.4.3 Viscosity

Rheological study was conducted to understand the change in viscosity due to accelerated aging. The study was conducted over the shear rate ranging from 0.1 to 1000 s^{-1}. The data reported are the **average values for the region where the data was almost constant (10-100 s^{-1}) (Figure 2.17).** The results obtained from rheological study for the unfiltered aged sample were note consistent. Also the unfiltered samples were exhibiting

the shear thinning behavior. Due to the larger size of the particles in the sample produced from the bark added feedstock, it was difficult to take the representative samples for analysis. The torque for the rheometer was exceeding the limit when the particles were used for the measurement. So the rheological study was performed for the samples aged after filtration. The maximum increase was observed for 80/20 CW/B sample and the viscosity increase was found to be 95.38% when it was aged for 48 hr. It was observed that the change in viscosity was not directly proportional to the amount of bark added. At lower shear rates (0.1 to 10 s^{-1}), the samples were showing shear thinning behavior and the viscosity becomes constant after that. This might be due to the presence of extractives, pyrolytic lignins and solids which led to exhibit Bingham fluid behavior (Lu et al., 2009).

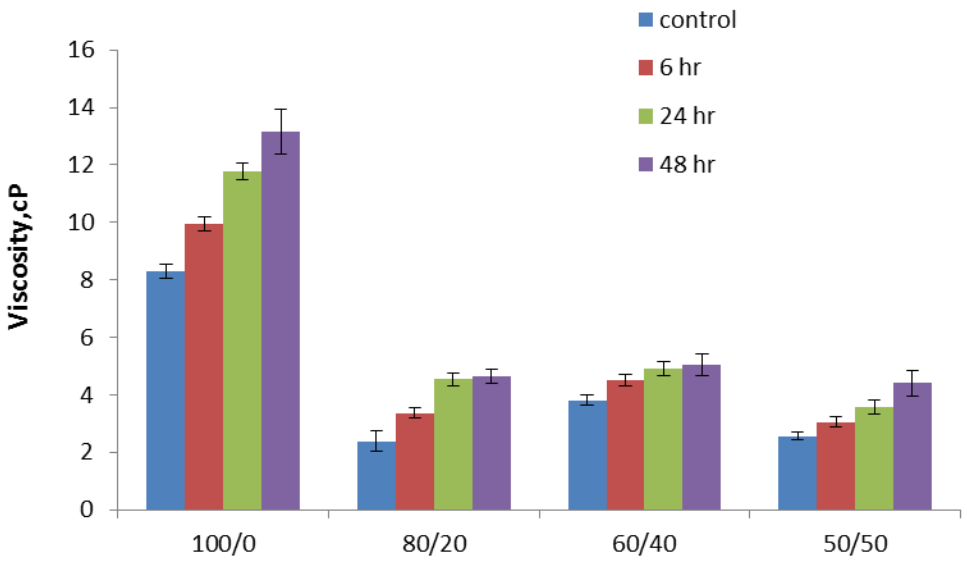

Figure 2.17 Average viscosity for filtered aged samples derived from different ratios of clear wood (CW) and bark: 100/0; 80/20; 60/40; 50/50 CW/B (wt%).

Error bars represent 95% confidence intervals.

Table 2.7 Viscosity increase (in %) for filtered aged samples derived from different ratios of clear wood (CW) and bark: 100/0; 80/20; 60/40; 50/50 CW/B (wt%).

	Viscosity increase (%)			
	100/0	**80/20**	**60/40**	**50/50**
6 h	20.05	41.93	18.08	19.32
24 h	42.06	91.78	28.40	39.92
48 h	58.52	95.38	32.51	71.99

2.3.4.4 FTIR spectroscopy

Pyrolysis oil is a mixture of as many as 400 organic compounds and aging is caused by several probable mechanisms leading to change in chemical composition (Diebold, 2000). FTIR spectroscopy was utilized to determine the change in chemical composition of pyrolysis oil during aging.

2.3.4.4.1 Pre-filtration

To determine the change in chemical composition with aging, the spectra for the sample aged for 48 h was compared with the spectra for the control. For the sample produced from 100/0 CW/B, peaks were observed at 48 h at 1153, 1124, 1034 cm^{-1} which was not seen at unaged samples. This indicates the occurrence of etherification and esterification reactions. For most of the samples aged for 48 h, increase in PHR was observed for C=O (stretching) (1700 cm^{-1}) and C-H, C=C-C (ring stretching) or N=O (stretching) (1515 cm^{-1}) which indicates the increase in aromatics and ketones. Decrease in C-O stretching was observed which indicates that the primary and secondary alcohols are reacting to produce aromatics or ketones. In all the samples decrease in O-H stretch

was observed irrespective of the increase in water content which could be due to the decrease in phenols and alcohols. Phenols can react with aldehydes to form resins.

2.3.4.4.2 Post-filtration

To understand the change in chemical composition due to the reactions while aging, the spectra for the control sample was compared with the one aged for 48 h. In all the filtered aged samples decrease in O-H stretch was observed like in unfiltered aged samples which might be due to the decrease in phenolic concentration. Two different reaction mechanisms seems to happen during aging which are the reaction of phenols with formaldehyde to form hemiformal in the absence of catalyst and the reaction of phenol with aldehyde to form resins and water (Diebold, 2000). Since these samples have less solids and alkali content this might lead to no-catalyst scenario for phenols to form hemiformal. Difference was observed with 100/0 CW/B sample from the bark samples in the carbonyl group stretch (1700 cm^{-1}). For 100/0 CW/B sample, increase in PHR was observed for C=O stretching whereas for the bark samples either it remained same or decreased. It could be possible that for 100/0 CW/B samples formation of ketone dominates the consumption of aldehyde. Significant peak was observed in all samples at 1515 cm^{-1} which indicates the formation of aromatics and aromatic amines. Increase in PHR at1515 cm^{-1} also indicates the increase in benzene ring vibration due to oxidation shown by decrease in carbon oxygen ration showing that oxidation occurred (Hilten and Das, 2010). Formation of esters due to esterification is shown by the appearance of peak at 1463 cm^{-1}. Decrease in PHR of the peak at 1053 cm^{-1} indicates the decrease in alcohols which could be esterification, acetalization (alcohols react with alcohols to form acetals) and hemiacetalization (alcohols react with aldehydes to form hemiacetal). The

alcohols and aldehydes can also oxidize to form carboxylic acids (Diebold, 2000). Another product that can form due to oxidation is organic peroxide and it can act as a catalyst polymerization of olefins (Diebold, 2000). Overall, no difference was observed in aging mechanisms with filtration.

2.3.4.4.3 Functional group changes in pyrolysis oil due to aging

Some of the changes in property of the pyrolysis oil due to aging reactions include decrease in pH due to the formation of carboxylic acid and increase in water content. The water content increases as it is a by-product in several aging reactions. The increase in water content is also due to polycondenstaion reaction. It will lead to decrease in heating value eventually (Lu et al., 2009). Due to some of the polymerization reactions, the viscosity increases. Acetalization and esterification helps the pyrolysis oil to move towards thermodynamic equilibrium. Thus the addition of alcohol is one of the methods used to increase the stability of the oil.

2.4 Conclusions

Effect of bark addition to the feedstock in the yield and physico-chemical properties of pyrolysis oil was studied by utilizing different ratios of pine clear wood and pine bark as feedstock. Yield of pyrolysis oil decreased when bark was utilized to produce pyrolysis oil attributed to high lignin content of bark. It was noted that oil yield was decreasing with the increase in amount of bark added. Visual inspection of pyrolysis oil produced from different ratios of pine clear wood and pine bark revealed that particulate loading and particle size were on higher side in the oil derived from bark added feedstock. Selective condensation of pyrolysis vapors was utilized and products

were collected separately with one fraction containing more water. Bark is rich in extractives, hence pyrolysis oil derived from 50/50 CW/B (wt%) contained waxy materials and they formed a top layer in high water content fractionated sample causing phase separation. Significant change in properties of pyrolysis oil was observed with the addition of bark. Bark addition led to increase in water content and solids content in the pyrolysis oil; with the increase proportional to the amount of bark added. Quick settling of lignin derived solid materials was observed in the samples with high water content. Bark addition led to some changes in chemical composition such as increased water, phenols, alcohols, ethers, esters, aromatics and decreased aldehydes, ketones and carboxylic acids.

Post-condensation filtration of pyrolysis oil reduced the solids content (measured as MIM, wt%) to as low as 0.09%. Reduction in solids content was more for the pyrolysis oil derived from bark added feedstock compared to the oil produced from clear wood as the crude filtration technique could remove the bigger size particles. Removal of particles led to decrease in viscosity and the sample produced from 100/0 CW/B was more viscous compared to other samples.

Accelerated aging studies based on water content showed that removal of char particles aided in slowing down the aging process. Pyrolysis oil derived from CW and CW/B behaved in a similar fashion during aging. Water content increased for both the unfiltered and filtered samples, but the percentage increase was less for filtered samples when aged for 48 h. Very little difference in water content was observed in both filtered and unfiltered samples when aged for 6 h and 24 h. Results obtained from solids content and viscosity measurement for unfiltered aged samples were not consistent due to the

non-homogeneity of the samples. Very small increase in solids content was observed when the samples were aged for 48 h. Removal of solids did not prevent the viscosity increase during aging. Surprisingly, increase in water content and viscosity was more for 80/20 CW/B compared with other samples. A possible explanation for this scenario could be as follows: As lignin requires wider temperature for complete degradation, more lignin in feed stock (60/40 CW/B and 50/50 CW/B) faced partial degradation and ended up in char which was removed by filtration. Hence filtered samples from the above mentioned feedstocks had less impact of lignin derived material during aging.

Pyrolysis oil had negative impacts such as increased solids, water and viscosity by the addition of bark and it also varied with the amount of bark added. Post-condensation filtration retarded the rate of aging in all the samples. Bark addition does not seem to have more impact on change in properties of pyrolysis oil during aging. But the physical appearance and initial properties of pyrolysis oil derived from bark added feedstock does not favor the addition of bark in the feedstock.

2.5 References

Agblevor, F., Besler, S., Montane, D., and Evans, R. (1995). Influence of inorganic-compounds on char formation and quality of fast pyrolysis oils. (Amer chemical soc PO box 57136, Washington, DC 20037-0136), p. 8 – cell.

Akhtar, J., and Saidina Amin, N. (2012). A review on operating parameters for optimum liquid oil yield in biomass pyrolysis. Renew. Sustain. Energy Rev. 16, 5101–5109.

Ba, T., Chaala, A., Garcia-Perez, M., and Roy, C. (2003). Colloidal Properties of Bio-Oils Obtained by Vacuum Pyrolysis of Softwood Bark. Storage Stability. Energy Fuels 18, 188–201.

Ba, T., Chaala, A., Garcia-Perez, M., Rodrigue, D., and Roy, C. (2004). Colloidal Properties of Bio-oils Obtained by Vacuum Pyrolysis of Softwood Bark. Characterization of Water-Soluble and Water-Insoluble Fractions. Energy Fuels 18, 704–712.

Bridgwater, A.V. (1999). Principles and practice of biomass fast pyrolysis processes for liquids. J. Anal. Appl. Pyrolysis 51, 3–22.

Bridgwater, A.V., Meier, D., and Radlein, D. (1999). An overview of fast pyrolysis of biomass. Org. Geochem. 30, 1479–1493.

Czernik, S., Johnson, D.K., and Black, S. (1994). Stability of wood fast pyrolysis oil. Biomass Bioenergy 7, 187–192.

Diebold, J.P. (2000). A review of the chemical and physical mechanisms of the storage stability of fast pyrolysis bio-oils (National Renewable Energy Laboratory Golden, CO).

Elliott, D.C., Oasmaa, A., Preto, F., Meier, D., and Bridgwater, A.V. (2012). Results of the IEA Round Robin on Viscosity and Stability of Fast Pyrolysis Bio-oils. Energy Fuels 26, 3769–3776.

Energy Information Administration (EIA). (2013). International Energy Outlook 2013. Washington, DC: US Department of Energy.

Hilten, R.N., and Das, K.C. (2010). Comparison of three accelerated aging procedures to assess bio-oil stability. Fuel 89, 2741–2749.

Ingram, L., Mohan, D., Bricka, M., Steele, P., Strobel, D., Crocker, D., Mitchell, B., Mohammad, J., Cantrell, K., and Pittman, C.U. (2007). Pyrolysis of Wood and Bark in an Auger Reactor: Physical Properties and Chemical Analysis of the Produced Bio-oils. Energy Fuels 22, 614–625.

"Interpretation of FTIR Spectra", http: //www.science-and-fun.de/tools/, accessed on 03/15/14.

Kuptsov, A. H.; Zhizhin, G. N. Handbook of Fourier Transform Raman and Infrared Spectra of Polymers; Elsevier: New York, 1988; pp 8, 10, and 11.

Li, Q., Steele, P.H., Yu, F., Mitchell, B., and Hassan, E.-B.M. (2013). Pyrolytic spray increases levoglucosan production during fast pyrolysis. J. Anal. Appl. Pyrolysis 100, 33–40.

Lu, Q., Li, W.-Z., and Zhu, X.-F. (2009). Overview of fuel properties of biomass fast pyrolysis oils. Energy Convers. Manag. 50, 1376–1383.

McKendry, P. (2002a). Energy production from biomass (part 1): overview of biomass. Rev. Issue 83, 37–46.

McKendry, P. (2002b). Energy production from biomass (part 2): conversion technologies. Rev. Issue 83, 47–54.

McKendry, P. (2002c). Energy production from biomass (part 2): conversion technologies. Rev. Issue 83, 47–54.

Oasmaa, A., and Czernik, S. (1999). Fuel Oil Quality of Biomass Pyrolysis OilsState of the Art for the End Users. Energy Fuels 13, 914–921.

Oasmaa, A., Kuoppala, E., Gust, S., and Solantausta, Y. (2002). Fast Pyrolysis of Forestry Residue. 1. Effect of Extractives on Phase Separation of Pyrolysis Liquids. Energy Fuels 17, 1–12.

Oasmaa, A., Kuoppala, E., and Solantausta, Y. (2003). Fast Pyrolysis of Forestry Residue. 2. Physicochemical Composition of Product Liquid. Energy Fuels 17, 433–443.

Pretsch, E.; Buhlmann, P.; Affolter, C. Structure of Determination of Organic Compounds, s of Spectral Data; Springer: New York,2000; pp 245, 255, 263, 264, 286, 287, 291, and 293.

Nakanishi, K.; Solomon, P. H. Infrared Absorption Spectroscopy;Holden Day: Oakland, 1977; pp 14, 19, 25, 26, 31, and 3840.

Silverstein, R. M.; Webster, F. X. Spectrometric Identification of Organic Compounds; John Wiley & Sons, Inc.: Hoboken, NJ, 1998; pp. 82, 86, 87, 90-92, 94, 95, and 97.

”Sources of biomass,” http: //www.biomassenergycentre.org.uk/, accessed on 08/19/14.

CHAPTER III

EFFECTS OF CENTRIFUGAL FILTRATION ON PYROLYSIS OIL PROPERTIES

3.1 Introduction

Fast pyrolysis is a promising technology that produces a second generation biofuel known as pyrolysis oil which can be readily stored and transported (Czernik and Bridgwater, 2004). Unlike first generation biofuels, second generation biofuels do not compete with the food chain and they can be produced from wide variety of biomass types (de Miguel Mercader et al., 2010). Pyrolysis oil can be used as a combustion fuel in burners, furnaces, boiler systems, diesel engines, turbines and Stirling engines (Czernik and Bridgwater, 2004). Pyrolysis oil produced from wood contains over 300 compounds in small amounts and isolating any single compounds is complex and not commercially economical (Czernik and Bridgwater, 2004). Hence technologies needs to be developed to produce chemicals from whole pyrolysis oil or from major, easily separable fraction of pyrolysis oil (Czernik and Bridgwater, 2004).

Pyrolysis oil contains significant amounts of water, oxygenated organic compounds, and carbonaceous char (Shaddix and Tennison, 1998). Char particles present in pyrolysis oil are of micron and submicron in size (Elliott, 1994). The presence of char and diverse chemical composition of pyrolysis oil leads to high viscosity, high mass density, high surface tension, low heating value, and low pH compared with petroleum fuels (Agblevor and Besler, 1996; Elliott, 1994). In fast pyrolysis, char is

produced along with pyrolysis gases and vapors in varying amounts and particle sizes (Lehto et al., 2013; Scahill et al., 1997). Char fines leads to increased viscosity over time, such as during storage (Agblevor et al., 1995). Char particles are laden with alkali metals which leads to clogging and corrosion in combustion environments (Agblevor and Besler, 1996; Elliott, 1994). Also char/ash can cause secondary cracking reactions which leads to lower oil yield (Agblevor and Besler, 1996; Bridgwater and Peacocke, 2000; Diebold, 2000). Char which becomes entrained in the pyrolysis oil contain alkali metals that have been shown to catalyze 'aging' reactions (Bridgwater and Peacocke, 2000; Diebold and Czernik, 1997). Alkali metals/inorganics present in the char do not leach in to the oil during storage (Agblevor and Besler, 1996) and hence removal of char helps to mitigate the aging reactions.

Controlling the water content in pyrolysis oil is also important as higher water content can lead to phase separation and corrosion (Lehto et al., 2013). Water in pyrolysis oil has both positive and negative effects on the physical properties and subsequent applications of the oil (Lehto et al., 2013). Density, viscosity and heating value of pyrolysis oil decreases with increased water content (Lehto et al., 2013). Alternately, pyrolysis oil with high water content has lower viscosity, is easier to pump, and has better atomization properties (Lehto et al., 2013). When compared with diesel fuel, pyrolysis oil—with its high water content—has a lower combustion rate (Oasmaa and Czernik, 1999). The water present in pyrolysis oil includes moisture from the feedstock and water produced during pyrolysis (Mohan et al., 2006). Pyrolysis feedstock is typically dried to have a moisture content of less than10 wt% to reduce the water content in the oil product (Bridgwater et al., 1999). A study was conducted by Demirbas

to understand the effects of initial feedstock moisture content on pyrolysis oil yields using spruce wood, hazelnut shell and wheat straw as feedstocks. This study showed that the oil yield increased with the increase in the initial moisture content of the feedstock (Demirbas, 2004).

Some of the important parameters to be considered in evaluating the suitability of any liquid fuel for combustion include spray atomization quality, ignitability, droplet vaporization, sooting, and coking tendency (Shaddix and Tennison, 1998). It is difficult to ignite pyrolysis oil due to the presence of water which has high latent heat of vaporization (Lu et al., 2009). Hence pyrolysis oil requires more energy than petroleum fuels for ignition. Cetane number (CN) is a measure of a fuel's readiness auto-ignite. The CN for diesel is around 48 (Lu et al., 2009). High CN indicates a low ignition delay before combustion (Lu et al., 2009). Ikura et al. calculated the CN of neat pyrolysis oil using linear extrapolation after measuring the CN of a number of pyrolysis oil/diesel emulsions with different concentrations of pyrolysis oil, as it is difficult to measure the cetane number of neat pyrolysis oil. The CN of pyrolysis oil was calculated to be around 5.6 which is very low in comparison to diesel fuel (Ikura et al., 2003; Lu et al., 2009). Hence to utilize pyrolysis oil for combustion requires preheating the air or adding ignition improvers (Lu et al., 2009). The process of breaking a liquid fuel in to small droplets for spray combustion is called atomization (Lu et al., 2009). Spray atomization quality of any fuel is affected by viscosity and surface tension as the size of the droplet increases with the increase in viscosity and surface tension (Lu et al., 2009; Shaddix and Tennison, 1998). Thus, pyrolysis oil requires preheating to improve atomization by increasing viscosity. However heating it at higher temperatures (>80 °C) leads to

accelerated aging reactions that can significantly changing the properties of pyrolysis oil (Lu et al., 2009). So char particles need to be removed quickly and completely to allow for effective utilization and upgrading of pyrolysis oil (Hoekstra et al., 2009).

The water and char present in pryolysis oil—as it is produced—results in reduced oil quality and makes it unsuitable as a replacement for petroleum fuel. The presence of char also causes problems such as poisoning and deactivation of catalyst used in upgrading processes (Hoekstra et al., 2009). Therefore, the ability to generate a s pyrolysis oil with low char fines content and low water content is essential to meet the requirements of both the upgrading processes and the end-user applications (Lehto et al., 2013; Scahill et al., 1997).

Char particles can be separated during pyrolysis either from the gas phase (prior to condensation) or from the liquid pyrolysis oil product (after condensation). Cyclone filtration is the most commonly used filtration method where char is separated from the pyrolysis gas utilizing particle impaction on the cyclone walls (Bridgwater, 2012; Hoekstra et al., 2009). However cyclone filters are inefficient in separating solids when the cyclone is scaled up and when the particle size is below 10 μm (Oasmaa and Czernik, 1999). This inefficiency leads to carryover of some char into the liquid (Bridgwater et al., 1999). Another separation method is electrostatic precipitation, which is effective in removing particles not captured by cyclone; however, they require higher capital and operating costs (Scahill et al., 1997). Hot gas filtration is an another technique which helps to produce high quality, char-free oil (Diebold et al., 1994) with alkali metal concentration of <10 ppm (Scahill et al., 1997), but this process can lead to 10-20% reduction in oil yield during continuous run as the char forms a permanent cake on filter

surface and results in cracking the vapors (Bridgwater, 2003). Baghouse filter is a commonly used filter element for hot gas filtration; it becomes ineffective when the cake thickness is > 1 cm and back flushing is commonly used to dislodge the cake to minimize pressure loss (Diebold et al., 1994; Scahill et al., 1997). Though back flushing helps in reducing the pressure loss, there is a significant minimum pressure drop which is unavoidable. Oxidative regeneration helps in recovering the initial pressure drop but it leaves residual char on the filter surface which negates its use in removing char (Scahill et al., 1997).

Drawbacks with post-reaction filtration techniques created interest in developing in-situ filtration technique where filter elements are incorporated within the fluidized bed reactor to remove char from pyrolysis vapors as it is produced. The filters can be cleaned continuously by the sourcing action of bed particles which prevents an increase in pressure drop (Hoekstra et al., 2009). With in-situ filtration methods, reaction and separation processes are integrated which reduces residence time and prevents secondary cracking reactions (Hoekstra et al., 2009; Wang, 2006). The collected char still needs to be removed and gas removal from the reactor through the in-situ filter alters the hydrodynamics of the reactor (Bridgewater, 2004). With these methods, removal of solids and alkali metals resulting in slowing the aging reactions but it did not prevent them completely (Hoekstra et al., 2009).

Removing char particles from pyrolysis oil after condensation is extremely difficult due to the viscous nature of the oil and associated high energy requirement (Agblevor and Besler, 1996). The complex interaction between char and pyrolytic lignin forms a gel-like phase and it can clog the filters used in pressure filtration (Bridgwater,

2003). Adding solvents such as methanol and ethanol help to mitigate this problem by solubilizing the less soluble constituents and also dilution (Bridgwater, 2003). Javaid et al. studied utilizing membrane filtration for separating char particles from pyrolysis oil. Tubular ceramic membranes of 0.8 and 0.5 μm pore size were utilized, and the results showed that these membranes were effective in removing particles above 1 μm in size. Microfiltration did not chemically alter the main components of pyrolysis oil. Javaid et al. also performed fouling studies and observed cake formation in both of the tested membranes (Javaid et al., 2010). Postcondensation filtration helps in reducing the particulate loading but did not prevent aging reactions in pyrolysis oil(Naske et al., 2011). Char content in pyrolysis oil can be controlled by other methods such as changing the process conditions to limit pyrolytic lignin, increasing the degree of depolymerization of lignin derived material, utilizing feedstock with lower lignin content, and/or reducing char-lignin interactions (Bridgwater et al., 1999).

Pyrolysis oil produced from fast pyrolysis contains water which is present either in the dissolved form or as part of a microemulsion, and this water cannot be removed by distillation. Fractional condensation can be used to reduce the water content in one or more fractions which will help in increasing the heating value (Bridgwater et al., 1999; Mohan et al., 2006). But this might increase the operating cost and decrease the low molecular weight volatile components (Bridgwater et al., 1999). A study conducted by Westerhof et al. investigated the possibility of utilizing extraction to remove water from pyrolysis oil; this study showed that the water content in pyrolysis oil could be reduced by extraction but 50% of the organics were removed along with the water phase leading to lower yield of oil (Westerhof et al., 2007).

Char collected in the liquid may be separated by a cartridge or rotary filter but again faces the drawback of filter blockage. Char can be removed by centrifugation (Oasmaa and Peacocke, 2010) which overcomes the drawback of plugging of filter or cake formation over the filter. Centrifugation is commonly used for separating water from oil-water mixtures. Elliott studied the possibility of utilizing centrifugation to separate char and water from pine- and oak-derived pyrolysis oil. Results indicated that centrifugation is an effective technique for separating char but not water (Elliott, 1994). However, Ba et al. observed three phases when centrifugation was performed on pyrolysis oil derived from bark residue (Ba et al., 2004). The purpose of the present study is to understand the effectiveness of centrifugation in removing char and water from pyrolysis oil derived from pine clear wood, along with the impacts of separation time and feed temperature.

3.2 Methods and Materials

3.2.1 Pyrolysis oil

The pyrolysis oil samples used for this study were produced from pine clear wood feedstock using an auger reactor capable of processing 84 lb/h of biomass feedstock (Mississippi State University Sustainable Energy Research Institute). The feedstock drops into the reactor pipe through a rotary airlock valve which along with nitrogen purging (42 LPM) keeps oxygen from entering the reactor and process gases from exiting. Auger helps to mix the solid heat carrier with the biomass. The biomass and solid heat carrier then enters the reactor zone which is heated by electrical band heaters to 450 °C. Hot gases (~425 °C) produced from pyrolysis of biomass are then sent to 3 shell and tube condensers to condense the gases to pyrolysis oil. Char is collected in a bin through a

heat exchanger. The solid heat carrier is returned back to the reactor through a heated tube (450 °C).

3.2.2 Centrifuge and testing method

Centrifuge used for this study is a disc-stack centrifuge supplied by GEA Westfalia Separator, Inc. The centrifuge can be operated as a two-phase clarifier or three phase separator with the self-cleaning bowl. It has a bowl speed of 10,000 rpm with a total capacity of 1.0 l and solids holding space of 0.5 l. Separation time and feed temperature play a crucial role in effective separation of solids in the centrifuge. Separation time can be defined as the time between ejection (ejection of collected solids) cycles (GEA Westfalia 2012). Separation time depends on solids content and consistency in the feed, effective volume of solids holding space and separator throughput (GEA Westfalia 2012). When the separation time is set high, incomplete ejection of solids due to long time dwelling of solids in the bowl happens resulting in high solids content (GEA Westfalia 2012). When the product to be separated is less viscous best separation effect can be obtained (GEA Westfalia 2012). The terminal velocity increases with the decrease in viscosity of the medium to be separated. At high terminal velocities, the radial velocity will be higher and the separation will be improved. Raising the temperature of the feed helps in reducing the viscosity, thereby facilitating the effective separation. Tests were carried out for two phase separation (solid-liquid) utilizing different separation times such as 2 min, 5 min and 10 min; and different feed temperatures such as 25, 30, 35 and 40 °C. Hot water circulation system was used to increase the temperature of the feed. Three phase separation (Heavy liquid- light liquid-solid) was also attempted.

3.2.3 Characterization methods

3.2.3.1 pH

To measure pyrolysis oil pH, a Mettler Toledo SevenEasy S20 pH meter was used. Buffer solutions of pH 2, 4, 7, 10, and 12 were used to calibrate the meter. Three measurements were taken for each sample to obtain average pH values and 95% confidence interval (CI).

3.2.3.2 Water content

Water content was determined using Mettler Toledo's EasyPlus^{TM} KFV titrator following ASTM 203-01 method. Hydranal 5E titrant and Hydranal Chloroform-Methanol (CM) solvent were used. Three measurements were taken to obtain the average and 95% confidence interval (CI).

3.2.3.3 Solids content

Solids content in the pyrolysis oil were measured as weight percentage of Methanol Insoluble Materials (MIM wt %). Sample size of 1-3 mg was used for the solvent amount of 100 mL. The solution was filtered through the 1μm Whatman filter paper. The filter was then weighed after drying and the solid content was calculated based on the weight on the sample used initially.

3.2.3.4 Particle size distribution

An Olympus BX 51 optical microscope was used to collect the images of the pyrolysis oil by smearing the sample on the slide. Images were collected at 10X and 20X magnifications. ImageJ software (version 1.45s) was used for the analysis of particle size. Particle size distribution was also measured by dynamic light scattering technique using a

Brookhaven ZetaPALS analyzer. For DLS analysis, the samples were diluted to 0.1 mg/ml with a solution of 1.0 mM KNO_3 in DI water due to the technique's requirement of low concentration. The diameter of the particles by number was determined using Particle Solutions (v 2.0) software from Brookhaven.

3.2.3.5 FTIR spectroscopy

Attenuated total reflectance (ATR) FTIR spectroscopy was used for the identification of the functional groups present in the pyrolysis oil. The spectra were collected using Nicolet 6700 spectrometer with MIRacle accessory containing diamond-ZnSe crystal. DTGS detector was used with 4 cm^{-1} resolution and 256 scans. Thermo Electron Omnic software (version 8.2) was used for the analysis of spectra. A minimum of 3 spectra were collected for each sample and all spectra were ATR corrected.

3.3 Results and Discussion

3.3.1 Variation in Separation time

A trial run of 2-phase centrifugal filtration was performed suing three different separation times (ST): 2, 5, and 10 min.

Physicochemical properties such as pH, density, viscosity, solids content and water content were measured for the liquid phase after filtration and are shown in Table 3.1. Solids content in the liquid phase of the pyrolysis oil decreased as the separation time (ST) was reduced. This shows that setting high separation time leads to incomplete ejection of solids which eventually causes carryover of solids in to the liquid phase as the solids holding space gets filled up. Water content, pH and density were also measured for the separated liquid phase to understand how the property of the oil varies after

centrifugal filtration. It was noted that the measured water content of the liquid phase decreased as the amount of solids removed increased; this indicates that there is water associated with the solids that is removed along with the solids in the centrifugal filtration process. Density values for the liquid phase decreased with increasing solids removal, as is expected. Viscosity of the separated liquid also decreased with the increase in solids removed.

Table 3.1 Physicochemical properties of the separated liquid phase after two phase centrifugal filtration.

Properties	Control	Liquid phase		
		ST-10 min	ST-5 min	ST-2 min
pH	2.22 ± 0.03	2.38 ± 0.02	2.25 ± 0.01	2.41 ± 0.01
Density (g/ml)	1.42 ± 0.05	1.259 ± 0.10	1.209 ±0.08	1.18 ±0.07
Viscosity(cP)	28.65 ± 0.39	16.05 ± 0.21	10.05 ± 0.21	7.65 ± 0.21
Water content (wt. %)	29.22 ± 0.79	24.89 ± 0.63	24.56 ± 0.79	21.89 ± 0.47
Ethanol insoluble solids, EIM (wt%)	0.58 ± 0.05	0.34 ± 0.01	0.27 ± 0.01	0.05 ± 0.03

Average values are presented along with 95% confidence intervals. ST represents 'separation time.'

3.3.1.1 FTIR Spectroscopy

ATR-FTIR was utilized to determine the change in chemical composition caused by centrifugal separation.

3.3.1.1.1 Peak identification

The functional groups in the pyrolysis oil samples were identified from the peaks observed and they are summarized in Table 3.2. The peak identified in the absorbance range of 3370-3415 cm^{-1} is due to the stretching of O-H bond indicates the presence of alcohols, phenols and water. The presence of alkanes is shown by the peak around 2930 cm^{-1} which is due to the asymmetric stretching of C-H bond and vibration of aliphatic C-

H_2 and C-H_3 bonds. A consistent peak in the absorbance range of 1708-1715 cm^{-1} was observed in all the samples which is due to the stretching of C=O bonds of carbonyl groups and it indicates the presence of aliphatic ketones, conjugated aldehydes and alpha-beta unsaturated and benzoate esters. A peak was identified at around 1650 cm^{-1} which might have caused by C=C symmetrical stretching of unconjugated linear alkenes and C=O stretching of amides or intramolecular hydrogen bonded carboxylic acid. The absorbance peak at 1515 cm^{-1} caused by C=C-C (ring stretching)/N=O (stretching) indicates the presence of aromatics and aromatic nitro compounds. A peak was observed at 1463 cm^{-1} for all pyrolysis oil produced from the bark added feedstock. This peak was caused by the asymmetric C-H bending of alkanes. The absorbance peak at 1366 cm^{-1} is due to the symmetric deformation of C-H in methyl groups. A peak was observed at 1271-1274 cm^{-1} which is due to the asymmetric stretch of C-O bond in alkyl aryl ethers. Peaks were observed at 1153 cm^{-1} and 1123 cm^{-1} are due to deformation vibrations of C-H bonds in benzene rings and aromatic in plane C-H bending respectively. The absorbance peak at 1123 cm^{-1} may also be due to the stretching of C-O bond and it indicates the presence of unsaturated and cyclic tertiary alcohols. The absorbance peak found at 1052 cm^{-1} could correspond to the rocking vibration of C-H_3 bond or C-N stretching vibrations or stretching of C-O bond indicating the presence of aromatics or aliphatic amines or primary alcohols respectively. A peak was absorbed at 1035 cm^{-1} due to deformation vibrations of C-H bond in aromatic rings. Peaks were observed in the broad absorbance range of 775-570 cm^{-1} due to the stretching of C-Cl and a C-Br bond indicates the presence of alkyl halides. Two peaks observed around 1500 cm^{-1} and 1370 cm^{-1} together indicates the presence of aryl nitro compounds.

Table 3.2 Identification of peaks from FTIR spectra and corresponding functional groups.

Peak Wavenumber (cm^{-1})	Functional Groups	Compound Class(es)	References
3390-3412	O-H (stretching)	Phenols, Alcohols, Water	Pretsch, Nakanishi
	N-H/N-H_2(stretching)	Amines, Amides, Imines	www.science-and-fun.de
2927-2938	C-H,C-H_2,C-H_3 (stretching)	Alkanes, Ketones	Silverstein, Prtesch, Nakanishi
1708-1716	C=O (stretching)	Ketones, Aldehydes, Carboxylic acids	Silverstein, Prtesch, Nakanishi
1642-1657	C=C (stretching)	Alkenes	Silverstein, Kupotsav
	C=O (stretching)	Amides, Intramolecular hydrogen bonded carboxylic acids	www.science-and-fun.de
1515	C-H,C=C-C (ring stretching)/N=O (stretching)	Aromatics	Pretsch, Nakanishi
	NO_2 (asymmetric stretching)	Aromatic nitro compounds	www.science-and-fun.de
1463	C-H (deformation vibration/scissoring)	Alkanes	Pretsch, Nakanishi
	C-H (asymmetric deformation)	Ethers	www.science-and-fun.de
	C-H_2 (symmetric deformation)	Esters/Amides	www.science-and-fun.de
1360-1368	CO-CH_3 (bending)	Aromatics	Pretsch, Nakanishi
1265-1277	C-C,C-O,C=O (stretching)	Aromatics	Silverstein, Prtesch, Kupotsav
	C-N (stretching)	Aromatic amines	www.science-and-fun.de

Table 3.2 (Continued)

1123	C-O (stretching)	Saturated secondary alcohols, Unsaturated & cyclic tertiary alcohols, Ethers, Esters	Silverstein, Nakanishi, Kupotsav
	C-O-C stretching vibration	Aromatics	Nakanishi, www.science-and-fun.de
1052	$C-H_3$ (rocking)/C-C (skeleton)	Aromatics	Pretsch, Kupotsav, www.science-and-fun.de
	C-N stretching vibrations	Aliphatic amines	Silverstein, Prtesch, www.science-and-fun.de
	C-O (stretching)	Primary alcohols, Esters	Nakanishi, Kupotsav, www.science-and-fun.de
1032	C-H (deformation)	Ethers	Prtesch, Nakanishi, www.science-and-fun.de
	C-O (stretching)	Primary alcohols	Silverstein, Prtesch, Nakanishi
	C-N stretching vibrations	Aliphatic amines	www.science-and-fun.de
775-570	C-Cl/C-Br (stretching)	Alkyl halides	www.science-and-fun.de

3.3.1.1.2 Quantitative analysis.

No significant chemical composition changes between the control sample and centrifuged oil samples could be identified. So a peak height ratio method was used to quantify the presence of the major functional group peaks. Peak height ratio was calculated by dividing the height of a peak of interest by the peak height corresponding to the C-H stretch, which is not expected to deviate from sample to sample. In examining the peak height ratios (Figure 3.1), we see that the PHR for O-H stretch decreased for the centrifuged oils compared to the control sample. This result might be due to the removal of some water along with the solids. In addition, a peak was observed for the solids samples at 1452 cm^{-1} which was not seen in liquid phase samples, and indicates the

presence of aromatics and heavier molecular weight compounds. No significant peak was observed around 1600 cm^{-1} which indicates an absence of alkene stretching. An increase in C-O and C=O stretching related to primary and secondary alcohols was observed which could point to acetalization and hemiacetal formation. A decrease in C=O stretching was observed which narrows down the list of probable chemical mechanisms to those involving aldehydes and carboxylic acids. The proposed decrease in carboxylic acid content correlates well with the slight increase in pH that was observed.

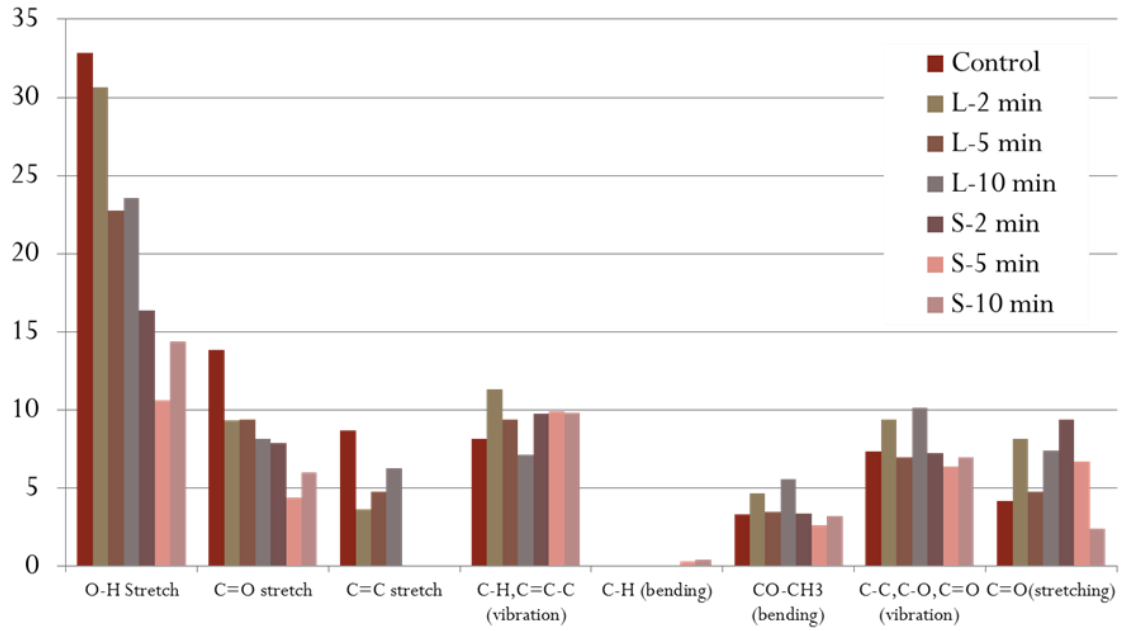

Figure 3.1 FTIR peak height analysis for solid (S) and liquid (L) samples obtained from centrifugal filtration after 2, 5, and 10 min.

Control sample values are also presented.

Particle size was analyzed using dynamic light scattering (DLS) technique (Figure 3.2). From the DLS data it can be observed that there is a decrease in the larger size

particles with centrifugation compared with the control sample. The particles in the centrifuged liquid for the separation time (ST) of 2 min are larger than those in the ST 10 min and 5 min samples, although the overall solids content (wt%) is less in the liquid phase of the ST 2 min sample.

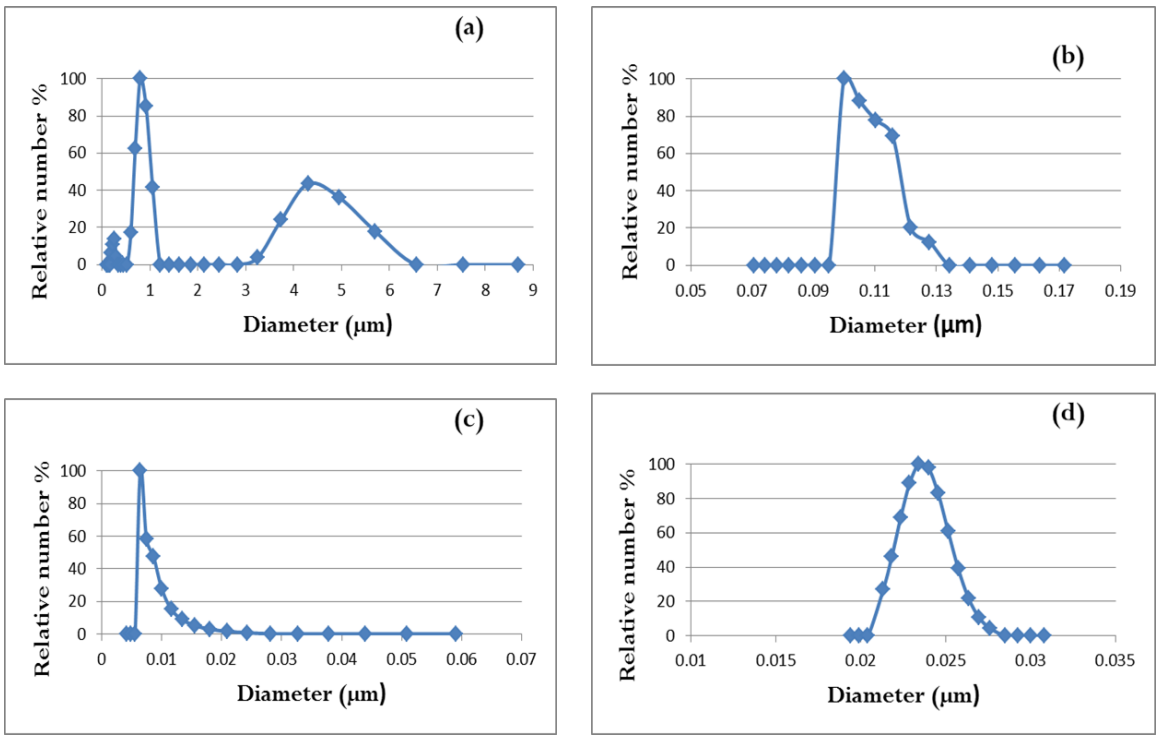

Figure 3.2 Particle size distribution via dynamic light scattering (DLS)

(a) Control; Liquid phase of separation times (b) 2 min; (c) 5 min,(d) 10 min.

3.3.2 Variation in Feed temperature

Two phase separation was performed with different feed temperatures of 25, 30, 35 and 40 °C and the resultant separated phases were analyzed to understand the effect of feed temperature on the effectiveness of separation. The separation time was constant at 10 min. The feed volume and the volume of the liquid phase outlet were measured and

the volume of solid collected is given as the difference between the feed and liquid phase, as shown in Table 3.3. More solids were separated when the temperature was increased (Table 3.4). The solids separated in the centrifuge has some oil and/or water associated with it, so solids content (as MIM) was also measured for the solid samples to know the actual mass of solids separated (Table 3.5). When the oil temperature was raised, the solids content of the resultant separated liquid phase was considerably reduced. Also the true solids removed are higher when the operation temperature was increased. So raising the feed temperature helps in enhancing solids separation. However, since pyrolysis oil 'ages' at high temperatures, the centrifugal filtration needs to ideally be performed just after condensation or the oil temperature raised to 40°C only just prior to centrifugation, if it has been stored at ambient or reduced temperatures for some period of time after production.

Table 3.3 Volumes of feed, separated liquid and solid phases.

Feed Temperature °C	Feed gal	Liquid gal	Solid gal	Liquid Volume %	Solid Volume %
25	3.07	2.7	0.37	87.95	12.05
30	4	3.65	0.35	91.25	8.75
35	3.6	3.1	0.5	86.11	13.89
40	3.06	2.1	0.96	68.63	31.37

Table 3.4 Solids contents of the liquid phase.

Temperature,°C	MIM (wt. %)
Control	0.50 ± 0.05
25	0.27 ± 0.03
30	0.26 ± 0.01
35	0.19 ± 0.02
40	0.13 ± 0.04

Table 3.5 Solids contents of the 'solids' phase.

Temperature,°C	MIM (wt. %)
25	2.82 ± 0.39
30	11.72 ± 0.17
35	7.41 ± 0.19
40	6.09 ± 0.45

Particle size distribution analysis was performed for the samples separated at different temperatures. The liquid samples collected were smeared onto microscopic slides and images collected using an Olympus Bx51 optical microscope with 10x magnification. Particle sizes were measured using ImageJ (1.45s) software (Figure 3.3). More particles were removed when the feed temperature was increased. Nearly 75 % of the particles were less than 10 μm in the control sample. Particle size of < 30 μm contributed more to the total number of particles in the control sample. Increasing feed temperature aided in removing more number of particles which is evident by the decrease in particle count. Most of the particles greater than 10 μm in diameter were removed when the feed temperature was raised to 40 °C.

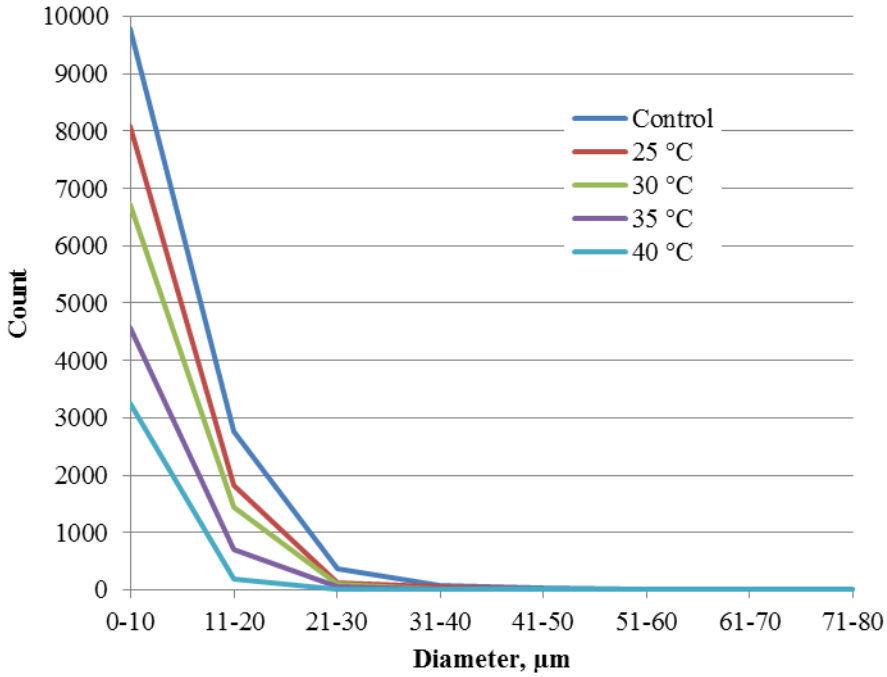

Figure 3.3 Particle sizes and count observed in pyrolysis oil samples centrifuged at different feed temperatures.

3.3.3 Three-phase separation trial

Trials for three-phase separation with the centrifugal filtration system were unsuccessful. In lab trials using a bench-top centrifuge three phase separation was not observed. Oil and water in pyrolysis oil forms an emulsion. Destabilization of the emulsion should enhance the oil-water separation.

3.4 Conclusions

Centrifugal separation is efficient for the removal of solids from pyrolysis oil but it could not force oil-water separation as the oil and water in pyrolysis oil forms an emulsion. It was clearly understood that separation time and feed temperature plays a crucial role in determining the effectiveness of solids separation. Overflow of solids was

observed when the separation time was set high than the requirement. Decrease in particle count in the separated liquid phase was observed with the increase in feed temperature. Almost all the particles of >10 μm size were removed when the feed temperature was set at 40 °C. Particle count of <10 μm size was reduced but centrifugal filtration could not remove them completely.

3.5 References

Agblevor, F.A., and Besler, S. (1996). Inorganic Compounds in Biomass Feedstocks. 1. Effect on the Quality of Fast Pyrolysis Oils. Energy Fuels 10, 293–298.

Agblevor, F., Besler, S., Montane, D., and Evans, R. (1995). Influence of inorganic-compounds on char formation and quality of fast pyrolysis oils. (Amer chemical soc PO BOX 57136, Washington, DC 20037-0136), p. 8 – cell.

Ba, T., Chaala, A., Garcia-Perez, M., Rodrigue, D., and Roy, C. (2004). Colloidal Properties of Bio-oils Obtained by Vacuum Pyrolysis of Softwood Bark. Characterization of Water-Soluble and Water-Insoluble Fractions. Energy Fuels 18, 704–712.

Bridgewater, A.V. (2004). Biomass fast pyrolysis. Therm. Sci. 8, 21–50.

Bridgwater, A.. (2003). Renewable fuels and chemicals by thermal processing of biomass. Chemreactor - 15 SI 91, 87–102.

Bridgwater, A.V. (2012). Review of fast pyrolysis of biomass and product upgrading. Overcoming Barriers Bioenergy Outcomes Bioenergy Netw. Excell. 2003 – 2009 38, 68–94.

Bridgwater, A.., and Peacocke, G.V.. (2000). Fast pyrolysis processes for biomass. Renew. Sustain. Energy Rev. 4, 1–73.

Bridgwater, A.V., Meier, D., and Radlein, D. (1999). An overview of fast pyrolysis of biomass. Org. Geochem. 30, 1479–1493.

Czernik, S., and Bridgwater, A.V. (2004). Overview of Applications of Biomass Fast Pyrolysis Oil. Energy Fuels 18, 590–598.

Demirbas, A. (2004). Effect of initial moisture content on the yields of oily products from pyrolysis of biomass. J. Anal. Appl. Pyrolysis 71, 803–815.

De Miguel Mercader, F., Groeneveld, M.J., Kersten, S.R.A., Way, N.W.J., Schaverien, C.J., and Hogendoorn, J.A. (2010). Production of advanced biofuels: Co-processing of upgraded pyrolysis oil in standard refinery units. Appl. Catal. B Environ. 96, 57–66.

Diebold, J.P. (2000). A review of the chemical and physical mechanisms of the storage stability of fast pyrolysis bio-oils (National Renewable Energy Laboratory Golden, CO).

Diebold, J.P., and Czernik, S. (1997). Additives To Lower and Stabilize the Viscosity of Pyrolysis Oils during Storage. Energy Fuels 11, 1081–1091.

Diebold, J., Czernik, S., Scahill, J., Phillips, S., and Feik, C. (1994). Hot-gas filtration to remove char from pyrolysis vapors produced in the vortex reactor at NREL. pp. 90–108.

Elliott, D.C. (1994). Water, alkali and char in flash pyrolysis oils. Biomass Bioenergy 7, 179–185.

Hoekstra, E., Hogendoorn, K.J.A., Wang, X., Westerhof, R.J.M., Kersten, S.R.A., van Swaaij, W.P.M., and Groeneveld, M.J. (2009). Fast Pyrolysis of Biomass in a Fluidized Bed Reactor: In Situ Filtering of the Vapors. Ind. Eng. Chem. Res. 48, 4744–4756.

Ikura, M., Stanciulescu, M., and Hogan, E. (2003). Emulsification of pyrolysis derived bio-oil in diesel fuel. Biomass Bioenergy 24, 221–232.

"Interpretation of FTIR Spectra", http: //www.science-and-fun.de/tools/, accessed on 03/15/14.

Kuptsov, A. H.; Zhizhin, G. N. Handbook of Fourier Transform Raman and Infrared Spectra of Polymers; Elsevier: New York, 1988; pp 8, 10, and 11.

Javaid, A., Ryan, T., Berg, G., Pan, X., Vispute, T., Bhatia, S.R., Huber, G.W., and Ford, D.M. (2010). Removal of char particles from fast pyrolysis bio-oil by microfiltration. J. Membr. Sci. 363, 120–127.

Lehto, J., Oasmaa, A., Solantausta, Y., Kytö, M., and Chiaramonti, D. (2013). Fuel oil quality and combustion of fast pyrolysis bio-oils. VTT Technol. 87, 79.

Lu, Q., Li, W.-Z., and Zhu, X.-F. (2009). Overview of fuel properties of biomass fast pyrolysis oils. Energy Convers. Manag. 50, 1376–1383.

Mohan, D., Pittman, Charles U., and Steele, P.H. (2006). Pyrolysis of Wood/Biomass for Bio-oil: A Critical Review. Energy Fuels 20, 848–889.

Naske, C.D., Polk, P., Wynne, P.Z., Speed, J., Holmes, W.E., and Walters, K.B. (2011). Postcondensation Filtration of Pine and Cottonwood Pyrolysis Oil and Impacts on Accelerated Aging Reactions. Energy Fuels 26, 1284–1297.

Oasmaa, A., and Czernik, S. (1999). Fuel Oil Quality of Biomass Pyrolysis OilsState of the Art for the End Users. Energy Fuels 13, 914–921.

Oasmaa, A., and Peacocke, C. (2010). Properties and fuel use of biomass-derived fast pyrolysis liquids. VTT Finl

.

Pretsch, E.; Buhlmann, P.; Affolter, C. Structure of Determination of Organic Compounds, s of Spectral Data; Springer: New York,2000; pp 245, 255, 263, 264, 286, 287, 291, and 293.

Nakanishi, K.; Solomon, P. H. Infrared Absorption Spectroscopy;Holden Day: Oakland, 1977; pp 14, 19, 25, 26, 31, and 3840.

Scahill, J., Diebold, J., and Feik, C. (1997). Removal of residual char fines from pyrolysis vapors by hot gas filtration. In Developments in Thermochemical Biomass Conversion, (Springer), pp. 253–266.

Shaddix, C.R., and Tennison, P.J. (1998). Effects of char content and simple additives on biomass pyrolysis oil droplet combustion. Symp. Int. Combust. 27, 1907–1914.

Silverstein, R. M.; Webster, F. X. Spectrometric Identification of Organic Compounds; John Wiley & Sons, Inc.: Hoboken, NJ, 1998; pp. 82, 86, 87, 90-92, 94, 95, and 97.

Wang, X. (2006). Biomass fast pyrolysis in fluidized bed: product cleaning by in-situ filtration (University of Twente).

Westerhof, R.J.M., Kuipers, N.J.M., Kersten, S.R.A., and van Swaaij, W.P.M. (2007). Controlling the Water Content of Biomass Fast Pyrolysis Oil. Ind. Eng. Chem. Res. *46*, 9238–9247.

CHAPTER IV

EMULSION DESTABILIZATION IN PYROLYSIS OIL TO ENHANCE SEPARATION BY CENTRIFUGATION

4.1 Introduction

Pyrolysis oil is a complex mixture of water, solid particles, and hundreds of organic compounds, with water the major component (Lu et al., 2009; Oasmaa and Czernik, 1999). Due to the hydrophilic nature of the carbohydrate-derived compounds, the water is very well dispersed within the pyrolysis oil mixture (Wang et al., 1997). However, the high water content in pyrolysis oil leads to drawbacks such as lower heating value, ignition delay, and reduced amount of material that undergoes combustion over a period of time. Another difficulty in utilizing pyrolysis oil is that phase separation can occur at high concentrations of water (>35 wt%) and lignin-derived materials (>40 wt%) (Lu et al., 2009; Oasmaa and Czernik, 1999). Phase separation can also occur during long term storage of pyrolysis oil (Oasmaa and Czernik, 1999)

Pyrolysis oil is a microemulsion containing a continuous aqueous phase that includes water-soluble compounds derived from holocellulose and a discontinuous phase derived from lignin macromolecules and containing hydrophobic compounds (Bridgwater, 2003). The microemulsion is stabilized by hydrogen bonding and formation of nano- and micro-sized micelles (Mohan et al., 2006). Stability of the microemulsion can be disrupted by an increase in water content over solubility limit of water in pyrolysis

oil (approx. 30-35 wt%) leading to the phase separation of hydrophilic lignin materials (Lu et al., 2009). The water present in pyrolysis oil is in the form of aldehyde hydrates and hydrogen bonded polar organic compounds which cannot be removed easily (Lu et al., 2009). The emulsion oil droplets are stabilized by electrostatic repulsion between droplets (Deluhery and Rajagopalan, 2005; Verbich et al., 1997). Electrostatic repulsion protects the emulsified oil droplets from coalescing into larger droplets and hence makes oil-water separation by gravitation difficult (Zouboulis and Avranas, 2000). If water could be removed from pyrolysis oil, the product would have a higher energy density. In order to separate water and oil in the pyrolytic emulsion, the emulsion needs to be destabilized.

Destabilization of emulsions can be achieved by physical, chemical or thermal methods (Cambiella et al., 2006). Chemical destabilization using coagulant salts followed by separation is a process widely used to remove oil from oil-water emulsions (Cambiella et al., 2006; Ríos et al., 1998). Chemical destabilization occurs through mechanisms such as double layer compression, charge neutralization, entrapment in a precipitate, and intraparticle bridging (Weber, 1972). Coagulant salts increase the ionic strength of the emulsion help to reduce the oil-oil electrostatic repulsions (Cambiella et al., 2006). The oil droplets can then coalesce with one another and grow larger in size, making its separation more feasible.

In the present work, a study was conducted to understand the effects of chemical destabilization on pyrolysis oil emulsion structure and separation via centrifugation. After anhydrous $CaCl_2$ was added, the mixture was centrifuged to separate the oil- and water-rich phases. Droplet size distribution and zeta potential were measured as a

function of $CaCl_2$ concentration to understand the destabilization process. Microscopy was used for visualizing coalescence of the oil droplets.

4.2 Materials and Methods

4.2.1 Pyrolysis oil

The pyrolysis oil samples used for this study were produced from pine clear wood feedstock using an auger reactor capable of processing 7 kg/h of biomass feedstock (Mississippi State University Forest Products Laboratory). This lab-scale reactor is constructed from a pipe 3″ in diameter and 40″ in length with 18″ of the auger heated. Heat is provided by five ceramic band heaters on the pipe exterior plus a heater inside the auger pipe. The feedstock drops into the reactor pipe through a rotary airlock valve which along with a nitrogen purge keeps oxygen from entering the reactor and process gases from exiting. Biomass is then fed through the heated zone by an auger operated at approximately 4.5 rpm. The residence time of the biomass in the heated zone (450 °C) is ~1 minute. Char drops out of the reactor into a sealed collection vessel and process gases (420 °C) are sent to the condensers for pyrolysis oil production. Multiple condensers are utilized in series at ~20 °C to condense the hot gases to oil. Physical properties of the resultant pyrolysis oil product are shown in Table 4.1.

Table 4.1 Average physical properties along with 95% confidence intervals for pyrolysis oil produced from pine clear wood.

Property	Value
pH	2.40 ± 0.07
Density, g/ml	1.09 ± 0.05
Water content, wt%	29.38 ± 0.40
Solids content, MIM, wt%	0.180 ± 0.01

4.2.2 Solids removal via centrifugation

A Hermle Labnet Z206 lab-scale centrifuge with fixed angle rotor was used for this study. Solids from the oil were removed to facilitate the accurate measurement of droplet size. To achieve maximum solids separation efficiency, the maximum speed (6000 rpm) and serial centrifugation (3 x 35 min) was utilized. A clear delineation between the separated solids and the liquid could not be seen through the centrifuge vial wall due to the dark color of the oil. In order to avoid pulling solids out with the liquid, the liquid 'sample', as investigated in this study, was an aliquot removed from top most portion of the liquid layer. Note that ~<10% of the liquid was left with the solids on the bottom of the tube. Samples were weighed and these measurements are shown in 4.2, including top (liquid) and bottom (solid) sample weights, for all three runs. Loss due to transfer was calculated as the weight gain of the voided centrifuge tube after the separation process in order to measure the amount of liquid residue remaining in the tube.

Table 4.2 Summary of gravimetric measurements before and after centrifugation showing the total and separated sample weights.

Run	Total Sample (g)	Top (g)	Bottom (g)	Transfer Loss (g)	Top (wt%)	Bottom (wt%)	Transfer Loss (wt%)
I	53.91	45.88	7.25	0.78	85.10	13.45	1.45
II	45.88	39.7	5.49	0.69	86.53	11.97	1.50
III	39.7	35.53	3.67	0.50	89.50	9.24	1.26

After removal of the solids via centrifugation, this 'solids-free' pyrolysis oil was used to examine the emulsion and degradation of the emulsion. The supernatant (top phase) of Run III was utilized as the control for this study to avoid the interference of particles in oil droplet size measurement. Oil droplets in oil-water emulsion carries

negative charge due to the dielectric characteristics of water and oil and this emulsion can be destabilized using cationic demulsifier (Kemmer, 1988). Based on a literature review of salt coagulants (Cambiella et al., 2006; Ríos et al., 1998; Sulaymon and Thuaban, 2010), anhydrous calcium chloride ($CaCl_2$) (Sigma-Aldrich, ≥93.0% purity) was used as the coagulant to facilitate the destabilization of the emulsion. $CaCl_2$ has some advantages over other commonly used coagulants such as $AlCl_3$ and $FeCl_3$. $CaCl_2$ is less polluting and less expensive compared with $AlCl_3$ (Ríos et al., 1998) and has minimal effect on pH compared to $FeCl_3$ (Sulaymon and Thuaban, 2010). Salt was added at concentrations of 0.1, 0.3, 0.5 and 1.0 M. All of the $CaCl_2$ added emulsions were agitated in a vortex mixture to facilitate the dissolution of $CaCl_2$ and then the solution was allowed to stabilize without mixing for around 30 min. The samples were then centrifuged at 6000 rpm for 15 min.

4.2.3 Optical microscopy

An Olympus Bx51 optical microscope was utilized to observe droplet size and coalescence of the oil droplets upon the addition of the coagulant. The samples for microscopy were prepared by smearing the sample solution onto slides. Slides were prepared for the control and each of the four $CaCl_2$ concentrations before and after centrifugation

4.2.4 Dynamic light scattering

Droplet size distribution was measured by dynamic light scattering technique using a Brookhaven ZetaPALS analyzer. For DLS analysis, the samples were diluted to 0.1 mg/ml with a solution of 1.0 mM KNO_3 in DI water due to the technique's

requirement of low concentration. The diameter of the droplets by number was determined using Particle Solutions (v 2.0) software from Brookhaven.

4.2.5 Zeta potential

Zeta potential of the emulsions was measured using a Brookhaven zeta potential analyzer. Electrophoretic mobility of the emulsion was determined using A phase analysis light scattering (PALS) technique. The samples were diluted to 0.1 mg/ml using 1.0 mM KNO_3 in DI water due to the high levels of dilution required by the technique. Average values and 95% confidence intervals were obtained from ten runs for each sample.

4.2.6 pH

To measure pyrolysis oil pH, a Mettler Toledo SevenEasy S20 pH meter was used. Buffer solutions of pH 2, 4, 7, 10, and 12 were used to calibrate the meter. Three measurements were taken for each sample to obtain average pH values and 95% Confidence interval.

4.2.7 Water content

Water content was determined using Mettler Toledo's EasyPlus^{TM} KFV titrator following ASTM 203-01 method. Hydranal 5E titrant and Hydranal Chloroform-Methanol (CM) solvent were used. Three measurements were taken to obtain the average and 95% Confidence interval.

4.3 Results and Discussion

Phase separation was observed with $CaCl_2$ addition followed by centrifugation both visually (Figure 4.1) and by gravimetric measurement (Table 4.3). The separated oil

and water were transferred and the weights measured. Only a small amount of phase separation was observed with 0.1 M and 0.3 M $CaCl_2$. A significant amount of phase separation was observed with 0.5 M and 1.0 M $CaCl_2$. Masses of the separated oil and water phases are shown in Table 4.3.

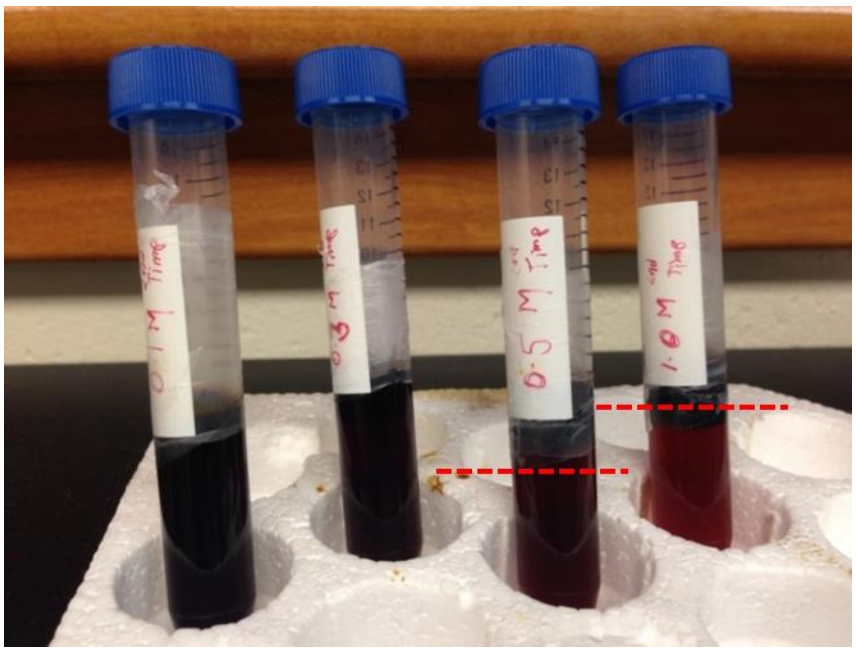

Figure 4.1 Oil-water separation after centrifugation in pyrolysis oil treated with $CaCl_2$. The dashed line delineates the phase interface which can be observed visually in 0.5 and 1.0 M samples. Separation could be determined with backlighting in 0.1 and 0.3 M samples

Table 4.3 Sample mass balance of oil and water during a two- phase separation based on chemical emulsion destabilization.

$CaCl_2$ concentration (M)	Initial Sample Weight (g)	Oil-rich (top) phase (g)	Water-rich (bottom) phase (g)	Transfer Loss (g)	Oil-rich phase (wt%)	Water-rich phase (wt%)
0.1	7.58 ± 0.09	1.52 ± 0.14	5.81 ± 0.22	0.25 ± 0.01	20.06 ± 2.12	76.65 ± 1.96
0.3	7.87 ± 0.10	1.87 ± 0.25	5.63 ± 0.15	0.37 ± 0.01	23.79 ± 2.92	71.48 ± 2.76
0.5	8.22 ± 0.03	2.12 ± 0.19	5.76 ± 0.20	0.33 ± 0.02	25.83 ± 2.38	70.16 ± 2.16
1.0	8.32 ± 0.08	2.29 ± 0.30	5.66 ± 0.23	0.37 ± 0.01	27.54 ± 3.37	68.00 ± 3.41

The stability of the oil-water emulsion is determined by the surface charge of the oil droplet. When the droplets are similarly charged, the electrostatic repulsion will be more than the attractive forces between them which prevents aggregation of droplets. Surface charge of particles and droplets can be measured as zeta potential which is a measure of electrophoretic mobility. Emulsions with high magnitude of zeta potential are more highly charged and exhibit high stability. As seen in 4.2, the zeta potential of the emulsion decreased with increased coagulant concentration and charge reversal was observed which indicates that destabilisation process was carried out by charge neutralisation (Al-Shamrani et al., 2002). The salt coagulant helped in overcoming the electrostatic barrier. This resulted in destabilization of the emulsion through aggregation of the oil droplets and enhanced separation of the oil and water phases.

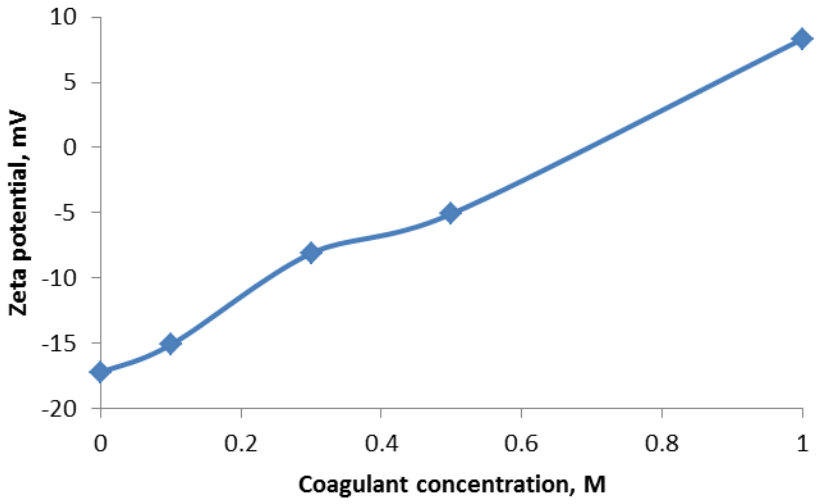

Figure 4.2 Zeta potential of pyrolysis oil as a function of added coagulant, $CaCl_2$ concentration.

Oil-water separation was evident with naked eye at $CaCl_2$ concentrations of 0.5 M or greater. Using optical microscopy, droplets of oil were observed in the $CaCl_2$ added samples (Figure 4.3). An increase in oil droplet size as $CaCl_2$ concentration increased was also observed. This result can clearly be seen at 1.0M $CaCl_2$ where the droplets are as large as 100 microns in diameter (Fig. 4.3e). No oil droplets were observed in the bottom/heavy aqueous phase after separating the oil and water phases using centrifugation (Fig. 4.3f).

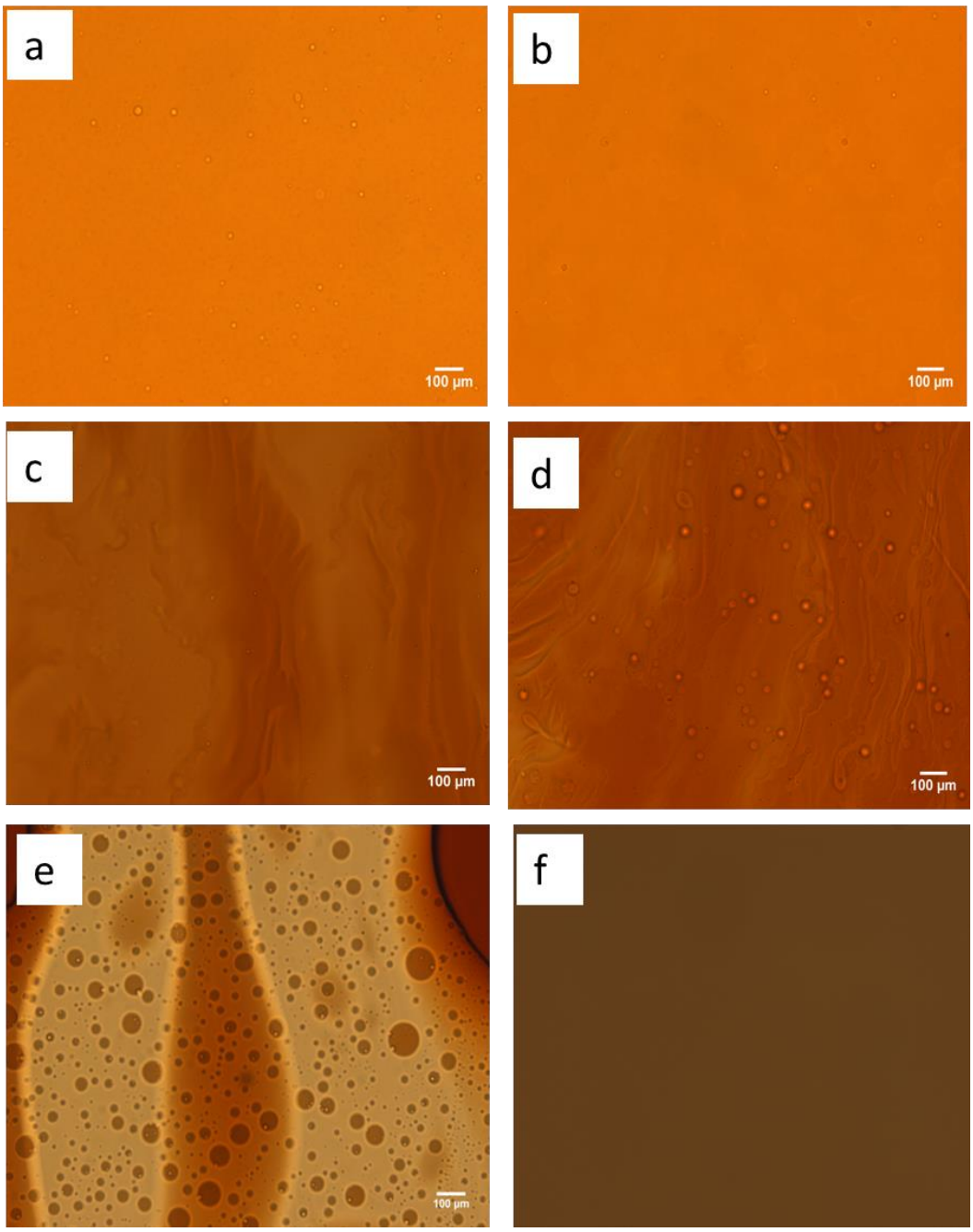

Figure 4.3 Representative optical micrographs at 10X magnification

(a) control; $CaCl_2$ added samples: (b) 0.1M, (c) 0.3M, (d) 0.5M, (e) 1.0M; (f) bottom phase after centrifugation.

In order to measure the change in average droplet size and the particle size distribution, dynamic light scattering (DLS) was utilized. The oil droplets initially have a

negative surface charge. Addition of the calcium cations neutralizes the negative surface charge and promotes coalescence (Cambiella et al., 2006). Coalescence causes an increase in droplet size; and is represented as a function of coagulant concentration in Figure 4.4; droplet size increased with coagulant concentration. After centrifugation the separated bottom phases were analyzed to determine droplet size distributions. Note that droplets with diameters greater than 2 µm were removed from the analysis. After centrifugation, no oil droplets were observed which confirmed separation of oil from the emulsion (Figure 4.5).

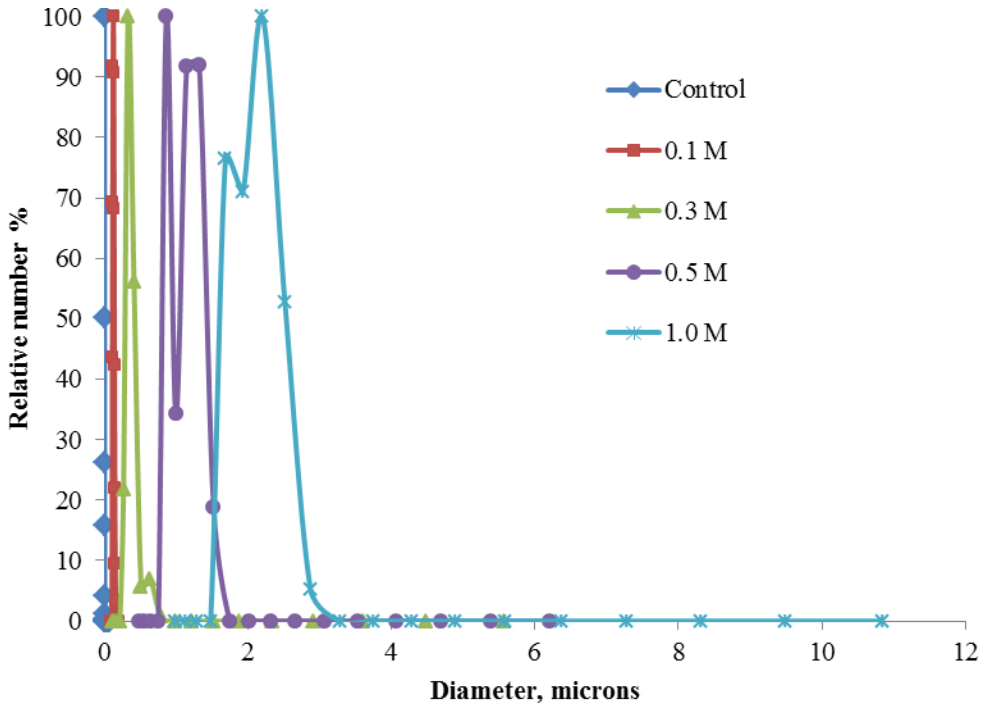

Figure 4.4 Emulsion droplet size distribution before centrifugation as a function of $CaCl_2$ concentration.

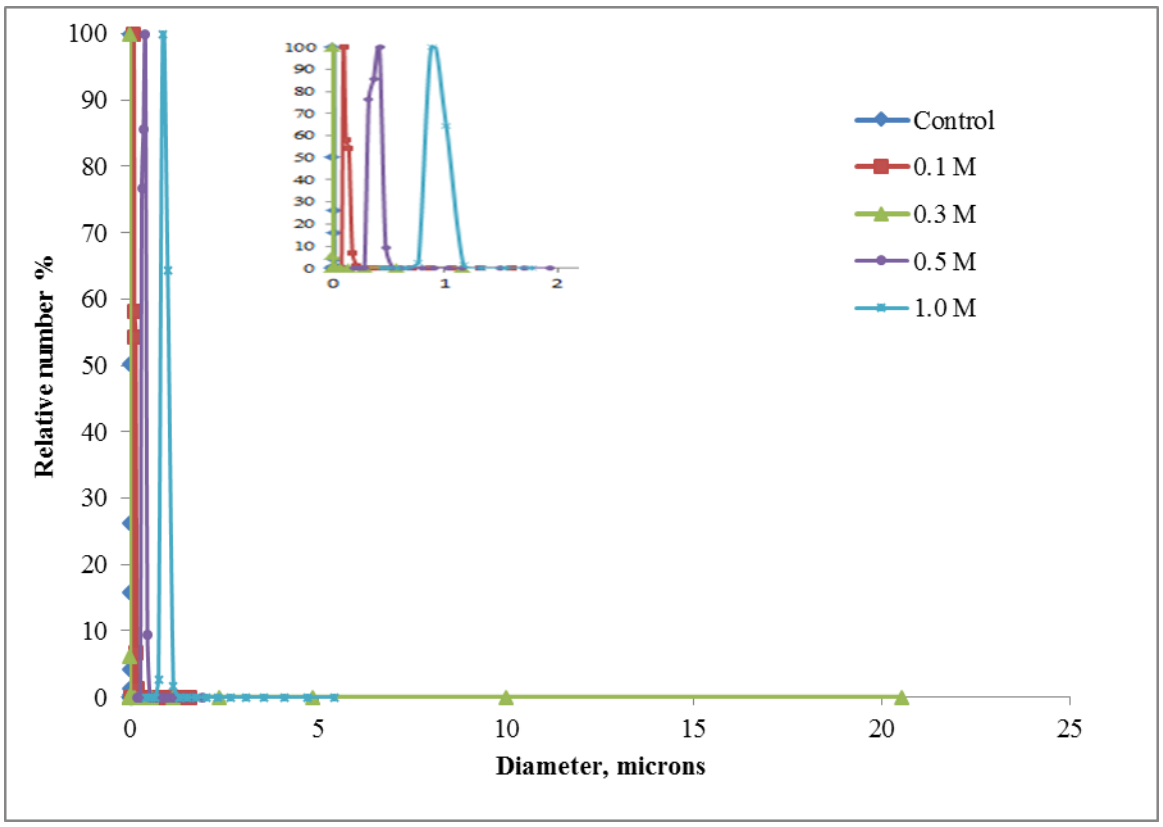

Figure 4.5 Droplet size distribution within the separated bottom phase after centrifugation as a function of $CaCl_2$ concentration.

pH values of separated top and bottom phases were also measured. $CaCl_2$ addition lowers pH and reduction in pH was more with increase in coagulant concentration (Table 4.4). SAWAIN et al., conducted a study to understand the effects of pH on the stability of oil and grease in wastewater and the results showed that the coalescence of oil droplets is strongly influenced by pH. Demulsification occurred when pH was reduced below 5 and more coalescence was observed at pH 1 (SAWAIN et al., 2009). pH of top phase was slightly higher than the bottom phase at any concentration of the coagulant (Table 4.4). This might have caused by the separation of $CaCl_2$ particles along with the bottom phase.

Table 4.4 Average pH values along with 95% confidence intervals for the separated bottom (B) and top (T) phases

Sample	pH
0.1 M (B)	2.19 ± 0.01
0.1 M (T)	2.41 ± 0.03
0.3 M (B)	1.98 ± 0.02
0.3 M (T)	2.10 ± 0.02
0.5 M (B)	1.76 ± 0.05
0.5 M (T)	1.82 ± 0.07
1.0 M (B)	1.36 ± 0.05
1.0 M (T)	1.54 ± 0.03

Water content was measured for separated top and bottom phases. Water content of the top phase was lesser than the bottom phase which indicates the removal of water from the top phase. Increased coagulant concentration aided in the oil-water separation which is shown by the decrease in water content of top phase (Table 4.5)

Table 4.5 Average water content (in wt%) along with 95% confidence intervals for the separated bottom (B) and top (T) phases

Sample	Water content
0.1 M (B)	30.99 ± 2.24
0.1 M (T)	21.03 ± 3.73
0.3 M (B)	32.08 ± 1.39
0.3 M (T)	20.19 ± 1.56
0.5 M (B)	33.89 ± 1.48
0.5 M (T)	20.23 ± 8.55
1.0 M (B)	34.84 ± 1.34
1.0 M (T)	17.48 ± 5.29

4.4 Conclusions

The addition of anhydrous $CaCl_2$ aided in destabilize pyrolytic oil-water emulsions. The concentration of coagulant played a key role in the extent of destabilization and thereby the effectiveness of oil-water separation using centrifugation. Efficient oil removal was observed at coagulant concentrations of 0.5 and 1.0 M which was observed visually and also demonstrated by the weight fraction of the separated oil. Microscopic examination also revealed the effect of coagulant concentration on droplet size and coalescence. Analysis of the droplet size distribution showed that after coagulant addition droplets aggregated to form larger droplets and after centrifuagtion all droplet larger than 2 microns had been removed. This study clearly demonstrates that chemical coagulation with $CaCl_2$ followed by centrifugation is an effective method for eenhancing oil and water separation in pyrolysis oil.

4.5 References

Bridgwater, A.. (2003). Renewable fuels and chemicals by thermal processing of biomass. Chemreactor - 15 SI 91, 87–102.

Cambiella, A., Benito, J.M., Pazos, C., and Coca, J. (2006). Centrifugal Separation Efficiency in the Treatment of Waste Emulsified Oils. Chem. Eng. Res. Des. 84, 69–76.

Deluhery, J., and Rajagopalan, N. (2005). A turbidimetric method for the rapid evaluation of MWF emulsion stability. Colloids Surf. Physicochem. Eng. Asp. 256, 145–149.

Lu, Q., Li, W.-Z., and Zhu, X.-F. (2009). Overview of fuel properties of biomass fast pyrolysis oils. Energy Convers. Manag. 50, 1376–1383.

Mohan, D., Pittman, Charles U., and Steele, P.H. (2006). Pyrolysis of Wood/Biomass for Bio-oil: A Critical Review. Energy Fuels 20, 848–889.

Oasmaa, A., and Czernik, S. (1999). Fuel Oil Quality of Biomass Pyrolysis OilsState of the Art for the End Users. Energy Fuels 13, 914–921.

Ríos, G., Pazos, C., and Coca, J. (1998). Destabilization of cutting oil emulsions using inorganic salts as coagulants. Colloids Surf. Physicochem. Eng. Asp. 138, 383–389.

SAWAIN, A., TAWEEPREDA, W., PUETPAIBOON, U., and SUKSAROJ, C. (2009). The Effect of pH on the stability of grease and oil in wastewater from biodiesel production process.

Al-Shamrani, A.A., James, A., and Xiao, H. (2002). Destabilisation of oil–water emulsions and separation by dissolved air flotation. Water Res. 36, 1503–1512.

Verbich, S.V., Dukhin, S.S., Tarovski, A., Holt, Ø., Saether, Ø., and Sjo¨blom, J. (1997). Evaluation of stability ratio in oil-in-water emulsions. Front. Colloid Chem. Int. Festschr. Profr. Stig E Friberg 123–124, 209–223.

Wang, D., Czernik, S., Montané, D., Mann, M., and Chornet, E. (1997). Biomass to Hydrogen via Fast Pyrolysis and Catalytic Steam Reforming of the Pyrolysis Oil or Its Fractions. Ind. Eng. Chem. Res. 36, 1507–1518.

Weber, W.J. (1972). Physicochemical processes for water quality control (Wiley Interscience).

Zouboulis, A.., and Avranas, A. (2000). Treatment of oil-in-water emulsions by coagulation and dissolved-air flotation. Colloids Surf. Physicochem. Eng. Asp. *172*, 153–161.

CHAPTER V

CONCLUSIONS AND FUTURE DIRECTIONS

It was found that the addition of pine bark to pine clear wood feedstock led to lower gravimetric oil yields. In addition, the properties of pyrolysis oil were negatively impacted. Specifically, increases in solids, water and viscosity resulted when bark was added to the feedstock, with the impact correlated to the weight fraction of bark added. When pyrolysis oil has high solids content and particles greater than 10 microns are present, filtration is required to make the pyrolysis oil sui for upgrading processes. Post-condensation filtration was found to retard the rate of aging for all clearwood and clearwood/bark samples. No correlation was observed with the amount of bark added and change in viscosity.

Centrifugal filtration was shown to be an effective post-condensation method for removing solids from pyrolysis oil. Separation time and feed temperature need to be configured for the effective separation, specifically to reduce re-uptake of settled particulate matter and increase the separation efficiency. Care should be taken while raising the feed temperature of the pyrolysis oil in order to enhance solids removal as the rate of aging increases at high temperatures.

Chemical stabilization using anhydrous $CaCl_2$ followed by centrifugal separation was effective for the removal of water from pyrolysis oil in lab scale. Emulsion stability was measured using zeta potential. Zeta potential for the pyrolysis oil without coagulant

addition was -17.23 and it decreased with the coagulant addition and zeta potential was as low as 8.31 with the coagulant concentration of 1.0 M. Destabilization of the pyrolytic oil-water emulsion occurred at the coagulant concentrations of 0.5 and 1.0 M. Hence addition of $CaCl_2$ as a coagulant at concentrations of 0.5 and 1.0 M enhanced separation of oil and water phases.

Based on the work presented, future efforts should include utilizing pilot plant-scale centrifugal filtration system for the pyrolysis oil produced from bark added feedstock. Emulsion destabilization studies should be carried out on the pilot plant, disk-stack centrifuge. The centrifugal filtration system at the pilot plant should be coupled with the pilot plant reactor with the required in-line volumetric flow rate measurements and feed heating to allow for continuous operation.

APPENDIX A

DESCRIPTION AND OPERATING INSTRUCTIONS FOR THE DISC STACK CENTRIFUGE

Centrifuges can be used for solid-liquid, liquid-liquid or solid-liquid-liquid separation. Centrifuge utilized in this study is a disk-stack high-speed centrifuge with self-cleaning bowl. The machine can be used either for clarification (removal of solids from a liquid) or for separation (separation of liquid mixtures with simultaneous removal of solids).

A.1 Operating Principles

The bowl of a centrifuge is rotated at high speed which produces high centrifugal force. Influence of centrifugal force leads to the rapid separation of mixtures. During separation the heavier components are moved to the bowl periphery and the lighter components are displaced to the center of the bowl. Figure A.1 shows the schematic of the operation of the centrifuge as a separator (purifier). The product to be purified is conveyed from the top. As the bowl rotates the liquid flows to the center of the bowl and is discharged under pressure by centripetal pump. The heavy liquid flows to the bowl periphery and is discharged by centrifugal force via separating disk. The separated solids collect in solids holding space and are ejected periodically at full bowl speed. A large number of conical disks place on top of one another forms the disk stack and it splits the mixture of two liquids based on density. Each disk has spacers with a defined interspaces and smooth surface which facilitates the solids to slide down and collect in the solids holding space. Automatic opening and closing of the bowl with the set separation time for desludging is facilitated by the solenoid valve in the operating water line. The centrifuge can be easily converted to separator or clarifier using a gasket and a lock ring. Figure A.2 shows the conversion of the bowl from purifier to clarifier. Figure A.3 shows

the schematic of the installed centrifugal filtration system along with the feed tank, product tanks and valves.

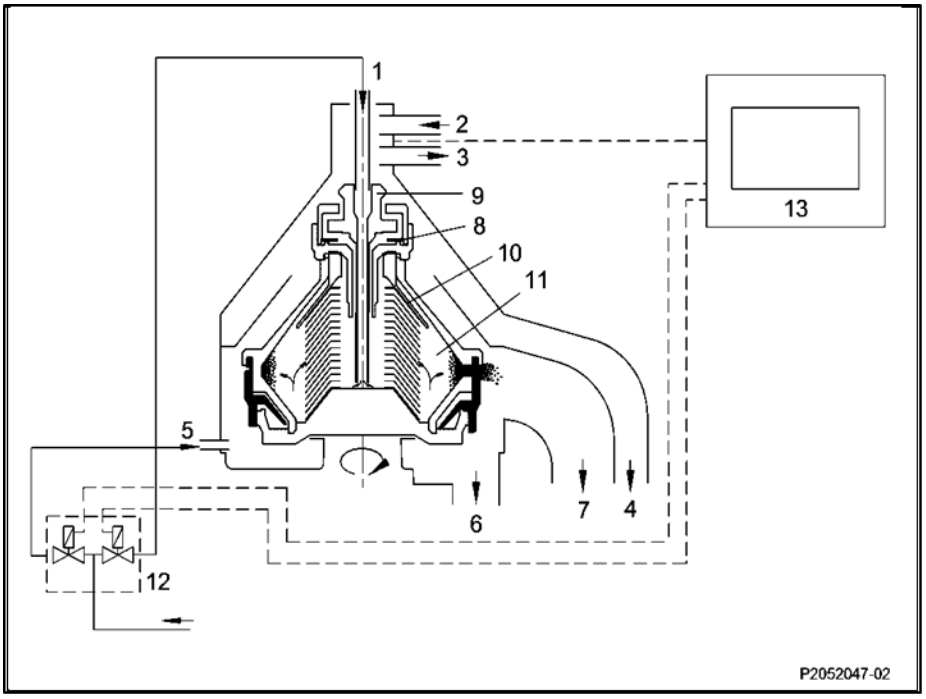

1. Filling and displacement water feed
2. Product feed
3. Light liquid discharge
4. Heavy liquid discharge
5. Operating water feed
6. Operating water discharge
7. Solids discharge
8. Regulating ring
9. Centripetal pump
10. Separating disk
11. Solids holding space
12. Solenoid valve block
13. Control unit

Figure A.1 Schematic of the operation of the centrifuge (GEA Westfalia, 2012)

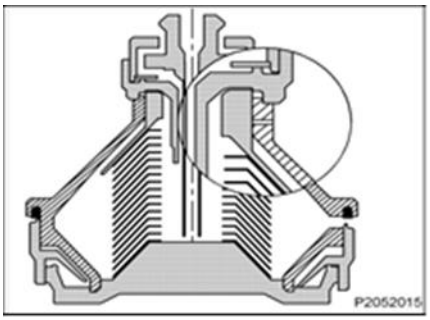

Separator bowl

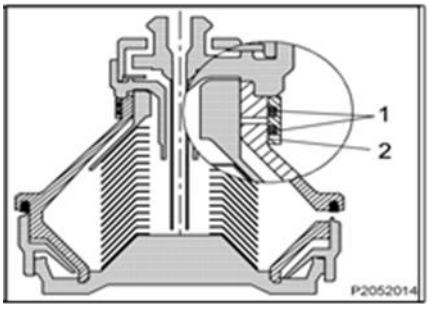

Clarifier bowl

1. Gasket
2. Lock ring

Figure A.2 Conversion of the bowl from separator to clarifier (GEA Westfalia 2012).

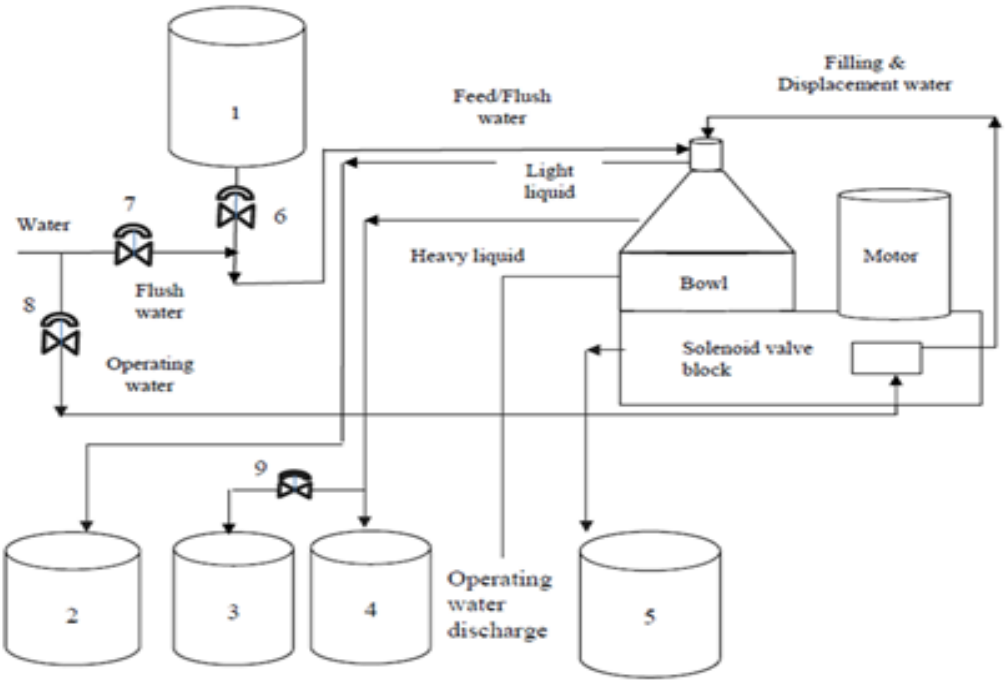

Item no	Description
1	Feed tank
2	Product tank-Light liquid
3	Product tank-Heavy liquid
4	Flush water collection tank
5	Solids collection tank
6	Feed valve
7	Flush water valve
8	Operating water valve
9	Valve-Clarified discharge line

Figure A.3 Assembly of centrifuge filtration unit at the MSU SERC pilot plant facility.

A.2 Requirements for Effective Filtration

A.2.1 Separation

The separation of liquid mixtures is possible only when they have different densities and do not form emulsions. Separation of liquid mixtures is facilitated by a regulating ring which adapts the bowl to the density difference between the liquids to be separated. Regulating ring should be chosen in a way that the inner diameter of the ring should correspond to the difference in density of the two liquids in the mixture. Three

rings with different inner diameters were provided along with the centrifuge by the manufacturer. Diameter with corresponding density of the liquid that can be handled, maximum and minimum density difference that can be handled and are summarized in Table A.1.

Table A.1 Diameter of required regulating ring based on the density of the light liquid

Density of the light liquid at 20 °C (g/mL)	Inner diameter of ring (mm)
0.8 to 0.84	36
0.84 to 0.90	41
0.90 to 0.93	44

(GEA Westfalia, 2012)

A.2.2 Clarification

Removal of solids strongly depends on separation time set for the centrifuge. After the elapse of the separation time the bowl opens to eject the collected solids out of the solids holding space of the centrifuge. If this time is set too long, overflowing of the solids in to the separated liquid space happens and if the time is set too short, sample loss increases with the increase in pressure loss. Separation is effective with the low viscosity of the product to be separated (GEA Westfalia 2012).

A.3 Operating Procedures

A.3.1 Starting the separator

Stepwise instructions for starting the separator are given below

- Switch on the control panel and check whether the mode of separation clarification or separation) is set as desired.
- Set the separation time.

- Check the oil level of the motor is up to the limit.
- Open the operating water line and check that the pressure is 2-2.5 bar.
- Check that the valves on the discharge side are open.
- Start the centrifuge. Starting time is 20-25 sec. The monitor will read 'accelerating'
- Once it finishes accelerating, open the feed valve and set the system to process mode.
- After the elapse of the set separation time, the bowl opens automatically to eject the collected solids.

A.3.2 Shutting down the separator

Stepwise instructions for starting the separator are given below

- Clean the centrifuge by operating it in the usual process mode using water.
- Close the discharge valve.
- Close the valves in the operating water line and feed line.
- Switch off the motor.
- Switch off the control panel.

A.4 References

GEA Westfalia, Centrifuge with self-cleaning bowl, Technical report 2052-9001-041/310, 2012.

APPENDIX B

SUMMARY OF STUDIES ON TESTING PYROLYSIS OIL IN COMBUSTION ENGINES

B.1 Summary

Pyrolysis oil has properties which do not support its use in diesel engines problems (Czernik and Bridgwater, 2004). Pyrolysis oil is difficult to ignite because of its lower heating value and high water content. Coking occurs due to the presence of thermally unstable compounds. Also, pyrolysis oil is corrosive and will degrade the materials used in standard engines.

However, environmental concerns related to conventional, petroleum-based fuels have led to research on ways to make pyrolysis oil more amenable to use in combustion engines. Frigo et al. showed that flash pyrolysis oil needs alcohol addition to allow for self-ignition in engines. Their study also showed that engine seizure may occur due to the deposits of carbonaceous material, and that the acidity of the oil may cause fast erosion of steel parts (Frigo et al., 1998). A study conducted at the VTT Technical Research Centre in Finland on a single cylinder, direct injection Lister Petter diesel engine showed that at least 5 vol% of nitrated alcohol should be added to pyrolysis oil for s engine operation, and even at 9 vol% alcohol addition there was a delay in ignition that required igniter modification. Also coke formation and clogging of injection nozzles was observed (Solantausta et al., 1993). Another study conducted at VTT showed that modifications are required to the injection pump and other engine elements to make them resistant to the acidic nature of pyrolysis oil (Solantausta et al., 1994a). In a study conducted by Solantausta et al., it was found that there was a need to readjust the injection system to adapt to the large variability in the properties of pyrolysis oil (Solantausta et al., 1994b). Researchers at the University of Florence conducted a study to test the suitability of pyrolysis oil-diesel emulsions as transportation fuel with the

emulsions prepared with the aid of surfactants. The emulsion showed better ignition characteristics than pyrolysis oil alone, but the high cost of surfactants and higher corrosiveness of the emulsion were the drawbacks of this approach (Chiaramonti et al., 2003). Some property specifications necessary for pyrolysis oil to meet current engine requirements include a solids content <0.1 wt %, a viscosity ranging between 10-20 cSt, and improved lubricity (Oasmaa et al., 2005). Prior studies have shown that utilizing pyrolysis oil in diesel engines is possible with modifications to existing equipment and stabilization of the properties of pyrolysis oil. These two issues need to be examine more, in order to identify a low cost, high value upgrade that would allow pyrolysis oil to be used for energy productions, transportation fuels, and more.

B.2 References

Chiaramonti, D., Bonini, M., Fratini, E., Tondi, G., Gartner, K., Bridgwater, A.V., Grimm, H.P., Soldaini, I., Webster, A., and Baglioni, P. (2003). Development of emulsions from biomass pyrolysis liquid and diesel and their use in engines—Part 2: tests in diesel engines. Biomass Bioenergy 25, 101–111.

Czernik, S., and Bridgwater, A.V. (2004). Overview of Applications of Biomass Fast Pyrolysis Oil. Energy Fuels 18, 590–598.

Frigo, S., Gentili, R., Tognotti, L., Zanforlin, S., and Benelli, G. (1998). Feasibility of using wood flash-pyrolysis oil in diesel engines (SAE Technical Paper).

Oasmaa, A., Peacocke, C., Gust, S., Meier, D., and McLellan, R. (2005). Norms and Standards for Pyrolysis Liquids. End-User Requirements and Specifications. Energy Fuels 19, 2155–2163.

Solantausta, Y., Nylund, N.-O., Westerholm, M., Koljonen, T., and Oasmaa, A. (1993). Wood-pyrolysis oil as fuel in a diesel-power plant. Bioresour. Technol. 46, 177–188.

Solantausta, Y., Nylund, N., Oasmaa, A., Westerholm, M., and Sipilä, K. (1994a). Preliminary tests with wood-derived pyrolysis liquid as fuel in a stationary diesel engine. pp. 26–28.

Solantausta, Y., Nylund, N.-O., and Gust, S. (1994b). Use of pyrolysis oil in a test diesel engine to study the feasibility of a diesel power plant concept. Biomass Bioenergy 7, 297–306.